Several Hfq-dependent alterations in physiology of Yersinia enterocolitica O:3 are mediated by derepression of the transcriptional regulator RovM

Leskinen, K., Pajunen, M. I., Varjosalo, M., Fernández-Carrasco, H., Bengoechea, J. A., & Skurnik, M. (2017). Several Hfq-dependent alterations in physiology of Yersinia enterocolitica O:3 are mediated by derepression of the transcriptional regulator RovM. Molecular Microbiology. DOI: 10.1111/mmi.13610

Published in:
Molecular Microbiology

Document Version:
Peer reviewed version

Several Hfq-dependent alterations in physiology of *Yersinia enterocolitica* O:3 are mediated by derepression of the transcriptional regulator RovM

Katarzyna Leskinen[1], Maria I. Pajunen[1], Markku Varjosalo[2,3], Helena Fernández-Carrasco[4], José A. Bengoechea[4], and Mikael Skurnik[1,5*]

[1]Department of Bacteriology and Immunology, Medicum, Research Programs Unit, Immunobiology, University of Helsinki, Finland; [2]Institute of Biotechnology, University of Helsinki; [3]Biocentrum Helsinki, Finland: Finnish Institute of Molecular Medicine, Finland, [4]Centre for Experimental Medicine, Queens University Belfast. Belfast, UK, and [5]Division of Clinical Microbiology, Helsinki University Hospital, HUSLAB, Helsinki, Finland.

***Address for correspondence:**

Mikael Skurnik
P.O.Box 21 (Haartmaninkatu 3)
FIN-00014 UNIVERSITY OF HELSINKI
FINLAND
tel: +358-2491 26464
fax: +358-2941 26382
mikael.skurnik@helsinki.fi

Running title: Hfq and RovM in *Yersinia enterocolitica* O:3

Keywords: Yersinia enterocolitica, *hfq*, *rovM*, *rovA*

Summary

In bacteria, the RNA chaperone Hfq enables pairing of small regulatory RNAs with their target mRNAs and therefore is a key player of post-transcriptional regulation network. As a global regulator, Hfq is engaged in the adaptation to external environment, regulation of metabolism and bacterial virulence. In this study we used RNA-sequencing and quantitative proteomics (LC-MS/MS) to elucidate the role of this chaperone in the physiology and virulence of *Yersinia enterocolitica* serotype O:3. This global approach revealed the profound impact of Hfq on gene and protein expression. Furthermore, the role of Hfq in the cell morphology, metabolism, cell wall integrity, resistance to external stresses and pathogenicity was evaluated. Importantly, our results revealed that several alterations typical for the *hfq*-negative phenotype were due to derepression of the transcriptional factor RovM. The overexpression of RovM caused by the loss of Hfq chaperone resulted in extended growth defect, alterations in the lipid A structure, motility and biofilm formation defects, as well as changes in mannitol utilization. Furthermore, in *Y. enterocolitica* RovM only in the presence of Hfq affected the abundance of RpoS. Finally, the impact of *hfq* and *rovM* mutations on the virulence was assessed in the mouse infection model.

Introduction

Yersinia enterocolitica is a gram-negative pathogen causing yersiniosis, the third most common zoonotic foodborne disease in the European Union (Virtanen *et al.*, 2011). The most common clinical manifestation of yersiniosis is self-limited gastroenteritis that is restricted to the intestinal tract, however, extraintestinal manifestations and postinfectious sequelae are also occasionally encountered. Common clinical symptoms among young adults are pseudoappendicitis and secondary immunological reactions which may lead to reactive arthritis and erythema nodosum (Virtanen *et al.*, 2011, Huovinen *et al.*, 2010).

The species *Y. enterocolitica* consists of heterogeneous group of strains classified into 6 biotypes (1A, 1B, 2, 3, 4 and 5) and over 70 serotypes (Wauters *et al.*, 1987). Due to the presence of virulence plasmid (pYV) the strains of biotypes 1B and 2-5 are considered pathogenic. The serotypes O:3, O:5,27, O:8 and O:9 are most commonly associated with the human infections (EFSA, 2014). The pathogenic potential of these bacteria resides on many essential virulence factors, encoded by genes located on both the virulence plasmid and chromosome. Major virulence determinants include lipopolysaccharide (LPS), specific adhesion and invasion proteins (Ail, Inv, YadA), as well as Type III Secretion System (T3SS) with its effector proteins (YopE, YopH, YopM, YopO, YopP, YopT). It is well established that the biosynthesis and expression of these factors undergo specific and precise regulation that takes place at both the transcriptional and translational levels, yet the regulation mechanisms are still poorly understood (Schiano & Lathem, 2012).

One of the newly discovered post-transcriptional regulatory circuits is based on small regulatory RNAs (sRNAs). Most sRNAs are within the range of 50 – 200 nucleotides in length and they regulate specific mRNA targets either by modulation of mRNA stability and/or by altering the access of mRNA to ribosomes (Livny & Waldor, 2007, Murina & Nikulin, 2015). Hfq, an RNA chaperone required for maintaining the stability and function of many sRNAs, has been recognized as a central component of global post-transcriptional regulation network (Vogel & Luisi, 2011). It interacts by binding AU-rich sequences of target mRNA and enable pairing of sRNA and target mRNA. Hfq-dependent sRNAs usually act on *trans*-encoded mRNA and represses translation and/or accelerates degradation, yet mRNA activation is also possible. Recent studies using co-immunoprecipitation and subsequent detection of sRNAs and mRNAs led to identification of a large number of Hfq targets present in different bacterial species (Bilusic *et al.*, 2014, Chao *et al.*, 2012, Sittka *et al.*, 2008, Zhang *et al.*, 2003).

Hfq typically exerts its function through interactions with sRNAs. A deep RNA-sequencing approach identified ca. 150 sRNAs in *Y. pseudotuberculosis* and 31 in *Y. pestis* (Beauregard *et al.*, 2013, Koo *et al.*, 2011, Nuss *et al.*, 2015, Schiano *et al.*, 2014). Another approach based on cDNA-cloning allowed verification of 43 novel sRNAs from *Y. pestis* (Qu *et al.*, 2012). For these species, the sRNA expression under different conditions and their role in bacterial virulence was studied (Koo *et al.*, 2011, Yan *et al.*, 2013) and it was observed that some sRNAs, although conserved in both *Yersinia* species, displayed different functions suggesting evolutionary changes in sRNA regulation networks of these two species (Koo *et al.*, 2011). In addition, it was found that the effect of the inactivation of the *hfq* gene can be either direct or indirect the latter via alterations in the expression of different regulators. In this respect, indications of interactions between the Hfq and Csr regulatory systems have been observed with different bacterial species. For example, in *Y. pseudotuberculosis* Hfq activates the expression of CsrB and CsrC, two sRNA molecules that repress the expression of CsrA (Bucker *et al.*, 2014, Heroven *et al.*, 2012). Also, in *E. coli* CsrA can bind to *hfq* mRNA and inhibit translation by blocking the ribosome binding site (Baker *et al.*, 2007). However, the effects of Hfq-inactivation always seem to be unique for each bacterial species. Due to its pleiotropic nature, many different defects were observed among Hfq-deficient strains: impaired growth, inability to cope with different types of environmental stresses, higher susceptibility to antimicrobial agents, defects in quorum sensing and host invasion. It has been proposed that the Hfq-deficient strains might be used as live attenuated vaccines as the virulence of the *hfq* mutants of many pathogens is highly reduced (Chao & Vogel, 2010, Hayashi-Nishino *et al.*, 2012, Geng *et al.*, 2009, Schiano *et al.*, 2010).

A recent study showed that Hfq has a profound influence on the fitness of *Y. enterocolitica* serotype O:8 strain by affecting the metabolism of carbohydrates, nitrogen, iron, fatty acids and ATP synthesis (Kakoschke *et al.*, 2014) as well as the expression of

several adhesins (Kakoschke *et al.*, 2016). Moreover, the inactivation of the *hfq* gene of the O:8 strain led to slower bacterial growth, decreased resistance to stress and impaired synthesis of urease, yersiniabactin, and biofilm formation (Kakoschke *et al.*, 2014). It was also shown that Hfq is essential for virulence in mice, and while it did not affect the production of Yops it was needed for proper translocation of T3SS effector proteins into host cells (Kakoschke *et al.*, 2016). The *hfq* mutant of *Y. pseudotuberculosis* presented hypermotility and increased production of a biosurfactant-like substance. Furthermore, it displayed decreased survival in macrophages, affected biofilm formation, impaired production of T3SS effector proteins and was highly attenuated in mouse model infection (Schiano *et al.*, 2010, Bellows *et al.*, 2012). Also in *Y. pestis* Hfq was implicated in the persistence inside of macrophages and resistance to stress, and likewise, the inactivation of the *hfq* gene led to attenuation (Geng *et al.*, 2009).

The *Y. pseudotuberculosis* RovM (for **r**egulator **o**f **v**irulence) is ca. 70% identical to the *E. coli* LysR homologue A (LrhA) that functions as a global transcriptional regulator of genes related to motility, chemotaxis and flagella synthesis. LrhA is known to interact directly with the promoter of the *flhDC* genes and to autoregulate the *lrhA* gene promoter, and thereby to affect indirectly the genes that are under the control of the FlhDC master regulon (Lehnen *et al.*, 2002). Moreover, in *E. coli* LrhA affects the levels of stationary-phase sigma factor σ^S (RpoS) (Gibson & Silhavy, 1999, Peterson *et al.*, 2006). In other bacteria, the LrhA homologs are known under diverse names and functions. The PecT of *Erwinia chrysanthemi* and HexA of *Erwinia carotovora* are 75-79% identical to LrhA, and were implicated to regulate several virulence determinants (Harris *et al.*, 1998, Castillo & Reverchon, 1997). In *Y. pseudotuberculosis* RovM requires H-NS to repress the invasin regulator RovA (Heroven & Dersch, 2006). Similar to *lrhA* also the *rovM* gene is autoregulated and this involves the RNA-binding protein CsrA through an unknown mechanism (Heroven *et al.*, 2008). Finally,

the RovM homolog of *Y. enterocolitica* O:3 is 88% identical to RovM of *Y. pseudotuberculosis* and ca. 70% identical to LrhA of *E. coli.*

In this study we used RNA-sequencing (RNA-seq) and quantitative proteomics (LC-MS/MS) to identify Hfq-dependent mRNAs and proteins of *Y. enterocolitica* serotype O:3, and to elucidate the role of this chaperone in the physiology and virulence of the pathogen. We show that deletion of *hfq* led to profound changes in gene and protein expression profiles, as well as to alterations in physiology and pathogenicity. Moreover, we report that several alterations in the *hfq* mutant were mediated by overexpression of RovM.

Results

Transcriptomic and proteomic profiling.

To detect genes regulated directly or indirectly by Hfq, deep RNA-seq analysis was performed for *Y. enterocolitica* serotype O:3 wild type strain 6471/76 (hereafter designated as YeO3) and its isogenic *hfq*-deficient derivative YeO3-*hfq*::Km. Total RNA was isolated from two biological replicas of bacteria grown in lysogeny broth (LB) to logarithmic phase (OD_{600} = 0.6) at room temperature (RT, 22°C) and at 37°C. Genes were considered to be significantly differentially expressed between the strains if the fold change (FC) in the relative normalized number of aligned sequence reads was >2, and the p-value of Student's T-test was <0.05 (see Experimental procedures). Under these relatively stringent criteria, the transcription of 346 genes at RT and 541 genes at 37°C, *i.e.,* ca. 8 and 12.5% of the *Y. enterocolitica* genes, respectively (Tables 2, S2 and S4) were altered in the *hfq* mutant. At RT, of the 346 genes 214 genes were down- and 132 up-regulated (Table S1), and at 37°C, of the 541 genes, 96 were down- and 445 up-regulated (Table S2). A total of 95 genes were differentially expressed both at RT and 37°C; 27 showed down- and 59 up-regulation (Table

S3). For 9 genes opposite changes took place depending on the growth temperature (indicated by exclamation marks in Table S3).

A subset of transcriptomics results was validated by quantitative RT-qPCR using newly isolated RNA. The RT-qPCR results were in perfect agreement with the RNA-seq data (Table S4), confirming the reliability of the RNA-seq results.

Total proteome samples in three biological replicas from the YeO3 and YeO3-*hfq*::Km strains, grown under exactly same conditions as for RNA-seq, were prepared for quantitative LC-MS/MS proteomic analysis. Also here the difference in protein abundance was considered significant if the FC was >2 with a p-value <0.05. Altogether 1570 (36.10%) of the 4349 proteins annotated for *Y. enterocolitica* serotype O:3 strain Y11 were identified from bacteria grown at 37°C. Out of them 119 proteins (7.58%) were differentially expressed; 101 (84.87%) over- and 18 (15.13%) under-expressed (Table S5). From bacteria grown at RT, on the other hand, altogether 1923 (44.22%) proteins were identified. Of these, 110 (5.72%) were differentially expressed; 69 (62.73%) over- and 41 (37.27%) under-expressed (Table S6). While the expression of altogether 212 different proteins was affected in the YeO3-*hfq*::Km strain, differential expression of 195 of them took place only at one of the growth temperatures. Only 17 of the proteins showed significant differences in abundance at both temperatures; fifteen were over-expressed and two, under-expressed. Nine of these Hfq-dependent proteins belonged to the metabolic pathways.

Taken together, the transcriptomic and proteomic profiling revealed profound differences in the expression of genes between the YeO3 and YeO3-*hfq*::Km strains with more affected genes in bacteria grown at 37°C than at RT. Based on the RNA-seq data, temperature in wild type bacteria does not regulate *hfq* expression thus making it unlikely that the distribution of the affected genes between the two temperatures would be due to

differences in Hfq baseline levels. Furthermore, both transcriptomics and proteomics demonstrated that >80% of the differentially expressed genes at 37°C were up-regulated. However, when bacteria were grown at RT the proteomics and transcriptomics data were not congruent as in RNA-seq most differentially expressed genes were down-regulated while in proteomics most differentially expressed proteins were up-regulated (Table 1).

The correlation between proteomics and transcriptomics analyses

Tables S5 and S6 list all the proteins with differential abundance identified in the proteomics analysis. We wanted to know whether this would correlate to the corresponding transcript levels. This was the case with ca. 47 and 69% of the proteins showing different abundance in LC-MS/MS study for bacteria grown at RT and 37°C, respectively, using the stringent criteria for differential expression. In bacteria grown at 37°C altogether 119 proteins had differential abundance (Table S5), and for 82 (69%) of them the transcriptomics results were concordant, but only 25 met the stringent criteria of differential expression in transcriptomics. The remaining 57 did not meet the stringent criteria used in the transcriptomics analysis. Altogether 36 proteins with significantly different protein abundance had an opposite but not significant pattern of gene expression. Finally, only one protein, succinate dehydrogenase flavoprotein subunit (YP_006005361.1) showed significantly different pattern of expression in both the transcriptome and proteome analyses under these conditions (Table S5).

In bacteria grown at RT, 110 proteins had differential abundance (Table S6). The RNA-sequencing and LC-MS/MS results were congruent for 52 (47%) of the proteins with differential abundance (Table S6). For 40 proteins (36%) the transcriptomics was congruent but did not meet the stringent criteria for differential expression. Only 18 (16%) of the proteins with significantly different protein abundance showed an opposite pattern of gene

expression, and out of these, only 2 genes, a putative sugar ABC transporter (YP_006005189.1) and the hemin transport protein HmuS, were considered to be significantly differentially expressed in both proteomics and transcriptomics studies (Table S6).

Functional classification of differentially expressed genes

Functional classification based on the Gene Ontology genome annotation of *Y. enterocolitica* Y11 (http://www.geneontology.org/) showed that differentially regulated genes were scattered among different functional classes (Fig. 1). The class of genes coding for the metabolic pathway enzymes was the best represented class accounting for 29.8% and 37.3% of all Hfq-dependent genes at RT and 37°C, respectively. In all functional classes, except for the motility and biofilm class where all the genes were down-regulated, both up- and down-regulation patterns were observed. Many of the differentially regulated genes encode inner or outer membrane-bound proteins that belong to the cell envelope and transporter/binding proteins classes, suggesting changes in the bacterial surface. Moreover, functional classification indicated that the iron metabolism of the YeO3-*hfq*::Km strain was differentially regulated.

Comparison of quantitative proteomic and transcriptomic results showed coherent patterns of differential regulation of several functional pathways (Table 2). Several outer membrane proteins including OmpX, OmpC, OmpF, OmpW and EnvZ were overexpressed in YeO3-*hfq*::Km especially at 37°C. Moreover, overexpression of the Cpx system components was observed in YeO3-*hfq*::Km. The Cpx system in *E. coli* functions as a stress response system that is induced upon damage to the cell envelope leading to subsequent activation of proteases and folding catalysts (Dorel *et al.*, 2006). Many phosphotransferase (PTS) systems turned out to be either up- or down-regulated in YeO3-*hfq*::Km. The PTS systems consist of two cytoplasmic energy-coupling proteins and different carbohydrate-

specific enzymes that catalyze carbohydrate translocation and phosphorylation. The PTS system optimizes the utilization of carbohydrates present in the environment through changes in the phosphorylation status of its components. Furthermore, in many bacteria the PTS systems with associated proteins have also been implicated in catabolite repression, inducer control and chemotaxis (Kotrba *et al.*, 2001). In the present study, the β-glucoside, fructose, glucitol/sorbitol, glucose, mannitol, mannose and *N*-acetylgalactosamine-specific enzymes were overexpressed in the YeO3-*hfq*::Km strain grown at 37°C. At RT only the enzymes involved in glucitol/sorbitol, glucose and mannitol utilization showed significant up-regulation. On the other hand, the cellobiose and chitobiose-specific PTS systems seemed to be significantly down-regulated in YeO3-*hfq*::Km grown at RT.

Influence of Hfq on the abundance of sRNAs

Due to the fact that Hfq functions as a chaperone of sRNAs, the differences in abundance of these molecules were investigated. Based on data obtained from the repository for bacterial sRNA (Li *et al.*, 2013) for the serotype O:8 a list of predicted 27 sRNAs was prepared (Table S7). Subsequently, the sequences of these sRNAs were blasted against the genomic DNA of *Y. enterocolitica* Y11 and the expression of selected regions was verified using the RNA-seq data.

The analysis showed that six sRNAs were affected by the lack of Hfq under at least one condition (Fig. S1). Two of them (*csrB* and *csrC*) that have been implicated in the global carbon storage regulatory system (Liu & Romeo, 1997), were downregulated under all studied conditions. CsrB and CsrC regulate the activity of CsrA, an RNA-binding protein, by sequestering its binding sites and thus preventing it from binding to its target mRNAs (Romeo, 1998, Weilbacher *et al.*, 2003). Moreover, the expression of *gcvB*, encoding a sRNA shown to repress the *dppA* gene in *Y. pestis* (Koo *et al.*, 2011), and *fnrS* was downregulated at 37°C. Whereas, two sRNA species, *rrpA* and *sroB*, were more abundant

in the YeO3-*hfq*::Km strain. In other bacterial species *gcvB*, *fnrS* and *sroB* are known to interact with Hfq protein (Chao *et al.*, 2012, Durand & Storz, 2010, Rasmussen *et al.*, 2009)

Influence of Hfq on transcriptional regulators

Interestingly, the expression of transcriptional regulators OmpR, RovA, PhoB, RovM and RpoS were altered in YeO3-*hfq*::Km. While the *ompR* and *rovM* genes were up-regulated (more strongly at 37°C, even 40-fold for *rovM* in RNA-seq), the *phoB, rovA* and *rpoS* were downregulated (Table 2). One could then speculate that certain phenotypic changes in YeO3-*hfq*::Km were due to changes in the expression levels of these regulators. Indeed, the loss of Hfq affected the RovA regulon in a similar way as loss of *rovA* including the downregulation of hemin genes, *flgN, cutC* and upregulation of *ompF, ompW, ompX*, and *gltJ* (Cathelyn *et al.*, 2007).

The overexpression of RovM in* hfq *mutant

Overexpression of RovM in YeO3-*hfq*::Km was clearly demonstrated by both transcriptomics and proteomics in this work and confirmed by RT-qPCR (Fig. 2A and Tables 3 and S4). While the RovM protein level in wild type bacteria grown at 37°C was too low to allow its detection by mass spectrometry, it was clearly identified from all the YeO3-*hfq*::Km samples (Fig. 2A). At RT both RNA-seq and proteomics indicated a 8-9-fold overexpression, however, at 37°C RNA-seq indicated a 39.8-fold overexpression (Table 2).

As RovM homologues are transcriptional regulators in other bacteria we wanted to elucidate its role as a regulator in *Y. enterocolitica* O:3. We used a genetic approach to assess which phenotypic features of YeO3-*hfq*::Km resulted of the subsequent overexpression of RovM. In strain YeO3-*rovM* the *rovM* gene was inactivated, in the double-mutant strain YeO3-*rovM-hfq*::Km both the *rovM* and *hfq* genes were inactivated and in strain YeO3/pMMB207-*rovM* the *rovM* gene was under an IPTG-inducible promoter. The

phenotypes of these strains were compared to those of the wild type and YeO3-*hfq*::Km strains as described next.

Due to the fact that many of the RovM homologs tightly control their own synthesis the regulation mechanism of RovM expression was assessed. The 300 bp long fragment upstream of the *rovM* gene showed 83% identity with equivalent region of *Y. pseudotuberculosis* and *Y. pestis*. However, the *lrhA* regulatory region of *E. coli* showed no significant similarity with that of *Y. enterocolitica* O:3. In order to verify the presence of autoregulation mechanism in *Y. enterocolitica* the *rovM* promoter fragment was cloned into the promoter reporter vector pLux232oT (see Experimental Procedures for details) and luminescence was measured in different strains (Fig. 2B). Light production in YeO3-*rovM*/pLux232oT-*rovM* bacteria was about half of that in YeO3/pLux232oT-*rovM* bacteria. In contrast, overexpression of RovM in YeO3/pMMB207-*rovM,* pLux232oT-rovM resulted in over 10-fold increase in light production. Moreover, the *rovM* promoter showed no activity in *E. coli* background. Overall, these results indicate the presence of an autoregulatory circuit for the *Y. enterocolitica* O:3 *rovM* gene.

In order to determine whether the overexpression of the *rovM* gene in the *hfq* mutant is mediated through CsrA, the *csrA* gene was overexpressed in the wild type strain (YeO3/pMMB207-*csrA*). The RT-qPCR results showed that the abundance of the *csrA* transcript in YeO3-*hfq*::Km and YeO3/pMMB207-csrA strains was comparable. At RT, the CsrA overexpression in both the *hfq* mutant and wt bacteria activated strongly the transcription of the *rovM* gene (9,42 ± 1,90 and 8,86 ± 0,92 -fold, respectively) and repressed the *rovA* transcription (0,22 ± 0,01 and 0,55 ± 0,02 –fold, respectively). We also demonstrated using the *rovM* promoter reporter construct plux232oT-rovM that the CsrA overexpression increased the *rovM* promoter activity ca. 2-fold (Fig. 2B).

297 In order to determine the influence of the RovM overexpression on the gene expression
298 in YeO3-*hfq*::Km mutant the transcriptomes of the YeO3-*rovM* and YeO3/pMMB207-*rovM*
299 bacteria were determined and compared. The analysis showed that in *Y. enterocolitica* 55
300 genes are under direct or indirect regulation of RovM (Table 3). The comparison between
301 the transcriptomes of the YeO3/pMMB207-*rovM* and YeO3-*hfq*::Km bacteria showed
302 general coherence in the expression of these 55 RovM-regulated genes. In both the strains
303 the elevated levels of RovM resulted in higher levels of several transcripts including outer
304 membrane protein X, three members of the PTS system, and several other enzymes.
305 Moreover, in both the strains the expression of *rovA* and *rpoS* was significantly repressed.
306 However, for five genes including the *malE* and *malM* genes from the maltose operon, an
307 opposite pattern of expression was observed.

308 ***Influence of* Hfq *on growth in vitro***

309 Inactivation of the *hfq* gene in *Y. enterocolitica* O:8 and in *Y. pseudotuberculosis*
310 caused slower growth *in vitro* (Kakoschke et al., 2014, Schiano et al., 2010). In line with this,
311 the growth curves of the YeO3-*hfq*::Km bacteria in BHI broth were influenced at all tested
312 temperatures (4, 22, 37 and 42°C) (Fig. 3A-D), and also the stationary phase OD_{600} values
313 of the mutant bacteria were clearly below those of the wild type bacteria (Fig. 3E). The
314 growth defect was most prominent at 4 and 37°C (Fig. 3B and 3C). The growth curves of
315 the *in trans* complemented strain YeO3-*hfq*::Km/p*hfq* were almost identical to those of the
316 wild type bacteria, although it reached stationary phase a little later than the wild type strain.
317 These minor differences were likely due to plasmid-copy number effects. To determine
318 whether the growth defect was mediated by the overexpression of RovM, the growth curves
319 of the *rovM* mutant strains were also determined. While the YeO3-*rovM* strain showed no
320 growth defects (data not shown), overexpression of RovM in YeO3-*hfq*::Km appeared to be
321 partially responsible for the growth defect of the *hfq* mutant. The double-mutant YeO3-*rovM*-

hfq::Km grew faster at all tested temperatures when compared to the YeO3-*hfq*::Km bacteria, however, not as well as the wild type bacteria (Fig. 3A-D). Interestingly, the overexpression of *rovM* from the pMMB207-*rovM* plasmid did not cause any significant changes in the bacterial growth (data not shown). The growth phenotypes of the strains in LB and in BHI showed no difference except for the YeO3-*rovM-hfq*::Km strain which grew slower at 4°C in LB than in the rich BHI medium (data not shown). Taken together, these results showed that the loss of Hfq led to a growth defect in *Y. enterocolitica* O:3 and that this was at least partially due to overexpression of RovM.

Colony and cell morphology

In *Y. enterocolitica* serotype O:8, the inactivation of the *hfq* gene caused altered colony morphology (Kakoschke *et al.*, 2014). While all the O:3 strains in this study had similar colony morphologies on LB plates at 22° and 37°C, after 48 h incubation on CIN agar at RT the YeO3-*hfq*::Km strain formed small, dry and dark colonies surrounded by dark violet halo. This phenotype appeared to be completely caused by the overexpression of RovM as the double-mutant YeO3-*rovM-hfq*::Km produced typical pink bull's eye colonies (Fig. S2A-B). In coherence with the RNA-seq results, where YeO3-*hfq*::Km mutant displayed overexpression of genes involved in metabolism of mannitol, the growth on mannitol and CIN agar plates was affected. During the growth on mannitol plates both YeO3-*hfq*::Km and YeO3/pMMB207-*rovM* bacteria displayed larger halo surrounding the bacterial growth indicating higher rates of acidification of the medium (Fig. S2C). To find out whether the colony morphology was associated with the bacterial cell morphology, the bacterial cells were studied by electron microscopy (EM). Bacteria grown overnight at RT in tryptone broth (TB) medium (with gentle shaking) or on 0.3% TB agar plates were collected for EM analysis. In line with previous reports (Chao & Vogel, 2010, Kakoschke *et al.*, 2014), the YeO3-*hfq*::Km bacterial cells from both the solid and liquid media were significantly ($p = 2.19 \times 10^{-}$

347 [33]) elongated. The average length of wild type bacterial strain cells was 0.96 ± 0.15 µm,
348 whereas that of YeO3-*hfq*::Km was 1.89 ± 0.32 µm. (Fig. 4). The double-mutant YeO3-*rovM-*
349 *hfq*::Km cells retained the elongated cell morphology of YeO3-*hfq*::Km and the cells of
350 YeO3-*rovM* were identical to those of wild type bacteria. Moreover, the YeO3-*hfq*::Km
351 bacteria were visibly more dispersed when compared with wild type and did not form
352 aggregates (Fig. S3). The cell morphology of the trans-complemented strain YeO3-
353 *hfq*::Km/p*hfq* was normal. Overall, the above results indicated that the YeO3-*hfq*::Km strain
354 colony morphology but not the bacterial cell shape was due to the RovM overexpression.

355 ***Motility and biofilm production.***

356 Loss of Hfq impairs the motility of many bacterial species, reviewed in (Chao & Vogel,
357 2010). As LrhA affected in *E. coli* the expression of *flhDC* encoding the master regulator of
358 flagella biosynthesis (Lehnen *et al.*, 2002), we decided to evaluate the impact of Hfq and
359 RovM on swimming motility using the constructed set of strains. In line with earlier results
360 (reviewed in (Chao & Vogel, 2010)), the YeO3-*hfq*::Km strain displayed decreased motility
361 when tested on 0.35% agar TB plates while the wild type, YeO3-*hfq*::Km/p*hfq* and YeO3-
362 *rovM-hfq*::Km strains were motile (Fig. 5A). To determine whether the reduced motility on
363 soft agar plates was due to flagellation defect, flagellin levels were evaluated by
364 immunoblotting using anti-flagellin mAb 15D8 (Fig. 5B). Indeed, the flagellin production of
365 YeO3-*hfq*::Km was repressed while normal levels were present in the wild type, YeO3-
366 *hfq*::Km/p*hfq* and YeO3-*rovM-hfq*::Km bacteria. Hence, the results indicate that the
367 impairment in motility of YeO3-*hfq*::Km strain is due to the overexpression of RovM that
368 represses the production of flagellin.

369 As flagellae and fimbriae are involved in biofilm formation, the role of Hfq and RovM in
370 the biofilm development was assessed. Bacteria were incubated statically at RT for 72h in
371 polystyrene microtiter plate wells and attached bacteria quantified using the crystal violet

assay. The wild type strain biofilm formation was most pronounced in M9 medium, followed by MedECa and least in TB. In all media, the YeO3-*hfq*::Km bacteria formed significantly less biofilm than wild type bacteria, and they formed no biofilmin MedECa and TB (Fig. 5C). In all the studied media the double mutant YeO3-*rovM-hfq*::Km formed statistically more biofilm compared to YeO3-*hfq*::Km mutant (Student's T-test p-values were 1.8×10^{-8}, 6.4×10^{-8}, and 1.3×10^{-6} in TB, MedECa and M9, respectively). Moreover, the trans-complemented strain YeO3-*hfq*::Km/p*hfq* showed increased biofilm production (p-values were 1.4×10^{-10} and 5.3×10^{-5} in MedECa and M9, respectively), presumably due to copy number effect. Overall, the RovM overproduction appeared to be responsible for the impairment of biofilm formation in the *hfq* mutant strain YeO3-*hfq*::Km.

Influence of RovM on RpoS and RovA expression

In *E. coli* LrhA represses the *rpoS* gene encoding the stationary phase sigma factor RpoS or σ^{38} (Peterson *et al.*, 2006). The transcriptomics and proteomics results indicated that inactivation of the *hfq* gene led to a decrease in the abundance of RpoS in *Y. enterocolitica* O:3 (Table 2). Moreover, the RNA-seq analysis revealed that the RovM overexpression from the pMMB207-*rovM* plasmid also resulted in decreased levels of *rpoS* transcript (Table 3). However, it is worth noting, that the sequencing was conducted for RNA isolated from bacteria growing in the logarithmic phase, whereas the stationary phase is the most optimal for RpoS expression. Therefore, we used immunoblotting to monitor at stationary phase the RpoS levels in wild type, YeO3-*hfq*::Km, YeO3-*hfq*::Km/p*hfq* and YeO3-*rovM-hfq*::Km bacteria. The results showed that the loss of *hfq* repressed the *rpoS* gene and decreased the level of σ^{38}, however, this was not reversed in the double mutant YeO3-*rovM-hfq*::Km (Fig. 6A). The RpoS levels were restored in the *trans*-complemented strain YeO3-*hfq*::Km/p*hfq*.

RovA is a transcriptional regulator of the MarR/SlyA family and its role in the virulence of *Yersinia* has been established (Cathelyn *et al.*, 2006, Lawrenz & Miller, 2007, Revell & Miller, 2000). In *Y. pseudotuberculosis* RovM interacts specifically with the regulatory region of the *rovA* gene negatively regulating its transcription (Heroven & Dersch, 2006). In order to evaluate the influence of RovM on the *rovA* transcription in *Y. enterocolitica* O:3 a quantitative RT-PCR was performed. Results showed that considerably more *rovA* transcript was detected in *rovM* negative strains, while overexpression of RovM resulted in decreased *rovA* mRNA abundance (Fig. 6B). Moreover, while there was a significant ($p = 0.004$) decrease in the *rovA* transcription in the YeO3-*hfq*::Km mutant, the knock-down of *rovM* gene in the *hfq* negative background restored and even increased the abundance of the *rovA* transcripts. Taken together, our results indicated that in *Y. enterocolitica* O:3 RovM functions as a repressor of *rovA* and that the decreased *rovA* expression in YeO3-*hfq*::Km mutant is mediated by the overexpression of RovM.

Resistance to environmental stresses.

During infection the *Y. enterocolitica* bacteria must resist the different stresses imposed by the host innate immune system and react adequately to the changes in the environment. Since inactivation of the *hfq* gene is highly pleiotropic it is also essential for virulence [reviewed in (Chao & Vogel, 2010)]. Therefore we assessed the YeO3-*hfq*::Km strain in several virulence-related stress experiments. The YeO3-*hfq*::Km bacteria were heat-sensitive in line with the impaired growth at 42°C (Fig. 3D); the mutant in contrast to wild type bacteria showed low survival rates after the exposure to 55°C (Fig. 7A). The heat-sensitivity was not caused by overexpression of RovM as the double-mutant YeO3-*rovM*-*hfq*::Km was also heat-sensitive. Heat-resistance was restored in the trans-complemented strain YeO3-*hfq*::Km/p*hfq*.

The YeO3-*hfq*::Km bacteria showed decreased ability to survive in acidic environment that mimics the passage through the stomach (Fig. 7A). Urease has been associated with acid-tolerance (De Koning-Ward & Robins-Browne, 1995, Gripenberg-Lerche *et al.*, 2000), and as both proteomics and transcriptomics (Table 2) indicated repression of the urease operon in YeO3-*hfq*::Km we assessed the urease activity of the strains. Indeed, YeO3-*hfq*::Km was urease-negative while the wild type and YeO3-*hfq*::Km/p*hfq* strains were urease-positive (Fig. 7B and S4). Repression of urease activity was not due to overexpression of RovM as the double-mutant YeO3-*rovM-hfq*::Km was urease-negative. However, the YeO3-*rovM-hfq*::Km strain presented intermediate tolerance to pH 2.5 (Fig. 7A) that is in line with the transcriptomic study that showed downregulation of the urease alpha- and beta-subunits in the YeO3/pMMB207-*rovM* strain (Table 3).

Mouse virulence

Finally, the virulence of YeO3-*hfq*::Km was tested in experimental mouse infection using the co-infection model (Skurnik *et al.*, 1999) where mice were infected with a mixture of YeO3 and YeO3-*hfq*::Km strains, as well as standard infection model where mice were infected with a single strain individually. Both intragastric (i.g.) and intraperitoneal (i.p.) routes of infection were investigated and the mice were not pretreated with the iron-chelating desferroxamine to avoid any possible immunosuppressive effects (Collins *et al.*, 2002).

Mouse virulence, i.g. coinfection experiments. In the co-infection model mice were infected with ca. $3x10^9$ CFU per mouse of a mixture of approximately equal doses of wild type and YeO3-*hfq*::Km bacteria. Subsequently, mice were killed two, five and nine days post-infection, the bacterial counts in different organs were performed, and the percentage of Km-resistant (Km^R) colonies was determined (Table 4). While the initial mixture contained 66% of Km^R bacteria, only 0-19% of Km^R bacteria were recovered from the Peyer's patches

444 of the infected mice. No Km^R bacteria were detected from the liver nor spleen samples. The
445 number of Km^R bacteria decreased over time, the average percentage decreased from 5.9%
446 on day 2 post-infection to 0.5% on day 9 post-infection (Table 4).

447 **Mouse virulence, i.g. single strain experiments.** Among the mice that were infected
448 i.g. with wild type, YeO3-*hfq*::Km, YeO3-*rovM-hfq*::Km and YeO3-*hfq*::Km/p*hfq* bacteria
449 individually using actual doses of ca. 10^9 CFU per mouse, a statistically significant
450 (p=0.0064) reduction in the number of YeO3-*hfq*::Km bacteria recovered from mice organs
451 five days post-infection was observed when compared to the wild type bacteria (Fig. 8 and
452 Table S8). The number of recovered bacteria was restored close to wild type levels with the
453 *trans*-complemented strain YeO3-*hfq*::Km/p*hfq*. The infection with the double mutant YeO3-
454 *rovM-hfq*::Km resembled that of the YeO3-*hfq*::Km mutant.

455 **Mouse virulence, i.p. single strain experiments.** To detect whether the infection
456 route played a role in the virulence of the *hfq* mutant, mice were also infected i.p. with wild
457 type, YeO3-*hfq*::Km and YeO3-*rovM-hfq*::Km bacteria with the actual doses of ca. 10^9 CFU
458 per mouse. In this case, the YeO3-*hfq*::Km and YeO3-*rovM-hfq*::Km bacteria both killed two
459 out of three mice within two days post-infection (Table S9), while all the wild type-infected
460 mice survived. There were no significant differences in the numbers of bacteria recovered
461 on day 5 post-infection from the different organs of the 5 day surviving mice infected with
462 wild type or YeO3-*hfq*::Km bacteria. Interestingly, the spleens of all these surviving i.p.
463 infected mice were almost 3-fold bigger that those of the i.g. infected mice (Table S10).

464 The very early death of the YeO3-*hfq*::Km and YeO3-*rovM-hfq*::Km but not the wild
465 type bacteria-infected mice suggested that it could be due to endotoxic shock caused by
466 LPS released from degrading bacteria. In immunoblotting analysis we did not find any
467 differences in the presence and amount of LPS on the surface of the bacterial cells (data

not shown). The altered cell morphology of the mutant bacteria could indicate cell wall defects, therefore, we determined the amount of LPS released into medium from the bacteria under vigorous shaking (Fig. S5). Dot-blotting demonstrated that 2-4 fold more LPS was released from the YeO3-*hfq*::Km and YeO3-*rovM-hfq*::Km bacteria when compared to wild type bacteria (Fig. S5, panel A). The endotoxin levels in the PBS supernatants measured by the Endosafe PTS system corroborated the dot-blotting (Fig. S5, panel B). The fragility of the mutant cell walls was further demonstrated by their increased susceptibility to SDS (Fig. S6). The endotoxicity of LPS depends on the lipid A acylation pattern such that penta- and hexa-acylated lipid A is far more endotoxic than tetra-acylated lipid A (Reines *et al.*, 2012, Trent *et al.*, 2006). As an immune-evasion strategy, to avoid endotoxicity, *Y. enterocolitica* deacylates its lipid A at 37°C by the activity of LpxR (Y11_05741) (Reines *et al.*, 2012). The transcriptomics revealed that the *lpxR* gene is 5-fold overexpressed at 37°C in the YeO3-*hfq*::Km bacteria (Table S2). Indeed, the structural analysis of the lipid A structure revealed differences between the wild type and hfq mutant bacteria grown at 37°C (Fig. S7). The results indicated that inactivation of the *hfq* gene actually increased the rate of deacylation of lipid A (i.e., reduced its endotoxicity), whereas the lipid A structure in the *hfq-rovM* double mutant was reversed to that of the wild type bacteria.

Discussion

In this study we combined two global approaches targeted at the identification of Hfq-dependent mRNAs (RNA-seq) and proteins (LC-MS/MS) to better understand the role of this RNA-chaperone in the physiology and virulence of *Y. enterocolitica* O:3. Here we show that several alterations typical for the *hfq*-negative phenotype were actually mediated by the overexpression of the transcriptional regulator RovM.

The role of Hfq in Yersinia species

Our results demonstrated that several hundred genes in *Y. enterocolitica* O:3 are either directly or indirectly regulated by Hfq. Similarly, high numbers of affected genes were identified for *hfq* mutants of *Salmonella enterica* and *Y. pestis* (Geng *et al.*, 2009, Sittka *et al.*, 2008). This indicates that Hfq plays an important role in gene regulation of *Y. enterocolitica* O:3. The data also showed that most of the differentially regulated genes were upregulated at 37°C. The results further showed that Hfq plays an important role for sugar metabolism, stress response, maintenance of outer membrane structure and for urease activity. The importance of Hfq as a post-transcriptional regulator was demonstrated by the fact that the abundance of numerous proteins was significantly altered even though no corresponding change was seen in transcriptomics (Tables S5 and S6). As many posttranscriptional and posttranslational mechanisms affect the protein abundances very seldom a 100% correlation between transcriptomics and proteomics is reached. Therefore we conclude that our results demonstrate the important role of Hfq as a post-transcriptional regulator.

In some cases a significant up- or down-regulation was only listed for one gene in an operon. Apparently, in some cases the stringent inclusion criteria had excluded some genes due to insufficient *p*-value (examples presented in Fig. S8). Thus, it is very likely that the total number of differentially expressed genes is an underestimate. However, it was previously shown that sRNAs can influence the regulation of operon transcription resulting in changes of the transcript length (Mellin *et al.*, 2014). Thus it is possible, that some of the operons showing discrepancies in the regulation of their genes are significant results that are affected by the loss of sRNA chaperone.

In other pathogenic *Yersinia* loss of Hfq has resulted in a growth defect. The YeO3-*hfq*::Km mutant presented similar growth pattern as the serotype O:8, showing an intermediate phenotype between marginally affected *Y. pseudotuberculosis* and notably

517 impaired *Y. pestis* (Geng *et al.*, 2009, Kakoschke *et al.*, 2014, Schiano *et al.*, 2010). We also
518 observed alterations in the bacterial metabolism such as utilization of mannitol visualized as
519 different growth phenotype on CIN agar and mannitol plates, similar to the phenotypes of *Y.*
520 *enterocolitica* O:8 *hfq* mutant (Kakoschke *et al.*, 2014). This phenotype was fully reverted in
521 the YeO3-*rovM-hfq*::Km double mutant bacteria. The comparison of proteomic studies
522 between the serotypes O:3 and O:8 showed an increase in abundance of several protein
523 chaperones and proteases indicating induction of the stress pathways. Moreover, both
524 serotypes showed alterations in iron and propanediol metabolism (Kakoschke *et al.*, 2014).
525 Both in *Y. enterocolitica* O:3 and in *Y. pestis*, loss of Hfq decreased the expression of
526 universal stress proteins, however, an opposite pattern was observed on heat shock protein
527 expression (Geng *et al.*, 2009). In coherence with the other *Yersinia* sp. (Geng *et al.*, 2009,
528 Kakoschke *et al.*, 2014, Schiano *et al.*, 2010), and some bacteria from other genera
529 (Guisbert *et al.*, 2007, Sittka *et al.*, 2007), we demonstrated that the Hfq of *Y. enterocolitica*
530 O:3 is involved in resistance to environmental stresses. Also, in line with Kakoschke *et al*.,
531 we observed repression of the urease genes (Fig. 7B and S6) that contributes to the reduced
532 resistance to acidic pH (Kakoschke *et al.*, 2014). Moreover, for the *Y. enterocolitica* serotype
533 O:8 an increase in abundance of three RovA-repressed proteins, i.e. OmpX, OppA and
534 TnaA, was reported, whereas in *Y. pestis* the expression of *rovA* was upregulated (Geng *et*
535 *al.*, 2009, Kakoschke *et al.*, 2014, Kakoschke *et al.*, 2016). However, our results showed
536 that unlike in serotype O:8, in serotype O:3 the loss of Hfq does not cause significant
537 changes in the structure of LPS O-antigen (Kakoschke *et al.*, 2016). Here, we showed that
538 in *Y. enterocolitica* O:3, in fact, Hfq together with RovM plays a role in *rovA* regulation. In all
539 pathogenic *Yersinia* species Hfq is crucial for virulence demonstrated by severe attenuation
540 of the *hfq* mutant in mouse infection experiments (Geng *et al.*, 2009, Lathem *et al.*, 2014,
541 Schiano *et al.*, 2010). In contrast to *Y. pseudotuberculosis* (Schiano *et al.*, 2010), lack of Hfq

in *Y. enterocolitica* O:3 caused impairment in bacterial motility and production of flagellin. Taken together, these results suggested that Hfq and its sRNA constellation exerts its gene regulation in a closely related manner between the two *Y. enterocolitica* serotypes, but has distinct dissimilarities between different *Yersinia* species.

Several* hfq *mutant phenotypes are indirect due to overexpression of RovM

Since the Hfq chaperone affects the global gene regulation it is assumed that some of the phenotypic features are indirect, due to alterations in the expression of different regulators. In this study, we observed alterations in expression of both the regulators and the genes belonging to their regulons. The proteomic and transcriptomic analyses revealed decreased expression of genes belonging to the RpoS regulon (Patten *et al.*, 2004), including the osmotically inducible protein OsmY, the cell division protein BolA, the HdeD protein, the superoxide dismutase [Cu-Zn] and the glutamate decarboxylase (Tables S2-S5). Analysis of the genes from the RovA regulon (Cathelyn *et al.*, 2007) showed decrease in the abundance of hemin transport protein HmuS and copper transport protein CutC, whereas strong upregulation was observed for the outer membrane porins like OmpX and OmpW, and for the genes of the glutamine metabolic pathway. Furthermore, even though OmpR is known to positively regulate the expression of urease in *Y. pseudotuberculosis* and thus enhance its survival in acid environment (Hu *et al.*, 2009), we observed here an adverse effect. In spite of upregulation of the *envZ* and *ompR* genes, the activity of urease was significantly decreased, suggesting that also other factors are involved in regulation of urease biosynthesis in *Y. enterocolitica* O:3. PhoB regulates the phosphate starvation response (Gao & Stock, 2015). The *phoB* gene was slightly repressed in the *hfq* mutant, and only one of the known PhoB targets (*pstS*) was affected and even that differently in proteomics and transcriptomics (Table S5).

In this study we also analyzed the effect of the RovM of overexpression in the Hfq-negative background. In the RNA-seq analysis we identified 55 genes that are under direct or indirect regulation of RovM (Table 3). In addition, comparison of YeO3/pMMB207-*rovM* and YeO3-*hfq*::Km transcriptomes showed a similar pattern of expression of RovM-dependent genes confirming that RovM overexpression was indeed responsible for the changes in expression of these genes in YeO3-*hfq*::Km bacteria. Importantly, both strains presented significantly decreased abundance of the *rovA* transcript, further suggesting that the expression of this gene in *Y. enterocolitica* is RovM-dependent and that its strong repression in the *hfq* mutant was due to elevated levels of RovM. The inactivation of the *rovM* gene in YeO3-*hfq*::Km strain allowed us to elucidate which of *hfq* phenotypes were mediated by RovM. This approach showed that the growth defect, colony morphology on CIN agar and motility were due to overexpression of RovM.

It is known that in *E. coli* several Hfq-dependent sRNA species regulate positively and negatively the *flhDC* genes that encode for the master regulator of motility (De Lay & Gottesman, 2012). In *Y. enterocolitica* the YenS sRNA was found to be a positive regulator of motility that acts through the modulation of YenI production. Moreover, the interplay between the levels of *yenI* and *yenS* led to either hypo- or hypermotility (Tsai & Winans, 2011). In our study, the *hfq* gene deletion caused a hypomotile phenotype, which was reversed by subsequent knock-out of *rovM*. Moreover, the single *rovM* mutant was hypermotile (data not shown). This allowed us to conclude that the motility defect of the *hfq* mutant was mediated by the overexpression of RovM that repressed the flagella biosynthesis. It is possible that similarly to LrhA of *E. coli*, RovM interacts directly with the *flhDC* promoter (Lehnen *et al.*, 2002). However, it is likely that the regulation of motility is more complex process that involves cooperation between many sRNA species and regulators and thus, the accumulation of RovM is not the sole factor affecting the motility in

591 the YeO3-*hfq*::Km strain. Furthermore, the defect of biofilm formation in YeO3-*hfq*::Km was
592 reversed in the double-mutant YeO3-*rovM-hfq*::Km. As flagella are important for biofilm
593 formation and contribute to both early attachment and maturation process (Reisner *et al.*,
594 2003, Kim *et al.*, 2008) it is likely that RovM affects the production of biofilm through
595 repressing the flagellation. Interestingly, the trans-complemented strain YeO3-*hfq*::Km/p*hfq*
596 formed more biofilm than wild type bacteria in MedECa and M9. It is possible that the
597 expression of *hfq* from the pTM100 plasmid resulted in higher than physiological abundance
598 of Hfq that eventually led to opposite alterations in regulation of biofilm production (Kim *et*
599 *al.*, 2008, Raczkowska *et al.*, 2011).

600 ***Influence of Hfq on* rovM *regulation***

601 In contrast to majority of the LysR-type regulators, but similar to *rovM* and *hexA*, the
602 YeO3 *rovM* was also under positive autoregulation. With RovM and HexA no direct binding
603 of the proteins to their respective promoter regions was detected (Harris *et al.*, 1998,
604 Heroven & Dersch, 2006). Indeed, most of the LysR-type regulators interact with coeffectors
605 - small molecules, mainly metabolites or intermediates of a biochemical pathway they
606 regulate (Schell, 1993). In addition, expression of *rovM* in *Y. pseudotuberculosis* is regulated
607 by the Csr system (Heroven *et al.*, 2008).

608 The Csr system in bacteria consists of CsrA protein and two non-coding RNAs, CsrB
609 and CsrC. CsrA is an RNA-binding protein that was shown to act as both positive and
610 negative regulator of target mRNAs (Wei *et al.*, 2001). The regulatory RNAs antagonize the
611 function of CsrA by binding to it and titrating it from the mRNA targets (Romeo, 1998,
612 Weilbacher *et al.*, 2003). It was previously shown, that in *Y. pseudotuberculosis* the CsrA
613 protein can induce the expression of RovM. Moreover, the non-coding CsrC RNA molecule
614 is considered to participate in the medium-dependent control of *rovM* expression (Heroven

615 *et al.*, 2008). In our study we observed downregulation of two non-coding RNAs showing
616 homology to *E. coli* CsrC and CsrB. Neither the transcriptomic nor the proteomic analyses
617 revealed any alterations in the abundance of the CsrA protein. Nevertheless, it is possible,
618 that decrease in abundance of regulatory Csr-RNAs resulted in reduction of CsrA
619 sequestration, therefore leading to an increase in the active (free) form of CsrA. Our results
620 show that the CsrA overexpression in YeO3 indeed increased the *rovM* transcription. The
621 similar abundance of the *rovM* and *rovA* transcripts in both the YeO3-*hfq*::Km and
622 YeO3/pMMB207-*csrA* bacteria (grown at RT) indicates that CsrA mediates the derepression
623 of the *rovM* gene in the *hfq* mutant. The CsrB and CsrC sRNAs do not depend on the Hfq
624 protein (Sittka *et al.*, 2008), but the alterations in their abundance might be a result of
625 changes in the bacterial metabolism. However, at 37°C the CsrA overexpression resulted in
626 only minor increase in the *rovM* transcript abundance indicating that other factors can also
627 influence the *rovM* transcription. Considering the high conservation of the Csr-system and
628 of the RovM sequences between *Yersinia* species, it is plausible that this regulatory network
629 is shared between these species. Although the importance of the *rovM* promoter region in
630 this regulation was shown, the study of Heroven *et al*. did not reveal the exact molecular
631 mechanism of the *rovM* gene activation indicating that the influence of CsrA is most probably
632 indirect and occurs through one or more transcriptional regulators (Heroven *et al.*, 2008).
633 Other work based on transcriptome analysis revealed that a quorum-sensing regulatory
634 protein EsaR could activate the expression of the *lrhA* gene of *Pantoea stewartii*
635 (Ramachandran *et al.*, 2014). Therefore, it is possible that the activation of the *rovM*
636 transcription is affected by additional regulator(s).

637 ***RpoS and resistance to environmental stresses.***

638 Optimal growth during the stationary phase and under unfavorable environmental
639 conditions requires the alternative sigma factor RpoS (Tanaka *et al.*, 1993, Badger & Miller,

1995) that in *E. coli* and *Salmonella* is Hfq-dependent explaining to some extent the decreased resistance to different environmental stresses (Muffler *et al.*, 1996, Brown & Elliott, 1996). In *E. coli* LrhA was demonstrated to repress the RpoS translation by a mechanism that requires Hfq by repressing a positive sRNA-regulator (Peterson *et al.*, 2006). The translation of *rpoS* transcript is repressed by an extensive secondary structure present in its 5' untranslated region that sequesters the Shine-Dalgarno site (Brown & Elliott, 1997). Four sRNAs are known to regulate the translation of *rpoS*, namely, DsrA, RprA and ArcZ that enhance the translation and OxyS, which negatively affects the RpoS synthesis (Majdalani *et al.*, 2002, Mandin & Gottesman, 2010, Sledjeski *et al.*, 1996, Zhang *et al.*, 1998). The positive regulation occurs through binding of the sRNA to the 5'-leader region of *rpoS* thereby opening up the inhibitory structure and provides the access for the ribosome to the Shine-Dalgarno site. The BSRD repository for bacterial small regulatory RNA (http://kwanlab.bio.cuhk.edu.hk/BSRD) identified two of these non-coding RNAs, RprA and ArcZ (SraH), from the genome of *Y. enterocolitica* O:3. The analysis of RNA-seq data revealed differential expression of RprA (Fig S2), while the expression of ArcZ could not be unquestionably detected. Moreover, all these sRNA species utilize Hfq as a chaperone for efficient regulation of the RpoS synthesis (Majdalani *et al.*, 2002, Mandin & Gottesman, 2010, Sledjeski *et al.*, 1996, Zhang *et al.*, 1998). The decreased amount of RpoS protein observed in all *hfq* mutants of *Y. enterocolitica* O:3 could thus be due to the inhibition of translation initiation. Our results showed that both *hfq* mutation and overexpression of *rovM* led to a decrease in the abundance of *rpoS* mRNA in *Y. enterocolitica* O:3 (Fig. 6 and Table 2 and 3), yet the subsequent knock-down of *rovM* gene in YeO3-*hfq*::Km did not restore the synthesis of RpoS (Fig. 6). Therefore, we conclude that in *Y. enterocolitica* O:3 overexpression of RovM represses the transcription of *rpoS*. However, as the knock-out of

rovM in the *hfq* mutant was not enough to restore the synthesis of RpoS it is assumed that Hfq is needed for efficient translation of the *rpoS* transcript.

Our results showed, that similarly to RovM in *Y. pseudotuberculosis* and *Y. enterocolitica O:8*, RovM represses the *rovA* gene in *Y. enterocolitica* O:3 (Heroven & Dersch, 2006, Lawrenz & Miller, 2007). In *Y. enterocolitica* serotype O:8 RovA controls the expression of *inv*, however, in serotype O:3 this regulation is prevented due to presence of an insertion sequence in the *inv* regulatory region (Uliczka *et al.*, 2011). It was shown that RovM in *Y. pseudotuberculosis* interacts specifically with certain DNA fragments, including a 30 bp regulatory region upstream of the *rovA* gene presumably leading to structural alterations of this region and resulting in prevention of transcription (Heroven & Dersch, 2006).

We also showed that the YeO3-*hfq*::Km strain was more sensitive to heat, acid and oxidative stress in line with observations made with other bacterial species [reviewed in (Chao & Vogel, 2010)]. Hfq-mediated adaptation to stress conditions is common in bacteria (Robertson & Roop, 1999, Torres-Quesada *et al.*, 2014) and it is generally associated with increased abundance of Hfq-dependent RNAs (Moller *et al.*, 2014). It is likely that some stress phenotypes of YeO3-*hfq*::Km are due to changes in the RpoS levels. In *Y. enterocolitica* O:8 lack of RpoS caused sensitivity to oxidative stress, high osmolarity, low pH and starvation but did not affect the production of the virulence factors like Invasin, Ail, YadA and Yops (Badger & Miller, 1995, Iriarte *et al.*, 1995).

The role of Hfq in virulence

The YeO3-*hfq*::Km bacteria were significantly attenuated in i.g. infected mice, in line with *hfq* mutants of *Y. pestis* and *Y. pseudotuberculosis* (Geng *et al.*, 2009, Schiano *et al.*, 2010) and of other bacterial pathogens [reviewed in (Chao & Vogel, 2010, Michaux *et al.*,

688 2014, Zeng *et al.*, 2013)]. The *hfq* mutant could be partially complemented *in trans.* This
689 may be due to loss of the complementing plasmid during the *in vivo* infection, as the
690 experiment was conducted without any addition of antibiotics.

691 Interestingly, the YeO3-*hfq*::Km mutant bacteria were recovered from the organs of the
692 one surviving mouse on day 5 post-infection in comparable numbers to the wild type bacteria
693 (Table S9). Thus, one can speculate that the Hfq-dependent virulence properties appeared
694 to play most important role during the oral infection route. Indeed, in order to pass through
695 the stomach during the course of infection, *Y. enterocolitica* must be able to survive in low
696 pH environment. Unlike in other acid-tolerant bacteria, the mechanism of acid tolerance in
697 *Yersinia* is not multifactorial and depends mainly on the production of urease (De Koning-
698 Ward & Robins-Browne, 1995, Gripenberg-Lerche *et al.*, 2000). Missing of the urease
699 activity, considered as an important virulence factor in the murine model (Gripenberg-Lerche
700 *et al.*, 2000), is likely to attenuate YeO3-*hfq*::Km when the oral route of infection is used.
701 However, as the inactivation of the *hfq* gene caused wide and pleiotropic changes in the
702 bacterial physiology it is highly likely that also other factors are responsible for the
703 attenuation observed in the YeO3-*hfq*::Km strain.

704 The early deaths of the i.p. YeO3-*hfq*::Km but not of the wild type-infected mice was
705 intriguing and raised the speculation that this could be due to endotoxic shock. This
706 speculation is supported by the decreased SDS-resistance of the YeO3-*hfq*::Km bacteria
707 (Fig. S6) and increased release of endotoxin to culture supernatant (Fig. S5). These findings
708 as well as the significant alterations in the abundance of membrane proteins indicated that
709 the outer membrane of YeO3-*hfq*::Km bacteria might be compromised. This is in line with
710 the previously established importance of Hfq- and sRNA-mediated control of the outer
711 membrane biogenesis (Guillier *et al.*, 2006, Van Puyvelde *et al.*, 2013). Finally, we also
712 observed a small but potentially important Hfq-dependent change in the lipid A structure of

YeO3-*hfq*::Km bacteria (Fig. S7) indicating that the characteristic detoxification of LPS due to the LpxR activity was increased in this strain. This indicates lower endotoxicity of LPS produced by the *hfq* mutant and thus it would not explain the early deaths of the infected mice. However, it is worth noticing that this alteration was fully reversed by the inactivation of the *rovM* gene, showing that RovM is the factor that mediates the changes in the lipid A structure in the *hfq* mutant strain. This is in agreement with the previous findings showing that RovA is a negative regulator of *lpxR*, and therefore the RovM overexpression would cause decrease in RovA levels and subsequent increase in the abundance of LpxR (Reines *et al.*, 2012). Taken all this together, we conclude that the death observed in mice infected intraperitoneally with the YeO3-*hfq*::Km or YeO3-*rovM-hfq*::Km bacteria occurred due to the endotoxic shock caused by the increased release of the LPS from the mutant bacterial cells and not by changes in the toxicity of the LPS itself.

Taken together, the loss of Hfq protein led to significant attenuation of *Y. enterocolitica* O:3 in orally infected mouse model, most probably due to difficulties in passing through the acidic stomach and the reduced resistance to detergent action. On the other hand, the YeO3-*hfq*::Km bacteria survived as well as the wild type bacteria during i.p. infection.

Hfq/RovM regulation model

The results of the present work as discussed above led us to propose a model (Fig. 9) that illustrates the roles of Hfq and RovM in determining the phenotype of the *hfq* mutant of *Y. enterocolitica* O:3. In summary, we investigated a range of Hfq- and RovM-dependent processes in *Y. enterocolitica* and provided evidence that many alterations in gene expression observed in the *hfq* mutant were due to overexpression of RovM. Derepression of RovM caused upregulation of OmpX, LpxR, and PTS system (glucitol/sorbitol) genes, as well as downregulation of RovA, OsmY and urease alpha- and beta-subunits. The knockout

of the *hfq* gene itself resulted in alterations in expression of membrane proteins (OmpC, OmpF, OmpW, Cpx pathway), urease accessory proteins (UreD, UreE, UreF, UreG), carbohydrate metabolism genes (numerous genes of PTS systems), and different transcriptional regulators (OmpR, PhoB). Interestingly, both lack of Hfq and overexpression of RovM caused downregulation of RpoS, but the knockout of *rovM* in the *hfq* mutant could not restore the production of this sigma factor, suggesting that both Hfq and RovM are involved in the regulation of RpoS synthesis in an independent way. Our result showed that CsrA mediates the derepression of the *rovM* gene in the Hfq negative background, however, other factors are likely to be also involved.

The alterations of gene expression in the *hfq* and *rovM* mutants were reflected in the phenotypes. The RovM overexpression in the *hfq* mutant was responsible for changes in motility and biofilm formation, lipid A structure, mannitol utilization, and up to some extent also for the growth rate. In addition, we showed that many alterations observed in the *hfq* mutant of *Y. enterocolitica* O:3 were independent from the *rovM* gene derepression. This included the cell shape, stress-sensitivity and attenuation of virulence. These phenotypes are perhaps caused indirectly by other Hfq-dependent regulators or directly by the Hfq and Hfq-dependent regulatory sRNAs.

Experimental Procedures

Bacterial strains and plasmids and growth conditions. The bacterial strains and plasmids are listed in Table 5. Bacteria were grown aerobically in lysogeny broth (LB) (Bertani, 2004), in brain heart infusion (BHI) medium (Fluka) or on *Yersinia* selective agar supplemented with cefsulodin, irgasan and novobiocin (CIN-agar, Oxoid, UK) at either 37°C or RT. LB agar plates were prepared by adding 15 g of bacto agar to 1 L of LB. For electron microscopy, flagellin production and motility evaluation bacteria were grown in tryptone broth

761 (TB) (1% tryptone, 0.5% NaCl) and on tryptone agar plates (1% tryptone, 0.5% NaCl, 0.3%
762 bacto agar). For biofilm experiments the MedECa and M9 minimal media were used (Miller,
763 1972, Skurnik, 1985). Antibiotics were used when needed at the following concentrations:
764 kanamycin (Km) 100 µg ml^{-1}, streptomycin (Str) 50 µg ml^{-1}, chloramphenicol (Clm) 100 µg
765 ml^{-1}, ampicillin (Amp) 50 µg ml^{-1}. Expression of the *rovM* gene from plasmid pMMB207-*rovM*
766 was induced with 1 mM isopropyl-β-D-thiogalactopyranoside (IPTG).

767 **Construction of bacterial strains.** Allelic exchange was used to generate the *hfq*
768 knock-out mutant (Fig. S1A). The *hfq* gene with its flanking regions was amplified by the
769 PCR reaction using the BglII-flanked primers hfq-F1 and hfq-R1 (Table S11) and the
770 amplified 1367 bp fragment was introduced to BamHI-digested pUC18 (Yanisch-Perron *et*
771 *al.*, 1985). Subsequently, the created ca. 4 kb pUC18-*hfq* plasmid was used as a template
772 in plasmid PCR to delete the *hfq* gene. The primers hfq-F2 and hfq-R2 (Table S11) amplified
773 a ca. 3.65 kb fragment leaving only the *hfq* gene flanking regions to the fragment; the whole
774 *hfq* gene within the 365 bp sequence was deleted. The kanamycin resistance cassette (Km),
775 amplified as a 1156 bp fragment from pUC-4K using the Km-GB66-f and Km-GB66-r primers
776 (Table S11), was ligated with the 3.65 kb pUC18-*hfq* PCR product. The generated ca. 4.8
777 kb pUC18-*hfq*::Km plasmid served as a template for PCR with primers hfq-F1 and hfq-R1 to
778 amplify the 2158 bp DNA-fragment containing the *hfq* flanking regions and the Km cassette.
779 The fragment was cloned into pKNG101 (Kaniga *et al.*, 1991). The obtained suicide
780 construct pKNG101-*hfq::Km* was subsequently mobilized from *E. coli* strain ω7249 into the
781 wild type *Y. enterocolitica* serotype O:3 strain 6471/76. The suicide plasmid integrated via
782 homologous recombination into the host genome and generated a merodiploid strain.
783 Subsequent second site homologous recombination replaced the *hfq* gene by allelic
784 exchange. Sucrose selection was used to screen for the double recombinants that had
785 eliminated the pKNG101 plasmid carrying the *sacB* gene. The obtained strain was named

as YeO3-*hfq*::Km. The deletion of the *hfq* gene was validated with the PCR reaction using the hfq-F1 and hfq-F2 primers. The wild type strain generated the 1367 bp product and replacement of the *hfq* gene by the Km-cassette increased the size to 2158 bp. The mutation was also verified by the RNA-seq data.

The *rovM* knock-out mutants were generated by insertion mutagenesis using a single site homologous recombination approach (Fig. S1B). In brief, internal 437 bp fragment of the *rovM* coding sequence was PCR amplified using BamHI-site-containing primers M-rovM-F and M-rovM-R (Table S1). The BamHI-digested PCR product was ligated to BamHI-digested and SAP-treated suicide vector pKNG101. The obtained suicide construct pKNG101-*rovM* was subsequently mobilized into strains 6471/76 and YeO3-*hfq*::Km to generate single and double mutant strains YeO3-*rovM* and YeO3-*rovM*-*hfq*::Km. The correct integration of pKNG101-*rovM* into the genomes of YeO3-*hfq*::Km and 6471/76 was verified by PCR.

Construction of plasmids. To complement *in trans* the *hfq* mutant a plasmid carrying the wild type *hfq* gene was constructed (Fig. S9C). The full *hfq* gene with its own promoter region was amplified by PCR using the BglII-flanked primers hfq-F1 and hfq-F2 (Table S11) and the obtained 1367 bp fragment was ligated into BamHI-digested and SAP-treated mobilizable vector pTM100 to obtain the plasmid p*hfq*. The correct insertion of the fragment was verified by PCR. Subsequently, the plasmid was introduced to the YeO3-*hfq::*Km strain by mobilization generating the *in trans* -complemented strain YeO3-*hfq*::Km/p*hfq*.

To construct a plasmid carrying the wild type *rovM* gene for overexpression experiments the full-length *rovM* gene was amplified by PCR using primers G-rovM-F and G-rovM-R (Table S11) and the obtained fragment was ligated into EcoRI-digested and SAP-treated expression vector pMMB207 (Fig. S9C). The correct orientation of the *rovM* gene in

the obtained plasmid pMMB207-*rovM* was verified by PCR. Subsequently, the plasmid was introduced to 6471/76 strain by mobilization to obtain strain YeO3/pMMB207-*rovM*.

The full-length *csrA* gene of 6471/76 was amplified with Phusion DNA polymerase using primers csrA-F1 and csrA-R1 (Table S1). The obtained fragment was digested with BamHI and EcoRI and ligated into BamHI and EcoRI digested, SAP-treated pMMB207. The ligation mixture was electroporated into *E. coli* strain ω7249 cells. The resulting construct (pMMB207-*csrA*) was verified by restriction digestion and by sequencing with the csrA-R1 and pMMB207 specific primers. The constructed plasmid was then mobilized into the 6471/76, YeO3-*hfq*::Km and YeO3/ pLux232oT-*rovM* bacteria by diparental conjugation as described earlier (Biedzka-Sarek *et al.*, 2005) (Fig. S9D). The construction of *csrA* mutants was attempted as shown in Fig. S9E.

Promoter reporter constructs. The promoter region of the *rovM* gene was amplified by PCR using the primers with flanking restriction sites (Table S11). The PCR fragments were digested with BamHI, and ligated into similarly digested and SAP-treated reporter vector pLux232oT (Leskinen *et al.*, 2015a). Ligation products were introduced to *E. coli* S17-1λpir (Simon *et al.*, 1983). The correct introduction of the insert was confirmed by PCR. Through conjugation the promoter reporter vector was subsequently introduced to the wild type, YeO3-*rovM*, and YeO3/pMMB207-*rovM* strains.

Growth curves. Overnight cultures were diluted in fresh medium to an OD_{600} of 0.2 and 200 µl aliquots were distributed into honeycomb plate wells (Growth Curves Ab Ltd). The growth experiments were carried out at 4°, 22°, 37° and 42°C using the Bioscreen C incubator (Growth Curves Ab Ltd) with continuous shaking. The OD_{600} values were measured at every 10 or 15 min. The averages were calculated from values obtained for the bacteria grown in 9 parallel wells.

SDS-PAGE and immunoblotting. Proteins were separated using 5% stacking and 12% separating sodium dodecyl sulfate polyacrylamide gel electrophoresis (SDS-PAGE). After the run the material was either visualized by silver staining (Mortz *et al.*, 2001) or transferred onto nitrocellulose membrane (Protran, Whatman, pore size 0.45 µm). Transfer of the proteins from the SDS-PAGE gel onto the membrane was done using the semi-dry apparatus (Thermo Scientific Owl, USA). Subsequently, the membrane was blocked using 5% skimmed milk in TBST buffer (50 mM Tris-HCl, 150 mM NaCl, 0.05% Tween 20, pH7.6) for 1 h at RT. The membrane with primary antibodies diluted in blocking buffer was incubated for 16h at 4°C with gentle shaking. After washing 3 times with TBST, the membrane was incubated with suitable peroxidase-conjugated secondary antibodies (Dako Cytomation, Denmark; dilution 1:2000 in blocking buffer) for 1h at RT. Subsequently membrane was washed in TBST as before and drained in ECL solution (0.1M Tris-HCl pH 8.5, 1.25 mM luminol, 0.2 mM coumaric acid, 5.3 mM hydrogen peroxide) and exposed to light sensitive film (Kodak, USA).

Antibodies and antisera. The mouse flagellin-specific monoclonal antibody (mAb) 15D8 (Feng *et al.*, 1990) and rabbit anti-RpoS antiserum (Coynault *et al.*, 1996), as well as a peroxidase-conjugated secondary anti-mouse and anti-rabbit immunoglobulin antibodies (P0447and P0217, Dako Cytomation, Denmark) were used for protein visualization.

Total RNA extraction. The total RNA of bacteria grown at RT or 37°C was isolated using the SV Total RNA Isolation System (Promega). The quality of the isolated RNA, as well as the rRNA profile was determined using Bioanalyzer (Agilent). For each strain and growth condition two biological replicates were included.

RNA-seq. The RNA-seq and data analysis were performed at the FIMM Technology Centre Sequencing Unit (http://www.fimm.fi/en/technologycentre/). Sequencing was

performed for strains YeO3, YeO3-*hfq*::Km, YeO3-*rovM*, and YeO3-*rovM*/pMMB207-*rovM*. The ribosomal RNA was removed using Ribo-ZeroTM rRNA Removal Kit for Gram-negative Bacteria (Epicentre). Paired-end sequencing was performed on Illumina HISeq2000 sequencer (Illumina) with the read length of 90 nucleotides. The obtained sequencing reads were filtered for quality and aligned against the *Y. enterocolitica* strain Y11 genome (accession number FR729477) using the TopHat read aligner (Langmead *et al.*, 2009). The Cufflinks program (Trapnell *et al.*, 2013) was then used to obtain the fragments per kilobase of gene per million aligned fragments (FPKM) values for differential expression. The genes were considered differentially expressed if the fold change (FC) of the average values was >2, and the Student's T-test p-value was <0.01. The frequencies of mutant to wild type ratios followed the normal distribution indicating the accuracy of the assay. The RNA sequence data has been deposited to Gene Expression Omnibus (Acc. no GSE66516).

Quantitative RT-PCR. Overnight cultures of *Y. enterocolitica* strains were diluted to OD_{600} = 0.1 and grown at 22 or 37°C to an OD_{600}=0.6 in LB. The bacterial total RNA was isolated as described above. The extracted total RNA was diluted to the final concentration of 25 ng μl^{-1}. The quantitative RT-PCR was performed using the GoTaq 1-step RT-qPCR System (Promega) and the primers listed in Table S11. All the experiments were performed in triplicates. Relative quantification was used to compare the amount of a target nucleic acid present in the samples. The ratio between the reference and the test sample was calculated as follows: Ratio (reference/target) = $2^{Cq(ref) - Cq(target)}$. Each result is presented as the mean value of 3 independent results with their standard deviation.

Quantitative proteomics. Bacteria were grown overnight at RT in 3 ml of LB. Cultures were diluted 1:10 in fresh LB and incubated at either RT or 37°C for another 4h. Afterwards, the cells were harvested by centrifugation at 3000 g, washed with sterile PBS and adjusted to 2.5 x 10^8 cfu ml^{-1}. Subsequently 1 ml of each culture was pelleted, resuspended in lysis

buffer (100 mM ammoniumbicarbonate, 8M urea, 0.1% RapiGest^{TM}), sonicated for 3 min (Branson Sonifier 450, pulsed mode 30%, loading level 2) and stored at -70°C. Each sample was prepared in 3 parallels. Prior to digestion of proteins to peptides with trypsin, the proteins in the samples were reduced with TCEP and alkylated with iodoacetamide. Tryptic peptide digests were purified by C18 reversed-phase chromatography columns [15] and the MS analysis was performed on an Orbitrap Elite ETD mass spectrometer (Thermo Scientific), using Xcalibur version 2.7.1, coupled to an Thermo Scientific nLCII nanoflow HPLC system. Peak extraction and subsequent protein identification was achieved using Proteome Discoverer software (Thermo Scientific). Calibrated peak files were searched against the *Y. enterocolitica* O:3 proteins (Uniprot) by a SEQUEST search engine. Error tolerances on the precursor and fragment ions were ±15 ppm. and ±0.6 Da, respectively. For peptide identification, a stringent cut-off (0.5% false discovery rate) was used. For label-free quantification, spectral counts for each protein in each sample were extracted and used in relative quantitation of protein abundance changes.

Thermotolerance assay. Thermotolerance was tested as described earlier (Leskinen *et al.*, 2015b). Bacterial overnight cultures were diluted to obtain ca. 1,000 bacterial cells in 10 µl and transferred to a thermoblock heated to 55ºC. Serial 10-fold dilutions were prepared at start point and after 5 min. The number of viable bacteria was determined by plating 50 µl of the dilutions on LB plates.

Acid tolerance. Acid tolerance was tested as described earlier (Leskinen *et al.*, 2015b). Bacterial overnight cultures were diluted in PBS pH 2.0 supplemented with 1.4 mM urea to obtain ca. 1,000 bacterial cells in 10 µl. Bacteria were incubated at 37°C for 20 min and subsequently 10-fold dilutions were prepared and plated on LB plates to determine the number of bacteria.

907 **Urease test**. The production of urease was verified in urea broth (0.1% peptone, 0.1%
908 glucose, 0.5% NaCl, 0.2% KH_2PO_4, 0.00012% phenol red, 2% urea) (Stuart et al., 1945).
909 The broth was inoculated with the overnight cultures and incubated at RT or 37°C with
910 shaking. The test result was considered positive if the medium changed the color from
911 orange to red and negative if the final color was yellow. The absorbance of the medium was
912 measured at 565 nm.

913 **Motility assay.** Bacteria were grown overnight in 5 ml of tryptone broth at RT with
914 gentle shaking. Subsequently, 5 µl of each culture was applied in the middle of the tryptone
915 motility plates (1% tryptone, 0.5% NaCl and 0.35% agar) and incubated for 24h at RT.
916 Images of the plates were taken using GelLogic 200 Imaging System (Kodac) and the radius
917 of the bacterial growth was measured.

918 **Biofilm assay.** Biofilm formation was tested as described earlier (Blumer *et al.*, 2005)
919 with modifications. Overnight cultures in TB, M9 or MedECa were diluted 1:10 into the same
920 medium and 200 µl aliquots were transferred to the wells of 96-well polystyrene microtiter
921 plate (Nunc). After 72h of incubation at RT the wells were emptied, washed three times with
922 sterile phosphate-buffered saline (PBS; pH 7.2) and drained in an inverted position. To fix
923 the biofilm, wells were washed with 200 µl of methanol and left overnight to dry. Adhered
924 cells were stained by incubation with 200 µl of 0.1 crystal violet solution for 15 min. Non-
925 bound dye was removed by rinsing three times with distilled water. Wells were subsequently
926 filled with 200 µl of 96% ethanol and incubated 30 min at RT to solubilize the crystal violet.
927 Finally the absorbance of the dye was measured at 560 nm using the Labsystems iEMS
928 Reader MF.

929 **Electron microscopy.** Overnight grown bacteria were collected from tryptone motility
930 plates, washed with sterile PBS (pH 7.2) and resuspended in 0.1 M ammonium acetate.

Cells were allowed to sediment on carbon coated grids for 1 min. Subsequently, the samples were stained negatively using 1% uranyl acetate and examined with JEOL JEM1400 transmission electron microscope. Pictures were taken using the Olympus Morada CCD camera with the iTEM software. Average bacterial cell length was calculated based on the size of 50 random cells of certain strain.

Mouse experiments. Animal experiments were performed under the permit (no ESAVI/5893/04.10.03/2012) from the Animal Experiment Board in Finland. The 35 inbred female 6-8 week old BALB/c mice were purchased from Envigo (Blackthorn, UK). The mice were allowed to adjust to the housing conditions for 1 week after receipt from the breeder.

Bacteria were prepared as described earlier (Skurnik *et al.*, 1999) with modifications. Briefly, bacteria for the animal experiment were grown overnight in 100 ml of LB supplemented with appropriate antibiotics under aeration at RT. The bacteria were pelleted and resuspended in 10 ml of sterile PBS, pH 7.4. Three 1 ml portions were centrifuged down and after removal of the supernatant the mean bacterial mass was determined. Based on assumption that 100 mg (300 mg for YeO3-*hfq*::Km bacteria) of wet pellet contains about 10^{11} bacterial cells, the initial bacterial suspension was adjusted to 10^{10} or 10^{8} bacteria per ml. For the coinfection experiments the suspensions of wild type and YeO3-*hfq*::Km bacteria were mixed at the ratio of 1:1 and samples from subsequent 10-fold dilutions were plated in order to determine exact bacterial counts.

Mice were kept without solid food for 4-h before bacterial challenge. The bacterial suspension (100 µl for the single infection and a total of 200 µl for the co-infection model) was administered i.g. to the mice using a 20 gauge stainless-steel ball-tipped catheter, or i.p. using a 25G needle. After mice were killed, the Peyer's patches, spleen, and liver were aseptically removed, weighted and homogenized using the Ultra-Turrax T8 homogenizer

(IKA Labortechnik, Staufen, Germany) into 0.5, 0.5 and 1 ml of PBS, respectively. The number of *Y. enterocolitica* was determined by plating serially diluted samples on CIN agar plates without antibiotics. The limit of detection in this study was approximately 3000 CFU g^{-1} for spleen, 500 CFU g^{-1} for liver, and 7000 CFU g^{-1} for Peyer's patches. Subsequently, for the co-infection experiments the ratio of wild type to YeO3-*hfq*::Km colonies was determined by patching the colonies on CIN agar plates supplemented with kanamycin. In our earlier studies we have not seen any indications that the introduction of the kanamycin resistance GenBlock by allelic exchange into the bacterial genome would impact the fitness of the bacteria (Tamm *et al.*, 1993).

Acknowledgments

KL was supported by the Doctoral Programme in Biomedicine (DPBM) of University of Helsinki and Emil Aaltonen Foundation. MV was supported by the Sigrid Juselius Foundation and Biocenter Finland. Anu Wicklund is thanked for assistance with EM. Juha Laitinen is thanked for excellent technical assistance. The anti-flagellin mAb 15D8 and anti-RpoS antiserum were kind gifts from Scott Minnich and Francoise Norel, respectively. Work in MS laboratory was supported by the Academy of Finland grant (288701). Work in JAB laboratory was supported by Marie Curie Career Integration Grant U-KARE (PCIG13-GA-2013-618162) and Queen's University Belfast start-up funds. The authors confirm that there is no conflict of interest.

References

Babic, A., A.M. Guerout & D. Mazel, (2008) Construction of an improved RP4 (RK2)-based conjugative system. *Research in microbiology* **159**: 545-549.

Badger, J.L. & V.L. Miller, (1995) Role of RpoS in survival of *Yersinia enterocolitica* to a variety of environmental stresses. *Journal of bacteriology* **177**: 5370-5373.

Baker, C.S., L.A. Eory, H. Yakhnin, J. Mercante, T. Romeo & P. Babitzke, (2007) CsrA inhibits translation initiation of *Escherichia coli hfq* by binding to a single site overlapping the Shine-Dalgarno sequence. *Journal of bacteriology* **189**: 5472-5481.

Beauregard, A., E.A. Smith, B.L. Petrone, N. Singh, C. Karch, K.A. McDonough & J.T. Wade, (2013) Identification and characterization of small RNAs in *Yersinia pestis*. *RNA biology* **10**: 397-405.

Bellows, L.E., B.J. Koestler, S.M. Karaba, C.M. Waters & W.W. Lathem, (2012) Hfq-dependent, co-ordinate control of cyclic diguanylate synthesis and catabolism in the plague pathogen *Yersinia pestis*. *Molecular microbiology* **86**: 661-674.

Bertani, G., (2004) Lysogeny at mid-twentieth century: P1, P2, and other experimental systems. *Journal of bacteriology* **186**: 595-600.

Biedzka-Sarek, M., R. Venho & M. Skurnik, (2005) Role of YadA, Ail, and Lipopolysaccharide in Serum Resistance of *Yersinia enterocolitica* Serotype O:3. *Infection and immunity* **73**: 2232-2244.

Bilusic, I., N. Popitsch, P. Rescheneder, R. Schroeder & M. Lybecker, (2014) Revisiting the coding potential of the *E. coli* genome through Hfq co-immunoprecipitation. *RNA biology* **11**: 641-654.

Blumer, C., A. Kleefeld, D. Lehnen, M. Heintz, U. Dobrindt, G. Nagy, K. Michaelis, L. Emody, T. Polen, R. Rachel, V.F. Wendisch & G. Unden, (2005) Regulation of type 1 fimbriae synthesis and biofilm formation by the transcriptional regulator LrhA of *Escherichia coli*. *Microbiology* **151**: 3287-3298.

Brown, L. & T. Elliott, (1996) Efficient translation of the RpoS sigma factor in *Salmonella typhimurium* requires host factor I, an RNA-binding protein encoded by the *hfq* gene. *Journal of bacteriology* **178**: 3763-3770.

Brown, L. & T. Elliott, (1997) Mutations that increase expression of the *rpoS* gene and decrease its dependence on *hfq* function in *Salmonella typhimurium*. *Journal of bacteriology* **179**: 656-662.

Bucker, R., A.K. Heroven, J. Becker, P. Dersch & C. Wittmann, (2014) The pyruvate-tricarboxylic acid cycle node: a focal point of virulence control in the enteric pathogen *Yersinia pseudotuberculosis*. *The Journal of biological chemistry* **289**: 30114-30132.

Castillo, A. & S. Reverchon, (1997) Characterization of the *pecT* control region from *Erwinia chrysanthemi* 3937. *Journal of bacteriology* **179**: 4909-4918.

Cathelyn, J.S., S.D. Crosby, W.W. Lathem, W.E. Goldman & V.L. Miller, (2006) RovA, a global regulator of *Yersinia pestis*, specifically required for bubonic plague. *Proceedings of the National Academy of Sciences of the United States of America* **103**: 13514-13519.

Cathelyn, J.S., D.W. Ellison, S.J. Hinchliffe, B.W. Wren & V.L. Miller, (2007) The RovA regulons of *Yersinia enterocolitica* and *Yersinia pestis* are distinct: evidence that many RovA-regulated genes were acquired more recently than the core genome. *Molecular microbiology* **66**: 189-205.

Chao, Y., K. Papenfort, R. Reinhardt, C.M. Sharma & J. Vogel, (2012) An atlas of Hfq-bound transcripts reveals 3' UTRs as a genomic reservoir of regulatory small RNAs. *EMBO Journal* **31**: 4005-4019.

Chao, Y. & J. Vogel, (2010) The role of Hfq in bacterial pathogens. *Current opinion in microbiology* **13**: 24-33.

Collins, H.L., S.H. Kaufmann & U.E. Schaible, (2002) Iron chelation via deferoxamine exacerbates experimental salmonellosis via inhibition of the nicotinamide adenine dinucleotide phosphate oxidase-dependent respiratory burst. *Journal Immunology* **168**: 3458-3463.

Coynault, C., V. Robbe-Saule & F. Norel, (1996) Virulence and vaccine potential of *Salmonella typhimurium* mutants deficient in the expression of the RpoS (sigma S) regulon. *Molecular microbiology* **22**: 149-160.

De Koning-Ward, T.F. & R.M. Robins-Browne, (1995) Contribution of urease to acid tolerance in *Yersinia enterocolitica*. *Infection and immunity* **63**: 3790-3795.

De Lay, N. & S. Gottesman, (2012) A complex network of small non-coding RNAs regulate motility in Escherichia coli. *Molecular microbiology* **86**: 524-538.

Dorel, C., P. Lejeune & A. Rodrigue, (2006) The Cpx system of *Escherichia coli*, a strategic signaling pathway for confronting adverse conditions and for settling biofilm communities? *Research in microbiology* **157**: 306-314.

Durand, S. & G. Storz, (2010) Reprogramming of anaerobic metabolism by the FnrS small RNA. *Molecular microbiology* **75**: 1215-1231.

EFSA, (2014) The European Union summary report on trends and sources of zoonoses, zoonotic agents and food-borne outbreaks in 2013. *European Food Safety Authority*.

Feng, P., R.J. Sugasawara & A. Schantz, (1990) Identification of a common enterobacterial flagellin epitope with a monoclonal antibody. *Journal of general microbiology* **136**: 337-342.

Gao, R. & A.M. Stock, (2015) Temporal hierarchy of gene expression mediated by transcription factor binding affinity and activation dynamics. *mBio* **6**: e00686-00615.

Geng, J., Y. Song, L. Yang, Y. Feng, Y. Qiu, G. Li, J. Guo, Y. Bi, Y. Qu, W. Wang, X. Wang, Z. Guo, R. Yang & Y. Han, (2009) Involvement of the post-transcriptional regulator Hfq in *Yersinia pestis* virulence. *PloS one* **4**: e6213.

Gibson, K.E. & T.J. Silhavy, (1999) The LysR homolog LrhA promotes RpoS degradation by modulating activity of the response regulator *sprE*. *Journal of bacteriology* **181**: 563-571.

Gripenberg-Lerche, C., L. Zhang, P. Ahtonen, P. Toivanen & M. Skurnik, (2000) Construction of urease-negative mutants of *Yersinia enterocolitica* serotypes O:3 and O:8: role of urease in virulence and arthritogenicity. *Infection and immunity* **68**: 942-947.

Guillier, M., S. Gottesman & G. Storz, (2006) Modulating the outer membrane with small RNAs. *Genes Dev* **20**: 2338-2348.

Guisbert, E., V.A. Rhodius, N. Ahuja, E. Witkin & C.A. Gross, (2007) Hfq modulates the sigmaE-mediated envelope stress response and the sigma32-mediated cytoplasmic stress response in *Escherichia coli*. *Journal of bacteriology* **189**: 1963-1973.

Harris, S.J., Y.L. Shih, S.D. Bentley & G.P. Salmond, (1998) The hexA gene of *Erwinia carotovora* encodes a LysR homologue and regulates motility and the expression of multiple virulence determinants. *Molecular microbiology* **28**: 705-717.

Hayashi-Nishino, M., A. Fukushima & K. Nishino, (2012) Impact of *hfq* on the intrinsic drug resistance of *Salmonella enterica* serovar *typhimurium*. *Frontiers in microbiology* **3**: 205.

Heroven, A.K., K. Bohme & P. Dersch, (2012) The Csr/Rsm system of *Yersinia* and related pathogens: a post-transcriptional strategy for managing virulence. *RNA biology* **9**: 379-391.

Heroven, A.K., K. Bohme, M. Rohde & P. Dersch, (2008) A Csr-type regulatory system, including small non-coding RNAs, regulates the global virulence regulator RovA of *Yersinia pseudotuberculosis* through RovM. *Molecular microbiology* **68**: 1179-1195.

Heroven, A.K. & P. Dersch, (2006) RovM, a novel LysR-type regulator of the virulence activator gene rovA, controls cell invasion, virulence and motility of *Yersinia pseudotuberculosis*. *Molecular microbiology* **62**: 1469-1483.

Hu, Y., P. Lu, Y. Wang, L. Ding, S. Atkinson & S. Chen, (2009) OmpR positively regulates urease expression to enhance acid survival of *Yersinia pseudotuberculosis*. *Microbiology* **155**: 2522-2531.

Huovinen, E., L.M. Sihvonen, M.J. Virtanen, K. Haukka, A. Siitonen & M. Kuusi, (2010) Symptoms and sources of Yersinia enterocolitica-infection: a case-control study. *BMC infectious diseases* **10**: 122.

Iriarte, M., I. Stainier & G.R. Cornelis, (1995) The rpoS gene from *Yersinia enterocolitica* and its influence on expression of virulence factors. *Infection and immunity* **63**: 1840-1847.

Kakoschke, T., S. Kakoschke, G. Magistro, S. Schubert, M. Borath, J. Heesemann & O. Rossier, (2014) The RNA chaperone Hfq impacts growth, metabolism and production of virulence factors in Yersinia enterocolitica. *PloS one* **9**: e86113.

Kakoschke, T.K., S.C. Kakoschke, C. Zeuzem, H. Bouabe, K. Adler, J. Heesemann & O. Rossier, (2016) The RNA Chaperone Hfq Is Essential for Virulence and Modulates the Expression of Four Adhesins in Yersinia enterocolitica. *Scientific Reports* **6**: 29275.

Kaniga, K., I. Delor & G.R. Cornelis, (1991) A wide-host-range suicide vector for improving reverse genetics in gram-negative bacteria: inactivation of the blaA gene of *Yersinia enterocolitica*. *Gene* **109**: 137-141.

Kim, T.J., B.M. Young & G.M. Young, (2008) Effect of flagellar mutations on Yersinia enterocolitica biofilm formation. *Applied and environmental microbiology* **74**: 5466-5474.

Koo, J.T., T.M. Alleyne, C.A. Schiano, N. Jafari & W.W. Lathem, (2011) Global discovery of small RNAs in *Yersinia pseudotuberculosis* identifies *Yersinia*-specific small, noncoding RNAs required for virulence. *Proceedings of the National Academy of Sciences of the United States of America* **108**: E709-717.

Kotrba, P., M. Inui & H. Yukawa, (2001) Bacterial phosphotransferase system (PTS) in carbohydrate uptake and control of carbon metabolism. *Journal of bioscience and bioengineering* **92**: 502-517.

Langmead, B., C. Trapnell, M. Pop & S.L. Salzberg, (2009) Ultrafast and memory-efficient alignment of short DNA sequences to the human genome. *Genome biology* **10**: R25.

Lathem, W.W., J.A. Schroeder, L.E. Bellows, J.T. Ritzert, J.T. Koo, P.A. Price, A.J. Caulfield & W.E. Goldman, (2014) Posttranscriptional regulation of the *Yersinia pestis* cyclic AMP receptor protein Crp and impact on virulence. *mBio* **5**: e01038-01013.

Lawrenz, M.B. & V.L. Miller, (2007) Comparative analysis of the regulation of rovA from the pathogenic *Yersiniae*. *Journal of bacteriology* **189**: 5963-5975.

Lehnen, D., C. Blumer, T. Polen, B. Wackwitz, V.F. Wendisch & G. Unden, (2002) LrhA as a new transcriptional key regulator of flagella, motility and chemotaxis genes in *Escherichia coli*. *Molecular microbiology* **45**: 521-532.

Leskinen, K., M. Varjosalo, Z. Li, C.M. Li & M. Skurnik, (2015a) The expression of the *Yersinia enterocolitica* O:3 lipopolysaccharide O-antigen and outer core gene clusters is RfaH-dependent. *Microbiology*.

Leskinen, K., M. Varjosalo & M. Skurnik, (2015b) Absence of YbeY RNase compromises the growth and enhances the virulence plasmid gene expression of *Yersinia enterocolitica* O:3. *Microbiology* **161**: 285-299.

Li, L., D. Huang, M.K. Cheung, W. Nong, Q. Huang & H.S. Kwan, (2013) BSRD: a repository for bacterial small regulatory RNA. *Nucleic acids research* **41**: D233-238.

Liu, M.Y. & T. Romeo, (1997) The global regulator CsrA of *Escherichia coli* is a specific mRNA-binding protein. *Journal of bacteriology* **179**: 4639-4642.

Livny, J. & M.K. Waldor, (2007) Identification of small RNAs in diverse bacterial species. *Current opinion in microbiology* **10**: 96-101.

Majdalani, N., D. Hernandez & S. Gottesman, (2002) Regulation and mode of action of the second small RNA activator of RpoS translation, RprA. *Molecular microbiology* **46**: 813-826.

Mandin, P. & S. Gottesman, (2010) Integrating anaerobic/aerobic sensing and the general stress response through the ArcZ small RNA. *EMBO Journal* **29**: 3094-3107.

Mellin, J.R., M. Koutero, D. Dar, M.A. Nahori, R. Sorek & P. Cossart, (2014) Riboswitches. Sequestration of a two-component response regulator by a riboswitch-regulated noncoding RNA. *Science* **345**: 940-943.

Michaux, C., A. Hartke, C. Martini, S. Reiss, D. Albrecht, A. Budin-Verneuil, M. Sanguinetti, S. Engelmann, T. Hain, N. Verneuil & J.C. Giard, (2014) Involvement of *Enterococcus faecalis* small RNAs in stress response and virulence. *Infection and immunity* **82**: 3599-3611.

Michiels, T. & G.R. Cornelis, (1991) Secretion of hybrid proteins by the *Yersinia* Yop export system. *Journal of bacteriology* **173**: 1677-1685.

Miller, J.H., (1972) Experiments in Molecular Genetics. In.: Cold Spring Harbor, pp. 433.

Miller, V.L. & J.J. Mekalanos, (1988) A novel suicide vector and its use in construction of insertion mutations: osmoregulation of outer membrane proteins and virulence determinants in *Vibrio cholerae* requires *toxR*. *Journal of bacteriology* **170**: 2575-2583.

Moller, P., A. Overloper, K.U. Forstner, T.N. Wen, C.M. Sharma, E.M. Lai & F. Narberhaus, (2014) Profound impact of Hfq on nutrient acquisition, metabolism and motility in the plant pathogen *Agrobacterium tumefaciens*. *PloS one* **9**: e110427.

Morales, V.M., A. Backman & M. Bagdasarian, (1991) A series of wide-host-range low-copy-number vectors that allow direct screening for recombinants. *Gene* **97**: 39-47.

Mortz, E., T.N. Krogh, H. Vorum & A. Gorg, (2001) Improved silver staining protocols for high sensitivity protein identification using matrix-assisted laser desorption/ionization-time of flight analysis. *Proteomics* **1**: 1359-1363.

Muffler, A., D. Fischer & R. Hengge-Aronis, (1996) The RNA-binding protein HF-I, known as a host factor for phage Qbeta RNA replication, is essential for *rpoS* translation in *Escherichia coli*. *Genes & development* **10**: 1143-1151.

Murina, V.N. & A.D. Nikulin, (2015) Bacterial Small Regulatory RNAs and Hfq Protein. *Biochemistry (Mosc)* **80**: 1647-1654.

Nuss, A.M., A.K. Heroven, B. Waldmann, J. Reinkensmeier, M. Jarek, M. Beckstette & P. Dersch, (2015) Transcriptomic profiling of Yersinia pseudotuberculosis reveals reprogramming of the Crp regulon by temperature and uncovers Crp as a master regulator of small RNAs. *PLoS Genet* **11**: e1005087.

1135 Patten, C.L., M.G. Kirchhof, M.R. Schertzberg, R.A. Morton & H.E. Schellhorn, (2004) Microarray analysis of
1136 RpoS-mediated gene expression in *Escherichia coli* K-12. *Molecular genetics and genomics : MGG*
1137 **272**: 580-591.
1138 Peterson, C.N., V.J. Carabetta, T. Chowdhury & T.J. Silhavy, (2006) LrhA regulates rpoS translation in response
1139 to the Rcs phosphorelay system in *Escherichia coli*. *Journal of bacteriology* **188**: 3175-3181.
1140 Qu, Y., L. Bi, X. Ji, Z. Deng, H. Zhang, Y. Yan, M. Wang, A. Li, X. Huang, R. Yang & Y. Han, (2012) Identification
1141 by cDNA cloning of abundant sRNAs in a human-avirulent *Yersinia pestis* strain grown under five
1142 different growth conditions. *Future microbiology* **7**: 535-547.
1143 Raczkowska, A., K. Skorek, M. Brzostkowska, A. Lasinska & K. Brzostek, (2011) Pleiotropic effects of a Yersinia
1144 enterocolitica ompR mutation on adherent-invasive abilities and biofilm formation. *FEMS*
1145 *microbiology letters* **321**: 43-49.
1146 Ramachandran, R., A.K. Burke, G. Cormier, R.V. Jensen & A.M. Stevens, (2014) Transcriptome-based analysis
1147 of the *Pantoea stewartii* quorum-sensing regulon and identification of EsaR direct targets. *Applied*
1148 *and environmental microbiology* **80**: 5790-5800.
1149 Rasmussen, A.A., J. Johansen, J.S. Nielsen, M. Overgaard, B. Kallipolitis & P. Valentin-Hansen, (2009) A
1150 conserved small RNA promotes silencing of the outer membrane protein YbfM. *Molecular*
1151 *microbiology* **72**: 566-577.
1152 Reines, M., E. Llobet, K.M. Dahlstrom, C. Perez-Gutierrez, C.M. Llompart, N. Torrecabota, T.A. Salminen & J.A.
1153 Bengoechea, (2012) Deciphering the acylation pattern of *Yersinia enterocolitica* lipid A. *PLoS*
1154 *pathogens* **8**: e1002978.
1155 Reisner, A., J.A. Haagensen, M.A. Schembri, E.L. Zechner & S. Molin, (2003) Development and maturation of
1156 Escherichia coli K-12 biofilms. *Molecular microbiology* **48**: 933-946.
1157 Revell, P.A. & V.L. Miller, (2000) A chromosomally encoded regulator is required for expression of the *Yersinia*
1158 *enterocolitica inv* gene and for virulence. *Molecular microbiology* **35**: 677-685.
1159 Robertson, G.T. & R.M. Roop, Jr., (1999) The *Brucella abortus* host factor I (HF-I) protein contributes to stress
1160 resistance during stationary phase and is a major determinant of virulence in mice. *Molecular*
1161 *microbiology* **34**: 690-700.
1162 Romeo, T., (1998) Global regulation by the small RNA-binding protein CsrA and the non-coding RNA molecule
1163 CsrB. *Molecular microbiology* **29**: 1321-1330.
1164 Schell, M.A., (1993) Molecular biology of the LysR family of transcriptional regulators. *Annual review of*
1165 *microbiology* **47**: 597-626.
1166 Schiano, C.A., L.E. Bellows & W.W. Lathem, (2010) The small RNA chaperone Hfq is required for the virulence
1167 of *Yersinia pseudotuberculosis*. *Infection and immunity* **78**: 2034-2044.
1168 Schiano, C.A., J.T. Koo, M.J. Schipma, A.J. Caulfield, N. Jafari & W.W. Lathem, (2014) Genome-wide analysis
1169 of small RNAs expressed by Yersinia pestis identifies a regulator of the Yop-Ysc type III secretion
1170 system. *J Bacteriol* **196**: 1659-1670.
1171 Schiano, C.A. & W.W. Lathem, (2012) Post-transcriptional regulation of gene expression in *Yersinia* species.
1172 *Frontiers in cellular and infection microbiology* **2**: 129.
1173 Simon, R., U. Priefer & A. Puhler, (1983) A Broad Host Range Mobilization System for Invivo Genetic-
1174 Engineering - Transposon Mutagenesis in Gram-Negative Bacteria. *Bio-Technol* **1**: 784-791.
1175 Sittka, A., S. Lucchini, K. Papenfort, C.M. Sharma, K. Rolle, T.T. Binnewies, J.C. Hinton & J. Vogel, (2008) Deep
1176 sequencing analysis of small noncoding RNA and mRNA targets of the global post-transcriptional
1177 regulator, Hfq. *PLoS genetics* **4**: e1000163.
1178 Sittka, A., V. Pfeiffer, K. Tedin & J. Vogel, (2007) The RNA chaperone Hfq is essential for the virulence of
1179 *Salmonella typhimurium*. *Molecular microbiology* **63**: 193-217.
1180 Skurnik, M., (1984) Lack of correlation between the presence of plasmids and fimbriae in *Yersinia*
1181 *enterocolitica* and *Yersinia pseudotuberculosis*. *The Journal of applied bacteriology* **56**: 355-363.
1182 Skurnik, M., (1985) Expression of antigens encoded by the virulence plasmid of *Yersinia enterocolitica* under
1183 different growth conditions. *Infection and Immunology* **47**: 183-190.
1184 Skurnik, M., R. Venho, J.A. Bengoechea & I. Moriyon, (1999) The lipopolysaccharide outer core of *Yersinia*
1185 *enterocolitica* serotype O:3 is required for virulence and plays a role in outer membrane integrity.
1186 *Molecular microbiology* **31**: 1443-1462.

1187 Sledjeski, D.D., A. Gupta & S. Gottesman, (1996) The small RNA, DsrA, is essential for the low temperature
1188 expression of RpoS during exponential growth in *Escherichia coli*. *EMBO Journal* **15**: 3993-4000.
1189 Stuart, C.A., E. Van Stratum & R. Rustigian, (1945) Further Studies on Urease Production by *Proteus* and
1190 Related Organisms. *Journal of bacteriology* **49**: 437-444.
1191 Tamm, A., A.M. Tarkkanen, T.K. Korhonen, P. Kuusela, P. Toivanen & M. Skurnik, (1993) Hydrophobic domains
1192 affect the collagen-binding specificity and surface polymerization as well as the virulence potential
1193 of the YadA protein of Yersinia enterocolitica. *Mol Microbiol* **10**: 995-1011.
1194 Tanaka, K., Y. Takayanagi, N. Fujita, A. Ishihama & H. Takahashi, (1993) Heterogeneity of the principal sigma
1195 factor in *Escherichia coli*: the *rpoS* gene product, sigma 38, is a second principal sigma factor of RNA
1196 polymerase in stationary-phase *Escherichia coli*. *Proceedings of the National Academy of Sciences of*
1197 *the United States of America* **90**: 3511-3515.
1198 Taylor, L.A. & R.E. Rose, (1988) A correction in the nucleotide sequence of the Tn903 kanamycin resistance
1199 determinant in pUC4K. *Nucleic acids research* **16**: 358.
1200 Torres-Quesada, O., J. Reinkensmeier, J.P. Schluter, M. Robledo, A. Peregrina, R. Giegerich, N. Toro, A. Becker
1201 & J.I. Jimenez-Zurdo, (2014) Genome-wide profiling of Hfq-binding RNAs uncovers extensive post-
1202 transcriptional rewiring of major stress response and symbiotic regulons in Sinorhizobium meliloti.
1203 *RNA biology* **11**: 563-579.
1204 Trapnell, C., D.G. Hendrickson, M. Sauvageau, L. Goff, J.L. Rinn & L. Pachter, (2013) Differential analysis of
1205 gene regulation at transcript resolution with RNA-seq. *Nature biotechnology* **31**: 46-53.
1206 Trent, M.S., C.M. Stead, A.X. Tran & J.V. Hankins, (2006) Diversity of endotoxin and its impact on
1207 pathogenesis. *Journal of Endotoxin Research* **12**: 205-223.
1208 Tsai, C.S. & S.C. Winans, (2011) The quorum-hindered transcription factor YenR of Yersinia enterocolitica
1209 inhibits pheromone production and promotes motility via a small non-coding RNA. *Molecular*
1210 *microbiology* **80**: 556-571.
1211 Uliczka, F., F. Pisano, J. Schaake, T. Stolz, M. Rohde, A. Fruth, E. Strauch, M. Skurnik, J. Batzilla, A. Rakin, J.
1212 Heesemann & P. Dersch, (2011) Unique cell adhesion and invasion properties of *Yersinia*
1213 *enterocolitica* O:3, the most frequent cause of human Yersiniosis. *PLoS pathogens* **7**: e1002117.
1214 Van Puyvelde, S., H.P. Steenackers & J. Vanderleyden, (2013) Small RNAs regulating biofilm formation and
1215 outer membrane homeostasis. *RNA biology* **10**: 185-191.
1216 Wauters, G., K. Kandolo & M. Janssens, (1987) Revised biogrouping scheme of *Yersinia enterocolitica*.
1217 *Contributions to microbiology and immunology* **9**: 14-21.
1218 Wei, B.L., A.M. Brun-Zinkernagel, J.W. Simecka, B.M. Pruss, P. Babitzke & T. Romeo, (2001) Positive regulation
1219 of motility and *flhDC* expression by the RNA-binding protein CsrA of *Escherichia coli*. *Molecular*
1220 *microbiology* **40**: 245-256.
1221 Weilbacher, T., K. Suzuki, A.K. Dubey, X. Wang, S. Gudapaty, I. Morozov, C.S. Baker, D. Georgellis, P. Babitzke
1222 & T. Romeo, (2003) A novel sRNA component of the carbon storage regulatory system of *Escherichia*
1223 *coli*. *Molecular microbiology* **48**: 657-670.
1224 Virtanen, S.E., L.K. Salonen, R. Laukkanen, M. Hakkinen & H. Korkeala, (2011) Factors related to the
1225 prevalence of pathogenic *Yersinia enterocolitica* on pig farms. *Epidemiology and infection* **139**: 1919-
1226 1927.
1227 Vogel, J. & B.F. Luisi, (2011) Hfq and its constellation of RNA. *Nature reviews. Microbiology* **9**: 578-589.
1228 Yan, Y., S. Su, X. Meng, X. Ji, Y. Qu, Z. Liu, X. Wang, Y. Cui, Z. Deng, D. Zhou, W. Jiang, R. Yang & Y. Han, (2013)
1229 Determination of sRNA expressions by RNA-seq in *Yersinia pestis* grown in vitro and during infection.
1230 *PloS one* **8**: e74495.
1231 Yanisch-Perron, C., J. Vieira & J. Messing, (1985) Improved M13 phage cloning vectors and host strains:
1232 nucleotide sequences of the M13mp18 and pUC19 vectors. *Gene* **33**: 103-119.
1233 Zeng, Q., R.R. McNally & G.W. Sundin, (2013) Global small RNA chaperone Hfq and regulatory small RNAs are
1234 important virulence regulators in *Erwinia amylovora*. *Journal of bacteriology* **195**: 1706-1717.
1235 Zhang, A., S. Altuvia, A. Tiwari, L. Argaman, R. Hengge-Aronis & G. Storz, (1998) The OxyS regulatory RNA
1236 represses *rpoS* translation and binds the Hfq (HF-I) protein. *EMBO Journal* **17**: 6061-6068.
1237 Zhang, A., K.M. Wassarman, C. Rosenow, B.C. Tjaden, G. Storz & S. Gottesman, (2003) Global analysis of small
1238 RNA and mRNA targets of Hfq. *Molecular microbiology* **50**: 1111-1124.

1239

Table 1. Summary of differentially expressed genes and proteins identified in RNA sequencing and quantitative proteomic studies.

	22°C		37°C	
	RNA-seq	**LC-MS/MS**	**RNA-seq**	**LC-MS/MS**
Differentially expressed*	7.96%	5.72%	12.44%	7.58%
Up-regulated**	38.15%	62.73%	92.47%	84.87%
Down-regulated**	62.43%	37.27%	7.53%	15.13%

* percent of all genes detected with the method (in case of RNA-seq all genes annotated for *Y. enterocolitica* Y11 were taken under account).

** percent of differentially expressed genes

Table 2. A selection of Hfq-dependent genes of *Y. enterocolitica* O:3 from the differentially expressed genes and proteins determined by RNA sequencing and quantitative proteomics, respectively. Values are displayed as ratios of the mRNA or protein abundances of the YeO3-*hfq*::Km to the wild type bacteria. Values >1 and ↑ signs show increased ratios, while values <1 and ↓ signs show decreased ratios.

				22		37	
pathway	**gene ID**	**gene product**		**RNA-seq**	**LC-MS/MS**	**RNA-seq**	**LC-MS/MS**
outer membrane structures	Y11_32161	EnvZ	Osmolarity sensory histidine kinase EnvZ	1.35	ND	**2.78***	inf ↑
	Y11_12201	OmpC	Outer membrane protein C	1.01	ND	**2.35***	ND
	Y11_02741	OmpC	Outer membrane protein C	**0.18***	0.89	1.07	0.78
	Y11_04441	OmpF	Outer membrane porin F	1.74	1.11	**3.90***	2.77
	Y11_17401	OmpX	Outer membrane protein X	**11.27***	inf ↑	**16.33***	1.54
	Y11_10821	OmpW	Outer membrane protein W	1.70	6.67	**6.04***	ND
	Y11_21911	BamD	Outer membrane protein assembly factor BamD	1.69	ND	**2.27***	ND
regulators	Y11_32151	OmpR	Two-component system response regulator OmpR	1.49	**2.67***	**2.87***	**5.59***
	Y11_08441	RovA	Transcriptional regulator (homolog of SlyA)	**0.13***	0.19*	**0.40***	inf ↓
	Y11_21031	PhoB	Phosphate regulon transcriptional regulatory protein PhoB	**0.35***	ND	0.66	ND
	Y11_02141	RovM	LysR family transcriptional regulator (homolog of LrhA)	**7.77***	8.90*	**39.82***	inf ↑
Cpx signaling pathway	Y11_28731	CpxA	Copper sensory histidine kinase	**5.62***	inf ↑	**3.98***	inf ↑
	Y11_00691	CpxR	Transcriptional regulatory protein CpxR	0.71	ND	1.78	ND
	Y11_00701	CpxR	Transcriptional regulatory protein CpxR	1.06	ND	2.08	inf ↑
	Y11_28711	CpxP	Cpx signaling pathway,periplasmic inhibitor	**5.91***	36.21	**17.39***	2.14
	Y11_28721	CpxR	Copper-sensing two-component system response regulator	**4.61***	3.95	**4.61***	**5.83***
urea metabolism	Y11_41821	UreA	Urease subunit gamma	**0.12***	0.15	0.53	**0.53***
	Y11_41831	UreB	Urease subunit beta	**0.18***	**0.39***	0.62	0.62
	Y11_41841	UreC	Urease subunit alpha	**0.25***	**0.32***	0.76	**0.63***
	Y11_41851	UreE	Urease accessory protein UreE	**0.30***	**0.11***	0.78	**0.60***
	Y11_41861	UreF	Urease accessory protein UreF	**0.31***	inf ↓	1.03	ND
	Y11_41871	UreG	Urease accessory protein UreG	**0.27***	0.28	1.00	0.65
	Y11_41881	UreD	Urease accessory protein UreD	**0.36***	inf↓	1.20	ND
PTS system	Y11_02891		PTS system, beta-glucoside-specific IIB component PTS system, beta-glucoside-specific IIC component PTS system,beta-glucoside-specific IIA component (EC 2.7.1.69)	1.18	ND	**2.21***	ND

	Y11_03261		PTS system, fructose-specific IIB component PTS system, fructose-specific IIC component (EC 2.7.1.69)	0.75	ND	**4.25***	0.72
	Y11_03271		PTS system, fructose-specific IIB component PTS system, fructose-specific IIC component (EC 2.7.1.69)	0.61	ND	**4.62***	ND
	Y11_43211		PTS system, glucitol/sorbitol-specific IIA component (EC 2.7.1.69)	**6.71***	ND	**2.68***	ND
	Y11_43221		PTS system, glucitol/sorbitol-specific IIB component and second of two IIC components (EC 2.7.1.69)	**7.95***	16.6*	**4.90***	inf↑
	Y11_43231		PTS system, glucitol/sorbitol-specific IIC component (EC 2.7.1.69)	**4.51***	ND	**2.70***	inf↑
	Y11_05361		PTS system, glucose-specific IIB component PTS system, glucose-specific IIC component (EC 2.7.1.69)	**9.64***	10.54*	**6.65***	**5.07***
	Y11_30351		PTS system, mannitol-specific IIC component PTS system, mannitol-specific IIB component PTS system, mannitol-specific IIA component (EC 2.7.1.69)	0.84	3.23*	**4.69***	**2.67***
	Y11_06301		PTS system, mannose-specific IIA component PTS system, mannose-specific IIB component (EC 2.7.1.69)	1.97	0.95	**3.50***	1.05
	Y11_06281		PTS system, mannose-specific IID component (EC 2.7.1.69)	1.72	ND	**2.73***	ND
	Y11_12011		PTS system, N-acetylgalactosamine-and galactosamine-specific IIA component (EC 2.7.1.69)	0.95	ND	**3.12***	ND
	Y11_11981		PTS system, N-acetylgalactosamine-specific IIB component (EC 2.7.1.69)	1.73	ND	**9.52***	ND
	Y11_11991		PTS system, N-acetylgalactosamine-specific IIC component (EC 2.7.1.69)	2.30	ND	**18.80***	ND
	Y11_12001		PTS system, N-acetylgalactosamine-specific IID component (EC 2.7.1.69)	1.77	ND	**5.44***	ND
	Y11_25621		PTS system, sucrose-specific IIB component PTS system, sucrose-specific IIC component (EC 2.7.1.69)	0.80	ND	**2.09***	ND
	Y11_01621		PTS system, cellobiose-specific IIB component (EC 2.7.1.69)	**0.40***	ND	0.91	ND
	Y11_42011		PTS system, chitobiose-specific IIB component (EC 2.7.1.69)	**0.48***	ND	0.93	ND
stress response	Y11_22741	RpoS	RNA polymerase sigma factor RpoS	**0.28***	0.33	1.48	ND
cell division	Y11_20571	BolA	Cell division protein BolA	**0.29***	**0.13***	0.64	ND
mannitol utilization	Y11_30361	MtlD	Mannitol-1-phosphate 5-dehydrogenase (EC 1.1.1.17)	1.15	2.62	**2.29***	2.31
protein folding	Y11_42751	HscA	chaperone protein HscA	**3.92***	**2.59***	1.48	inf↑

ND, not detected,

Inf, the protein was detected only in the YeO3-*hfq*::Km mutant or the wild type strain thus preventing the ration calculation.

* statistically significant - >2-fold difference, p-value < 0.05

Table 3. RovM-dependent genes of *Y. enterocolitica* O:3 determined by RNA sequencing. Values are displayed as ratios that represent the mRNA abundance in YeO3/pMMB207-*rovM* strain compared with the YeO3-*rovM* mutant. Values >1 show increase and numbers <1, decrease in the abundance of respective mRNAs. The corresponding YeO3-*hfq*::Km to wild type ratios are presented on the right hand columns.

Gene	Protein names	RovM		Hfq	
		FC	p-value	FC	p-value
Y11_02141	Lysr family transcriptional regulator RovM	**16,93**	*0,015*	**7,77**	*0,048*
Y11_17401	Outer membrane protein X	**6,71**	*0,009*	**11,27**	*0,034*
Y11_18781	Uncharacterized protein	**2,55**	*0,002*	**1,53**	*0,231*
Y11_18211	Putative phosphatase	**2,45**	*0,016*	**3,88**	*0,004*
Y11_30241	Glyoxylate/hydroxypyruvate reductase B	**2,43**	*0,007*	**1,96**	*0,006*
Y11_24061	Putative outer membrane lipoprotein Pcp	**2,41**	*0,021*	**1,38**	*0,421*
Y11_31701	Epi-inositol hydrolase	**2,41**	*0,035*	**1,50**	*0,045*
Y11_43231	PTS system, glucitol/sorbitol-specific IIC component	**2,39**	*0,020*	**4,51**	*0,005*
Y11_43211	PTS system, glucitol/sorbitol-specific IIA component	**2,16**	*0,042*	**6,71**	*0,012*
Y11_02051	Acetate kinase	**2,15**	*0,044*	**2,78**	*0,134*
Y11_31691	5-keto-2-deoxygluconokinase uncharacterized domain	**2,10**	*0,034*	**2,03**	*0,000*
Y11_43221	PTS system, glucitol/sorbitol-specific IIB component	**2,02**	*0,007*	**7,95**	*0,042*
Y11_00921	Glucokinase	**2,02**	*0,037*	**1,41**	*0,120*
Y11_40141	Putative regulator	**0,50**	*0,050*	**0,55**	*0,045*
Y11_11071	Hnr protein	**0,47**	*0,025*	**0,30**	*0,002*
Y11_07101	Copper homeostasis protein CutC	**0,46**	*0,041*	**0,23**	*0,000*
Y11_43261	Uncharacterized protein	**0,45**	*0,003*	**0,86**	*0,641*
Y11_30751	Urocanate hydratase	**0,45**	*0,034*	**0,50**	*0,134*
Y11_00541	Putative N-acetylmannosamine-6-phosphate 2-epimerase	**0,44**	*0,034*	**0,63**	*0,174*
Y11_06711	Putative uroporphyrin-III c-methyltransferase	**0,44**	*0,007*	**0,20**	*0,005*
Y11_41831	Urease subunit beta	**0,44**	*0,001*	**0,18**	*0,006*
Y11_08901	Peptide transport system permease protein sapB	**0,44**	*0,022*	**0,37**	*0,023*
Y11_41961	Protein CrcB homolog	**0,43**	*0,010*	**0,45**	*0,015*
Y11_00561	N-acetylmannosamine kinase	**0,43**	*0,048*	**0,43**	*0,020*
Y11_41841	Urease subunit alpha	**0,42**	*0,043*	**0,25**	*0,013*
Y11_41871	Urease accessory protein UreG	**0,42**	*0,039*	**0,27**	*0,036*
Y11_11061	Hnr protein	**0,42**	*0,030*	**0,51**	*0,015*
Y11_22741	RpoS RNA polymerase sigma factor	**0,38**	*0,020*	**0,28**	*0,022*
Y11_07051	Phosphate starvation-inducible protein PhoH	**0,36**	*0,015*	**0,21**	*0,128*
Y11_39751	Htra protease/chaperone protein	**0,35**	*0,027*	**1,75**	*0,005*

Y11_09651	Uncharacterized protein	**0,34**	*0,037*	**0,65**	*0,537*
Y11_08981	Putative phage protein	**0,33**	*0,018*	**0,25**	*0,018*
Y11_37711	Glycerol dehydrogenase	**0,32**	*0,020*	**0,43**	*0,011*
Y11_13781	N-acetylneuraminate epimerase	**0,32**	*0,011*	**0,49**	*0,013*
Y11_27721	Maltose/maltodextrin ABC transporter MalE	**0,30**	*0,003*	**1,84**	*0,034*
Y11_37731	Phosphoenolpyruvate-dihydroxyacetone phosphotransferase subunit DhaL	**0,30**	*0,025*	**0,51**	*0,013*
Y11_41911	Putative exported protein	**0,30**	*0,025*	**0,25**	*0,010*
Y11_23851	Putative exported protein	**0,29**	*0,009*	**1,74**	*0,065*
Y11_37741	Phosphoenolpyruvate-dihydroxyacetone phosphotransferase, subunit DhaM	**0,28**	*0,030*	**0,53**	*0,010*
Y11_17471	DNA protection during starvation protein	**0,27**	*0,002*	**0,32**	*0,004*
Y11_18351	Putative starvation-inducible protein	**0,27**	*0,016*	**0,19**	*0,029*
Y11_27691	Maltose operon periplasmic protein MalM	**0,25**	*0,050*	**4,19**	*0,005*
Y11_37721	Phosphoenolpyruvate-dihydroxyacetone phosphotransferase, subunit DhaK	**0,24**	*0,020*	**0,53**	*0,003*
Y11_42561	Putative transport system permease protein	**0,23**	*0,040*	**0,42**	*0,025*
Y11_37461	Acetyltransferase	**0,19**	*0,020*	**0,19**	*0,037*
Y11_23791	Uncharacterized protein	**0,17**	*0,008*	**1,15**	*0,710*
Y11_38001	Osmotically inducible protein OsmY	**0,15**	*0,016*	**0,29**	*0,011*
Y11_08441	Transcriptional regulator RovA	**0,10**	*0,040*	**0,13**	*0,001*
Y11_25651	Glutamate decarboxylase	**0,10**	*0,042*	**0,18**	*0,001*
Y11_25661	Glutamate decarboxylase	**0,08**	*0,027*	**0,14**	*0,005*
Y11_14811	Beta-galactosidase	**0,08**	*0,008*	**0,66**	*0,358*
Y11_31801	Acetolactate synthase	**0,06**	*0,004*	**0,53**	*0,068*
Y11_07321	Sigma-fimbriae uncharacterized paralogous subunit	**0,05**	*0,005*	**0,09**	*0,076*
Y11_07311	Sigma-fimbriae uncharacterized paralogous subunit	**0,03**	*0,006*	**0,20**	*0,037*
Y11_31821	Transcriptional regulator of alpha-acetolactate operon alsR	**0,03**	*0,021*	**0,22**	*0,045*

1261

Table 4. The YeO3-*hfq*::Km bacteria are attenuated in i.g. infected mice. Shown are bacterial counts in mouse spleen, liver and Peyer's patches (PP) recovered at different time point after i.g. co-infection of the mice. Each mouse was infected with 200 µl of mixture containing a total of $3x10^9$ CFU of wild type and YeO3-*hfq*::Km bacteria. The proportion of the YeO3-*hfq*::Km colonies (Km^R) in the initial mixture was 66%.

Days post infection	Organ	Total CFU g^{-1} in the organs and percentage of Km^R colonies							
		Mouse 1	%Km^R	Mouse 2	%Km^R	Mouse 3	%Km^R	Mouse 4	%Km^R
2	Spleen	0	0	0	0	0	0	0	0
	Liver	0	0	0	0	3×10^3	0	0	0
	PP	2×10^6	3	7×10^6	19	1×10^8	1.5	5×10^7	0
5	Spleen	0	0	0	0	0	0	0	0
	Liver	4×10^2	0	0	0	5×10^2	0	0	0
	PP	4×10^5	9	3×10^6	0	8×10^6	0	4×10^6	0
9	Spleen	0	0	0	0	0	0	0	0
	Liver	0	0	0	0	0	0	0	0
	PP	3×10^6	0	9×10^5	2	4×10^6	0	0	0

1269 **Table 5.** Bacteria and plasmids used in this work.

Bacterial strains and plasmids	Description	Source or reference
***Yersinia enterocolitica* strains**		
YeO3	6471/76, serotype O:3, patient isolate, wild type	(Skurnik, 1984)
YeO3-*hfq*::Km	*hfq*::Km-GenBlock, Km^R	this work
YeO3-*hfq*::Km/p*hfq*	*hfq*::Km complemented with pTM100-*hfq*; Km^R, Clm^R	this work
YeO3-*rovM*	*rovM*::pKNG101, $Strep^R$	this work
YeO3-*rovM-hfq*::Km	*hfq* - *rovM* double mutant; Km^R, $Strep^R$	this work
YeO3/pMMB207-*rovM*	*rovM* strain with pMMB207-*rovM* plasmid (overexpression of *rovM* under the IPTG induced promoter); $Strep^R$, Clm^R	this work
YeO3/pLux232oT-*rovM*	6471/76, wild type strain carrying *rovM* promoter reporter vector pLux232oT-*rovM,* Km^R	this work
YeO3-*rovM*/ pLux232oT-*rovM*	*rovM*::pKNG101 carrying *rovM* promoter reporter vector pLux232oT-*rovM,* Km^R, $Strep^R$	this work
YeO3/pMMB207-*rovM*/ pLux232oT-*rovM*	*rovM* strain with pMMB207-*rovM* plasmid carrying *rovM* promoter reporter vector pLux232oT-*rovM,* Km^R, $Strep^R$, Clm^R	this work
S17-1λpir/ pLux232oT-*rovM*	*E. coli* S17-1λpir strain carrying *rovM* promoter reporter vector pLux232oT-*rovM,* Km^R	this work
YeO3/pMMB207-*csrA*	6471/76 strain with pMMB207-*csrA* plasmid (overexpression of *csrA* under the IPTG induced promoter); Clm^R	this work
YeO3-*hfq*::Km/pMMB207-*csrA*	YeO3-*hfq*::Km strain with pMMB207-*csrA* plasmid (overexpression of *csrA* under the IPTG induced promoter); Km^R, Clm^R	this work
YeO3/pMMB207-*csrA*/ pLux232oT-*rovM*	6471/76 strain with pMMB207-*csrA* plasmid carrying *rovM* promoter reporter vector pLux232oT-*rovM,* Km^R, Clm^R	this work
***Escherichia coli* strains**		
ω7249	B2163Λnic35, *E. coli* strain for suicide vector delivery, requirement for diaminopimelic acid, Km^R	(Babic *et al.*, 2008)
SY327λpir	recA56(λpir), *E. coli* strain for suicide vector delivery	(Miller & Mekalanos, 1988)
S17-1λpir	recA, λpir, *E. coli* strain for suicide vector delivery	(Simon *et al.*, 1983)
Plasmids		
pTM100	Mobilizable vector, pACYC184-oriT of RK2; Clm^R	(Michiels & Cornelis, 1991)
pUC18	Cloning vector; Amp^R	(Yanisch-Perron *et al.*, 1985)
pUC-4K	Origin of the Km-GenBlock cassette; Amp^R, Km^R	(Taylor & Rose, 1988)
pKNG101	Suicide vector; $Strep^R$	(Kaniga *et al.*, 1991)
pMMB207	Cloning vector derived from RSF1010	(Morales *et al.*, 1991)
pLux232oT	Promoterless reporter plasmid	(Leskinen *et al.*, 2015a)
pUC18-*hfq*	the flanked *hfq* gene cloned as a PCR-fragment into pUC18; Amp^R	this work
pUC18-*hfq*::Km	pUC18-*hfq* derivative with the internal part of hfq gene replaced with Km-GenBlock; Km^R, Amp^R	this work
pKNG101-*hfq*::km	*hfq*::Km-GenBlock fragment cloned into BamHI site of pKNG101; Km^R,, $Strep^R$	this work
pKNG101-*rovM*	the internal part of *rovM* gene cloned as a PCR-fragment into pKNG101; $Strep^R$	this work
pKNG101-*csrA*::CAT	the CAT gene with the flanking regions of *csrA* gene cloned into pKNG101; $Strep^R$, Clm^R	this work
pMMB207-*rovM*	overexpression plasmid; the complete *rovM* gene cloned as a PCR-fragment into pMMB207; Clm^R	this work
pMMB207-*csrA*	overexpression plasmid; the complete *csrA* gene cloned as a PCR-fragment into pMMB207; Clm^R	this work
pTM100-*hfq*	full *hfq* gene with the upstream promoter cloned as a PCR-fragment into pTM100; Clm^R	this work
pLux232oT-*rovM*	*rovM* promoter region cloned as a PCR fragment into the promoter reporter vector pLux232oT; Km^R	this work

Figure Legends

Figure 1. Functional classification of Hfq-dependent genes based on the Gene Ontology genome annotation of *Y. enterocolitica* Y11 (http://www.geneontology.org/). Shown are the down- and upregulated genes in selected functional classes in YeO3-*hfq*::Km bacteria grown at 22 and 37°C when compared to YeO3-wt bacteria.

Figure 2. Derepression of the *rovM* gene in *Y. enterocolitica* O:3 *hfq* mutant. **Panel A.** Spectral values obtained in quantitative proteomics study showed substantial increase in the RovM protein abundance in the YeO3-*hfq*::Km bacteria. The abundance of RovM protein in wild type bacteria grown at RT was below detection level. **Panel B**. The the *rovM* promoter activity in different *Y. enterocolitica* O:3 strains. The bacteria harboring the pLux232oT-*rovM* plasmid were grown in microtiter plates for 4h at 37°C before the level of bioluminescence was measured. The *rovM* promoter activity in the wild type bacteria was set to 100%. The graph presents the average luminescence values obtained from 16 replicates; error bars represent standard deviation. The statistical significances of the differences to wild type values are indicated above the bars, **** $p \leq 0.0001$.

Figure 3. The growth of *Y. enterocolitica* O:3 strains in BHI medium. Bacteria were cultured in BHI at 22°C (**Panel A**), 37°C (**Panel B**), 4°C (**Panel C**) and 42°C (**Panel D**). The symbols of the curves of the different strains are indicated on the right. Each data point represents the average of nine replicates. The error bars (in many data points covered by the symbol) indicate the standard deviations. Note the different time scale in the Y-axis in **Panel** C. **Panel E.** The maximal OD value reached by each strain during the growth at different temperatures. The statistical significance of the differences to wild type values are indicated above the bars, *** $p \leq 0.001$, **** $p \leq 0.0001$.

Figure 4. The influence of Hfq and RovM on the colony and cell morphology. **Panel A.** Transmission electron micrographs of wild type (left image) and YeO3-*hfq*::Km bacteria (right image) stained with uranyl acetate. **Panel B**. Average cell lengths of the bacteria based on measurements of 50 different bacterial cells for each strain. The error bars represent standard deviation.

Figure 5. The influence of Hfq and RovM on motility and biofilm formation. **Panel A.** Motility assay results. Bacterial strains were spotted on the Tryptone soft agar motility plate and incubated for 24h at RT. Subsequently the halo representing the bacterial growth was measured. The graph presents the values of 15 replicates for each strain. **Panel B.** Expression levels of flagellin determined using anti-flagellin mAb 15D8 in immunoblotting. Equal amounts of whole cell lysates of bacteria grown overnight in TB broth at 22°C were loaded in each lane. Loading controls are presented in the Fig. S10. **Panel C.** Effects of Hfq and RovM on biofilm formation in different media. Cultures of wild type, YeO3-*hfq*::Km, YeO3-*hfq*::Km/p*hfq* and YeO3-*hfq*::Km-*rovM* bacteria were grown in microtiter plates for 72h in tryptone broth, M9 or MedECa minimal media. The adherent cells were quantitated with crystal violet staining. The graph presents the average A_{560} values obtained from 16 replicates; error bars represent standard deviations. The statistical significances between the wild type and mutant strains are indicated above the bars, ** $p \leq 0.01$, *** $p \leq 0.001$, **** $p \leq 0.0001$.

Figure 6. Role of Hfq and RovM in expression levels of RpoS and RovA. **Panel A**. Abundance of the RpoS protein was determined using polyclonal anti-RpoS antiserum in immunoblotting. Equal amounts of whole cell lysates of bacteria grown overnight in LB at 22°C were loaded in each lane. The arrow indicates the RpoS protein band. Loading controls are presented in Fig. S11. **Panel B**. The relative levels of *rovA* expression in mutant bacteria compared to that of wild type bacteria (expressed as ratios when wild type value was set to

1) were determined by quantitative RT-PCR using the total RNA isolated from bacteria grown at 37°C. The statistical significances between the strains are indicated above the bars, ** $p \leq 0.01$, *** $p \leq 0.001$, **** $p \leq 0.0001$.

Figure 7. Stress response of the YeO3-*hfq*::Km bacteria. **Panel A.** Acid and temperature tolerance assays. Shown are the survival percentages of bacteria after 20 min incubation in PBS, pH 2.0, and after a 5 min exposure to 55ºC. **Panel B.** Urease activity of bacteria grown in urea broth supplemented with phenol red. The activity was measured as increase in absorbance at 565 nm. The error bars show standard deviations. The statistical significances are indicated above the bars, **** $p \leq 0.0001$.

Figure 8. Hfq is required for full virulence of *Y. enterocolitica* O:3. The mice were infected i.g. individually with ca 10^9 CFU per mouse. The bacterial loads in Peyer's patches were determined on day 5 post-infection and are show for each mouse. The horizontal bars indicate the CFU g^{-1} averages of each strain. (See also Table S8).

Figure 9. Working model of the Hfq and RovM regulatory network. Hfq inhibits the *rovM* gene transcription by decreasing the availability of free CsrA, though it is likely that also other Hfq-dependent factors may control the *rovM* transcription. The RovM overexpression affects the transcription of the *rovA*, *lpxR*, *osmY*, *ompX genes,* of two urease subunit genes*,* and of two genes from the PTS system. Hfq, independently of RovM, is required for the proper regulation of the expression of the urease accessory protein genes, the Cpx pathway elements, numerous PTS systems genes, and genes of different transcriptional regulators. The RovM appears to repress the expression of RpoS, but Hfq can affect the expression of this sigma factor also independently.

Figure 1

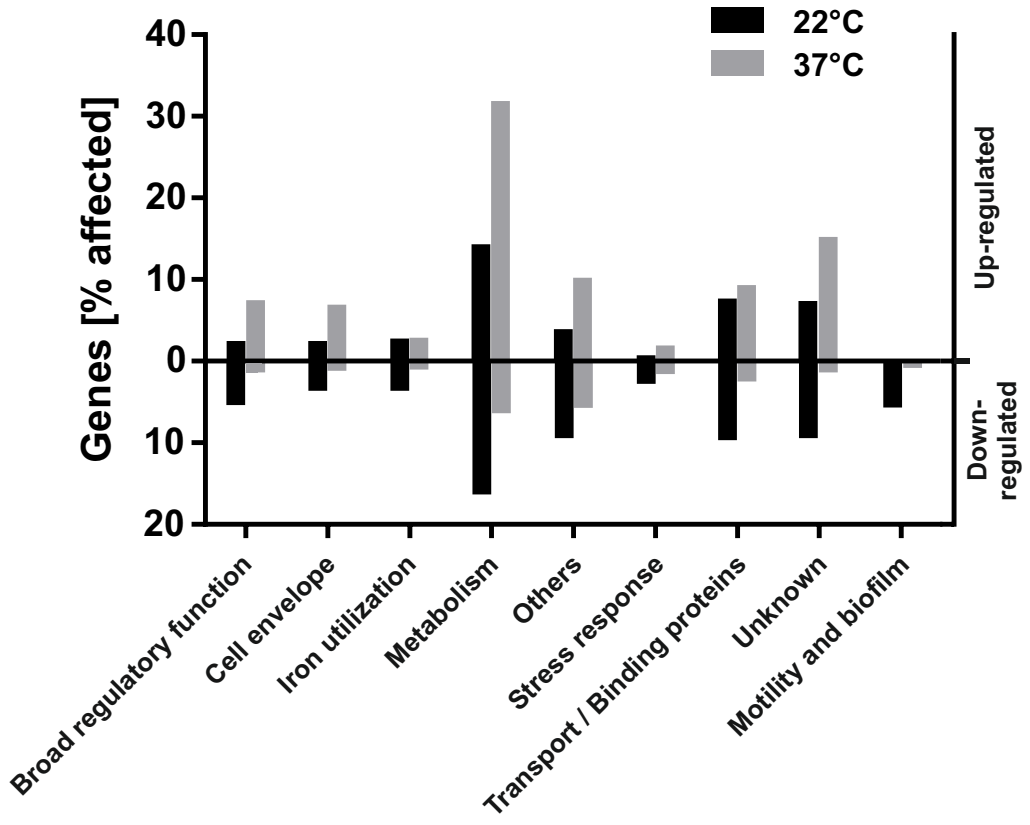
22°C
37°C
Genes [% affected]
40
30
20
10
0
10
20
Up-regulated
Down-regulated
Broad regulatory function
Cell envelope
Iron utilization
Metabolism
Others
Stress response
Transport / Binding proteins
Unknown
Motility and biofilm

Figure 2

A

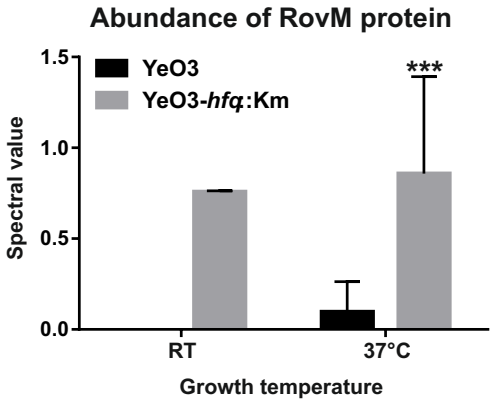
Abundance of RovM protein
YeO3
YeO3-*hfq*:Km
***
Spectral value
1.5
1.0
0.5
0.0
RT
37°C
Growth temperature

B

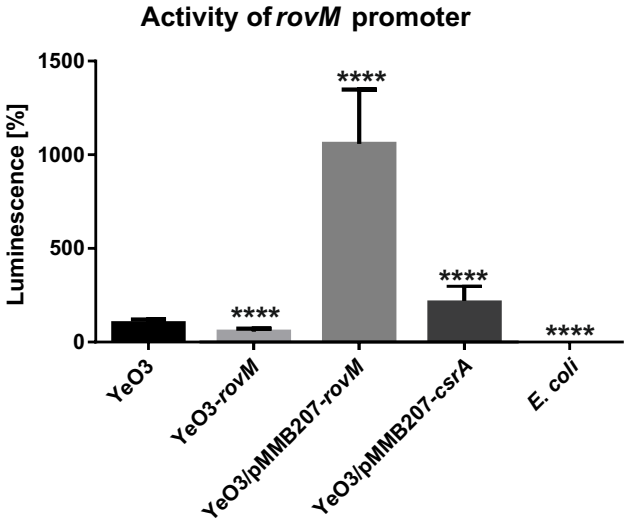
Activity of *rovM* promoter
Luminescence [%]
1500
1000
500
0
****
****
****
****
YeO3
YeO3-*rovM*
YeO3/pMMB207-*rovM*
YeO3/pMMB207-*csrA*
E. coli

Figure 3

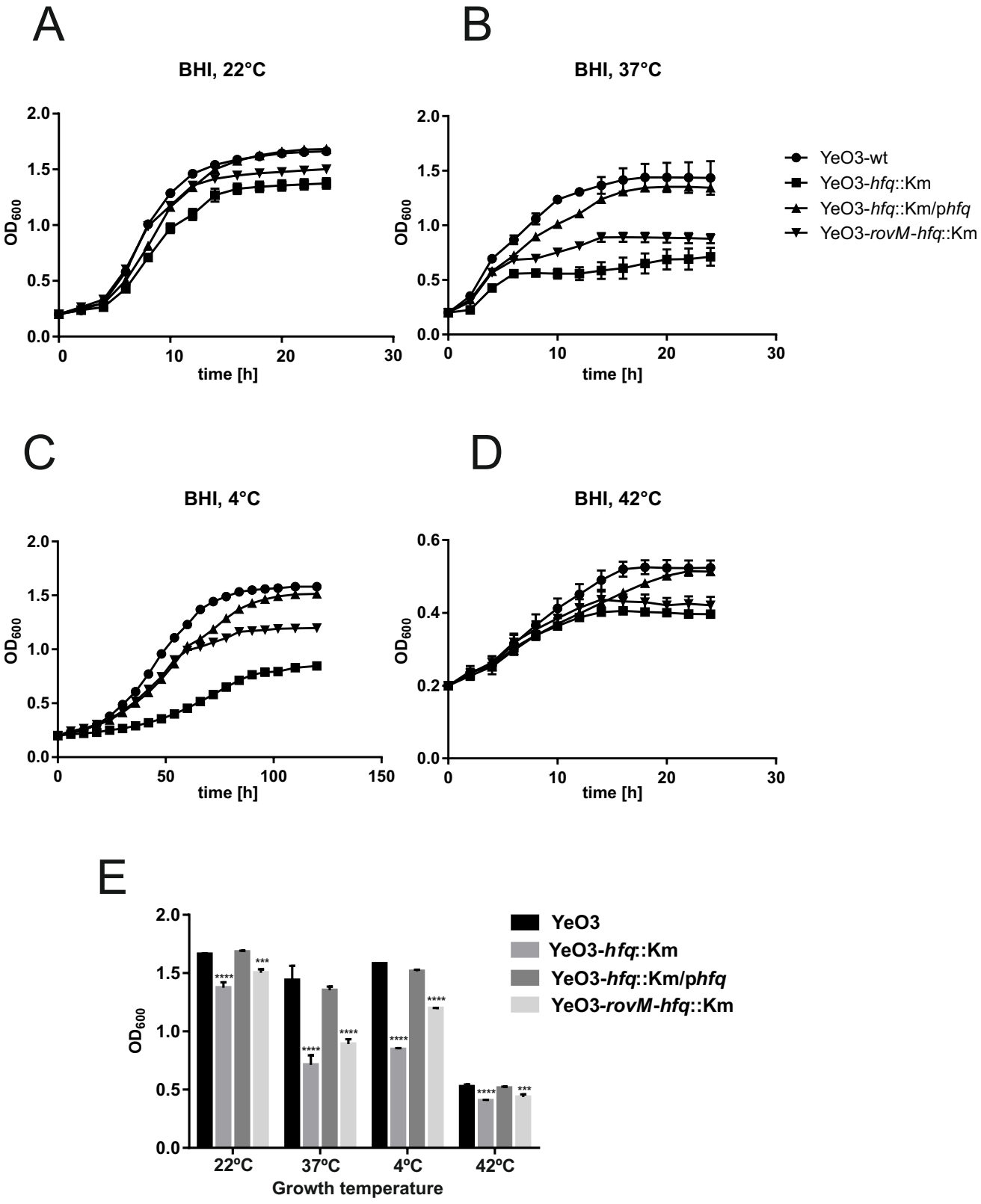
A
BHI, 22°C
B
BHI, 37°C
C
BHI, 4°C
D
BHI, 42°C
OD600
time [h]
YeO3-wt
YeO3-hfq::Km
YeO3-hfq::Km/phfq
YeO3-rovM-hfq::Km
E
YeO3
YeO3-hfq::Km
YeO3-hfq::Km/phfq
YeO3-rovM-hfq::Km
22ºC
37ºC
4ºC
42ºC
Growth temperature

Figure 4

A

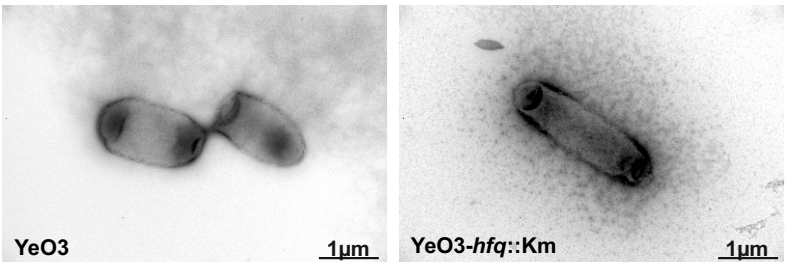
YeO3
1µm
YeO3-*hfq*::Km
1µm

B

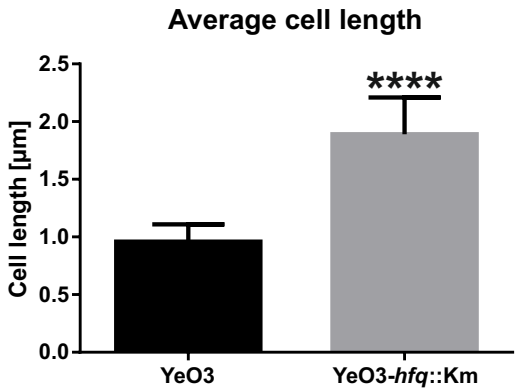
Average cell length
Cell length [µm]
2.5
2.0
1.5
1.0
0.5
0.0
****
YeO3
YeO3-*hfq*::Km

Figure 5

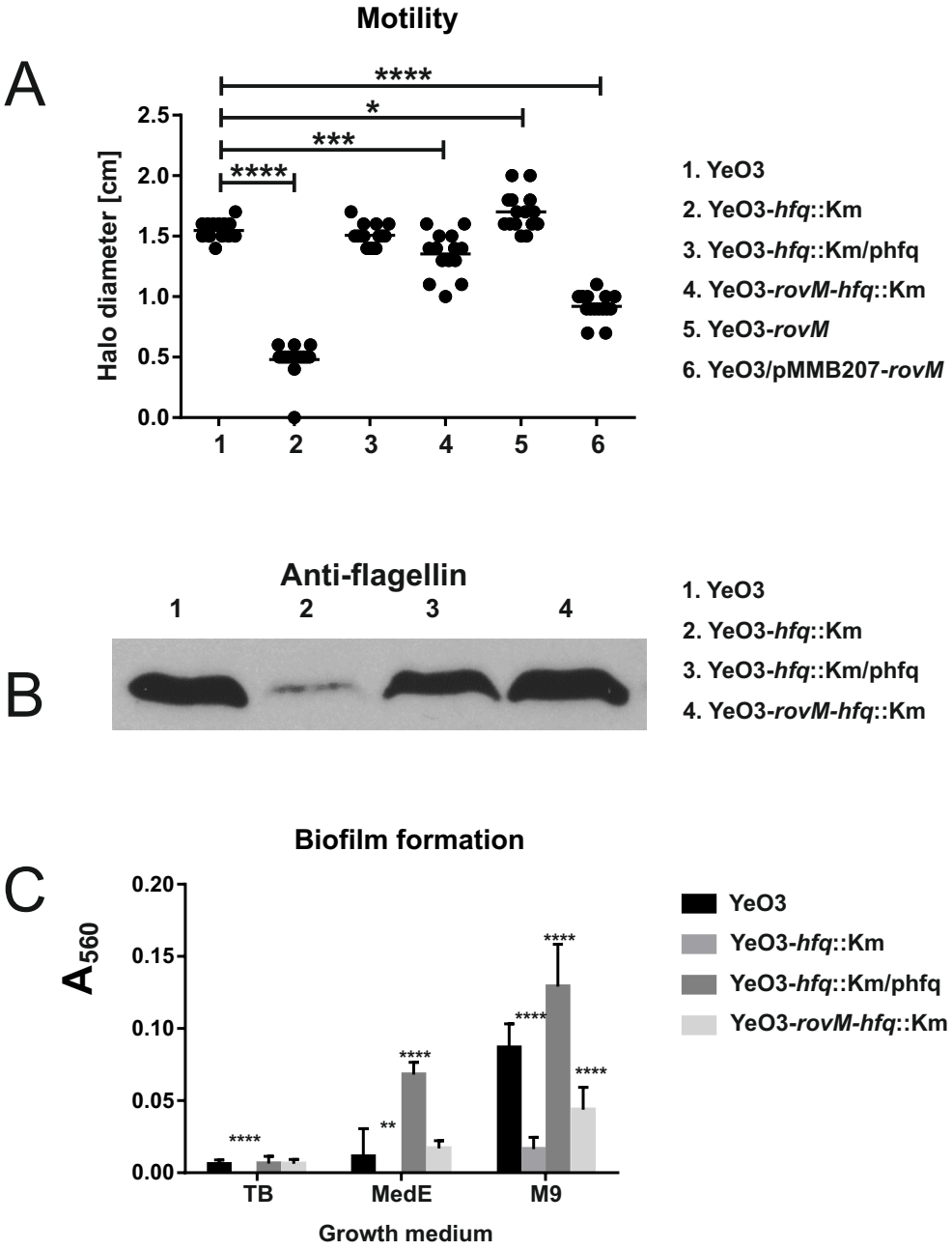
A
Motility
Halo diameter [cm]
2.5
2.0
1.5
1.0
0.5
0.0
****
*
***
****
1
2
3
4
5
6
1. YeO3
2. YeO3-hfq::Km
3. YeO3-hfq::Km/phfq
4. YeO3-rovM-hfq::Km
5. YeO3-rovM
6. YeO3/pMMB207-rovM
B
Anti-flagellin
1
2
3
4
1. YeO3
2. YeO3-hfq::Km
3. YeO3-hfq::Km/phfq
4. YeO3-rovM-hfq::Km
C
Biofilm formation
A560
0.20
0.15
0.10
0.05
0.00
****
**
****
****
****
****
TB
MedE
M9
Growth medium
YeO3
YeO3-hfq::Km
YeO3-hfq::Km/phfq
YeO3-rovM-hfq::Km

Figure 6

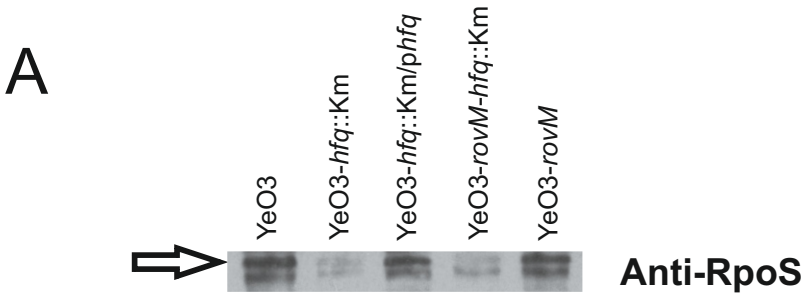
A
YeO3
YeO3-hfq::Km
YeO3-hfq::Km/phfq
YeO3-rovM-hfq::Km
YeO3-rovM
Anti-RpoS

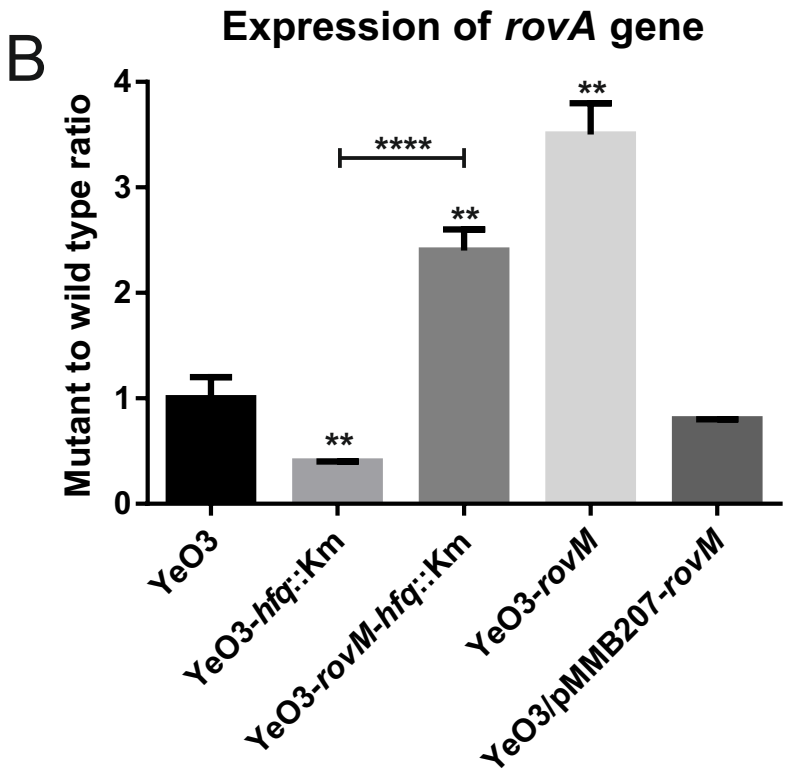
B
Expression of rovA gene
Mutant to wild type ratio
0
1
2
3
4
****
**
**
**
YeO3
YeO3-hfq::Km
YeO3-rovM-hfq::Km
YeO3-rovM
YeO3/pMMB207-rovM

Figure 7

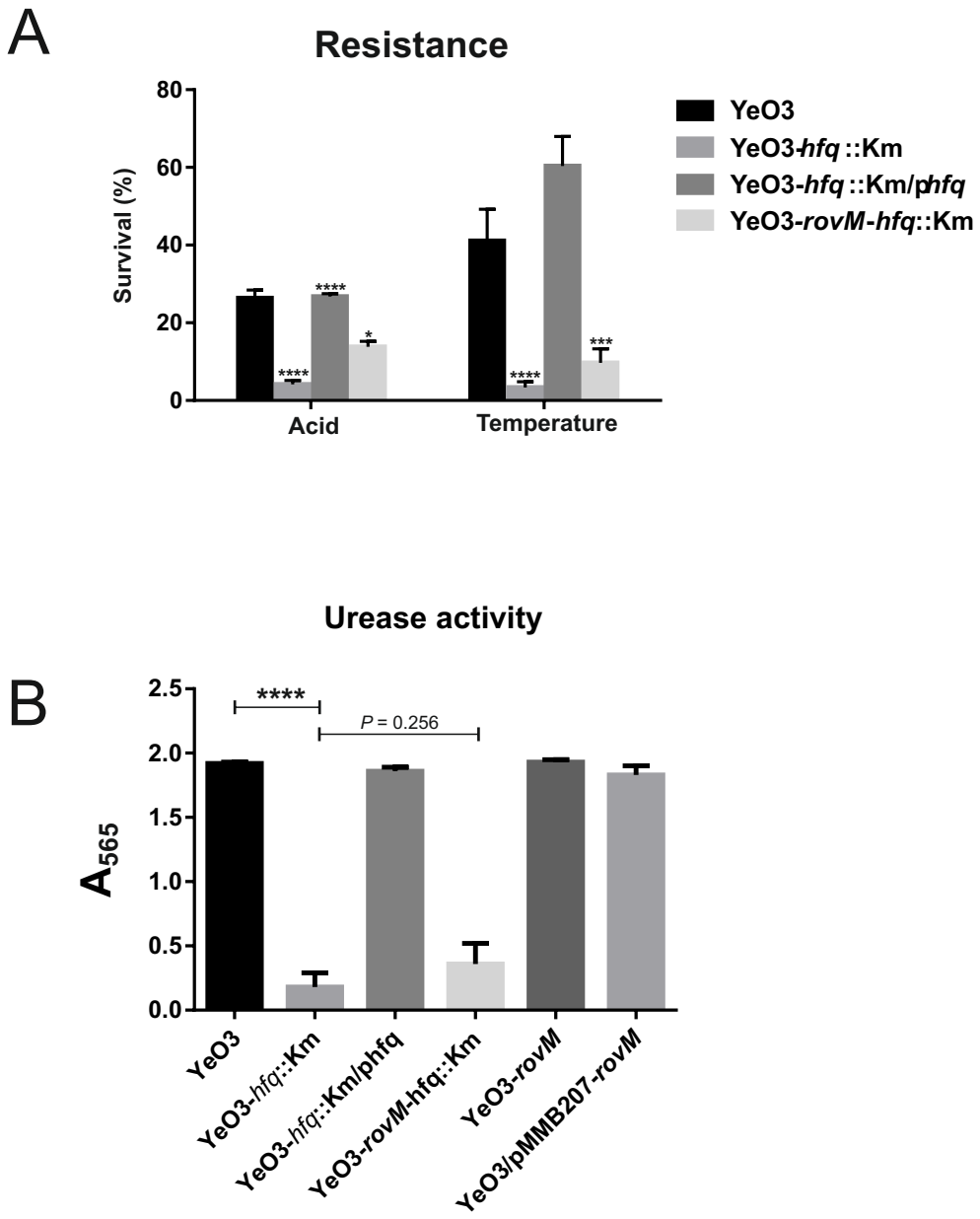
A
Resistance
Survival (%)
80
60
40
20
0
****
****
*
****
***
Acid
Temperature
YeO3
YeO3-hfq ::Km
YeO3-hfq ::Km/phfq
YeO3-rovM-hfq::Km
B
Urease activity
A565
2.5
2.0
1.5
1.0
0.5
0.0
****
P = 0.256
YeO3
YeO3-hfq::Km
YeO3-hfq::Km/phfq
YeO3-rovM-hfq::Km
YeO3-rovM
YeO3/pMMB207-rovM

Figure 8

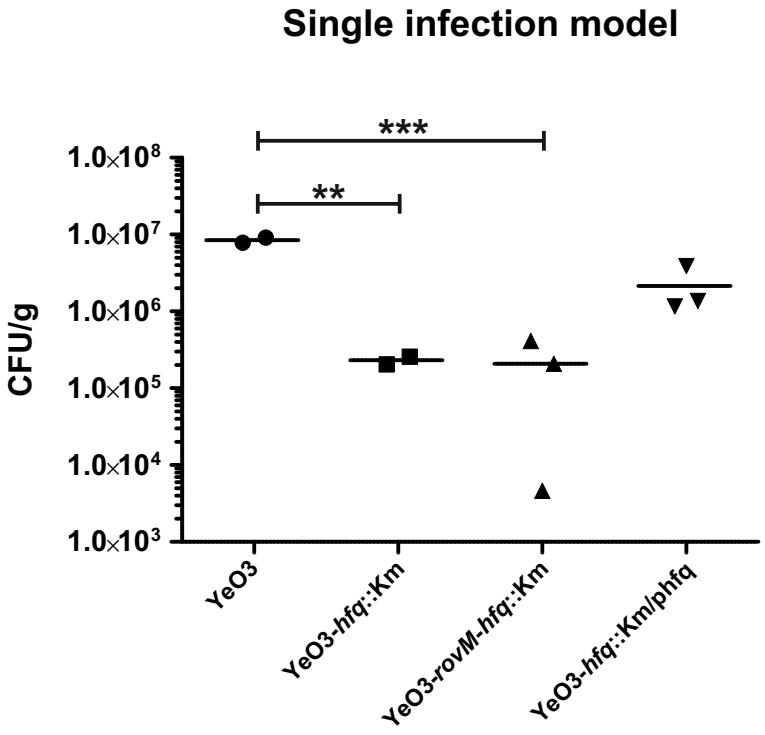
Single infection model
***
**
CFU/g
1.0×10^8
1.0×10^7
1.0×10^6
1.0×10^5
1.0×10^4
1.0×10^3
YeO3
YeO3-hfq::Km
YeO3-rovM-hfq::Km
YeO3-hfq::Km/phfq

Figure 9

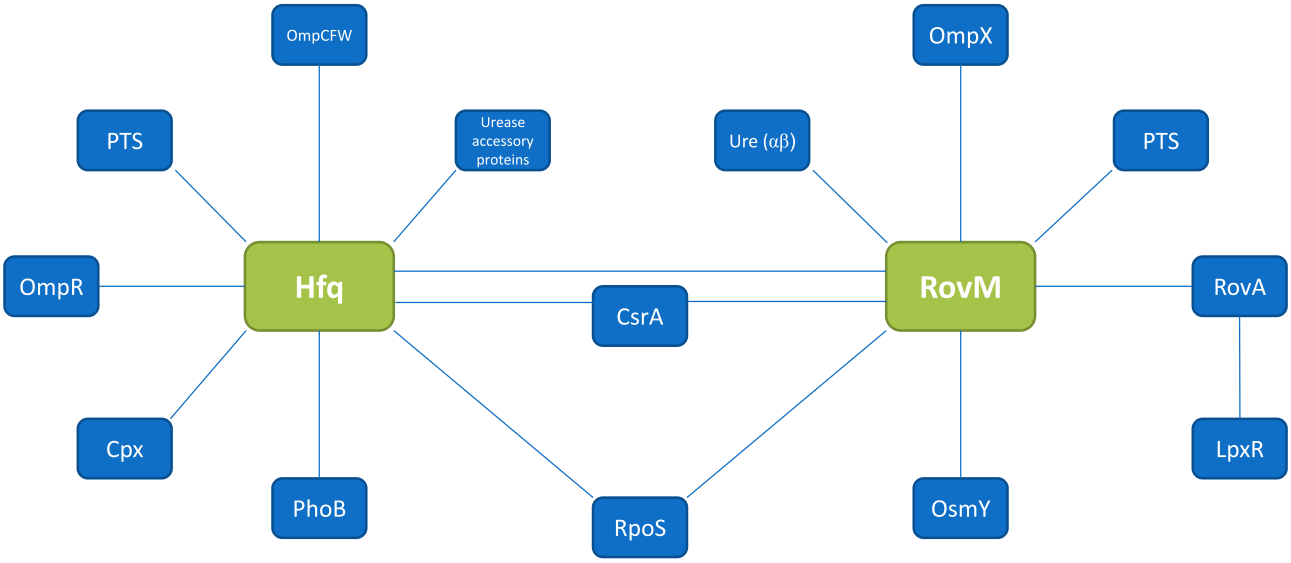
OmpCFW
PTS
Urease accessory proteins
OmpR
Hfq
CsrA
Cpx
PhoB
RpoS
OmpX
Ure (αβ)
PTS
RovM
RovA
LpxR
OsmY

SUPPLEMENTARY MATERIAL

Several Hfq-dependent alterations in physiology of *Yersinia enterocolitica* O:3 are mediated by derepression of the transcriptional regulator RovM

Katarzyna Leskinen[1], Maria I. Pajunen[1], Markku Varjosalo[2,3], Helena Fernández-Carrasco[4], José A. Bengoechea[4], and Mikael Skurnik[1,5*]

[1]Department of Bacteriology and Immunology, Medicum, Research Programs Unit, Immunobiology, University of Helsinki, Finland; [2]Institute of Biotechnology, University of Helsinki; [3]Biocentrum Helsinki, Finland: Finnish Institute of Molecular Medicine, Finland, [4]Centre for Experimental Medicine, Queens University Belfast. Belfast, UK, and [5]Division of Clinical Microbiology, Helsinki University Hospital, HUSLAB, Helsinki, Finland.

***Address for correspondence:**

Mikael Skurnik
P.O.Box 21 (Haartmaninkatu 3)
FIN-00014 UNIVERSITY OF HELSINKI
FINLAND
tel: +358-2491 26464
fax: +358-2941 26382
mikael.skurnik@helsinki.fi

Table S1. Genes differentially expressed between the wild type and the YeO3-*hfq*::Km mutant strains grown to logarithmic phase at RT. FC value is the ratio between the FPKM values of the YeO3-*hfq*::Km and wild-type strains. The values >1 indicate increase, while numbers <1 indicate decrease in the abundance of mRNA in the YeO3-*hfq*::Km strain.

GENE ID	GENE NAME	PROTEIN NAME	FC	P-VALUE
Y11_04281		Uncharacterized protein	**43,38**	0,0333
Y11_11701		Uncharacterized protein	**23,65**	0,0062
Y11_21001	*brnQ*	Branched-chain amino acid transport system carrier protein	**13,07**	0,0005
Y11_06951		Metal-dependent hydrolase related to alanyl-tRNA synthetase	**12,68**	0,0001
Y11_17401	*ompX*	Outer membrane protein X	**11,27**	0,0338
Y11_09491		Uncharacterized protein	**10,17**	0,0012
Y11_10651		Uncharacterized protein	**10,04**	0,0432
Y11_43201		Sorbitol-6-phosphate 2-dehydrogenase	**9,71**	0,0044
Y11_05361		PTS system, glucose-specific IIB component PTS system, glucose-specific IIC component	**9,46**	0,0010
Y11_31441		Glutamate dehydrogenase	**8,44**	0,0016
Y11_43221		PTS system, glucitol/sorbitol-specific IIB component and second of two IIC components	**7,95**	0,0425
Y11_02141	*rovM*	LysR family transcriptional regulator RovM (homolog of LrhA)	**7,77**	0,0485
Y11_43211		PTS system, glucitol/sorbitol-specific IIA component	**6,71**	0,0118
Y11_36101		tRNA dimethylallyltransferase	**6,10**	0,0017
Y11_28711		P pilus assembly/Cpx signaling pathway, periplasmic inhibitor/zinc-resistance associated protein	**5,91**	0,0038
Y11_03551		Serine transporter	**5,87**	0,0082
Y11_35641		Ferrichrome-iron receptor	**5,74**	0,0386
Y11_08251		Pyruvate kinase	**5,66**	0,0053
Y11_28731	*cpxA*	Copper sensory histidine kinase CpxA	**5,62**	0,0293
Y11_28111		Uncharacterized protein	**5,55**	0,0455
Y11_38291		Uncharacterized protein	**5,35**	0,0084
Y11_18531		Uncharacterized protein	**5,22**	0,0404
Y11_30051		50S ribosomal protein L34	**5,05**	0,0042
Y11_43191		Glucitol operon activator protein	**4,88**	0,0126
Y11_33791	*yifK*	Putative transport protein yifK	**4,71**	0,0135
Y11_28721	*cpxR*	Copper-sensing two-component system response regulator CpxR	**4,61**	0,0192
Y11_20991	*proY*	Proline-specific permease proY	**4,61**	0,0160
Y11_09481		Ng,NG-dimethylarginine dimethylaminohydrolase 1	**4,55**	0,0305
Y11_43231		PTS system, glucitol/sorbitol-specific IIC component	**4,51**	0,0049
Y11_23531		Uncharacterized protein	**4,47**	0,0050
Y11_26721		4-hydroxy-2-oxoglutarate aldolase	**4,24**	0,0321
Y11_27691	*malM*	Maltose operon periplasmic protein MalM	**4,19**	0,0049
Y11_19721	*ybbP*	Uncharacterized metabolite ABC transporter in Enterobacteriaceae	**4,10**	0,0054
Y11_18681		Membrane protein	**4,02**	0,0121
Y11_06251		Ferrichrome-iron receptor	**3,96**	0,0094
Y11_42751	*hscA*	Chaperone protein HscA (Hsc66)	**3,92**	0,0190
Y11_03541		L-serine dehydratase (EC 4.3.1.17)	**3,90**	0,0002
Y11_06341		L-serine dehydratase	**3,89**	0,0200

Y11_18211		Putative phosphatase	**3,88**	0,0045
Y11_03521		D-alanyl-D-alanine carboxypeptidase	**3,74**	0,0002
Y11_24931		Similarity with glutathionylspermidine synthase, group 1	**3,73**	0,0045
Y11_12371		Calcium/proton antiporter	**3,67**	0,0349
Y11_08531		Uncharacterized protein	**3,63**	0,0215
Y11_34111		Uncharacterized protein	**3,61**	0,0400
Y11_31951	*malT*	HTH-type transcriptional regulator MalT	**3,59**	0,0128
Y11_42711		Cysteine desulfurase	**3,57**	0,0068
Y11_40101		Peptide chain release factor 2 programmed frameshift-containing	**3,52**	0,0489
Y11_34551		Uncharacterized protein	**3,50**	0,0473
Y11_24921		UPF0441 protein Y11_24921	**3,48**	0,0082
Y11_38781		Uncharacterized protein	**3,47**	0,0126
Y11_18521	*ybgE*	Protein ybgE	**3,47**	0,0397
Y11_35161		Proton/glutamate symport protein @ Proton/aspartate symport protein	**3,47**	0,0413
Y11_42831		Uncharacterized protein	**3,46**	0,0374
Y11_41341		Methionine ABC transporter ATP-binding protein	**3,45**	0,0232
Y11_26001		Alcohol dehydrogenase	**3,32**	0,0357
Y11_05101		Putative membrane protein	**3,31**	0,0306
Y11_02761	*ampH*	Penicillin-binding protein AmpH	**3,27**	0,0100
Y11_27341		Lipid A biosynthesis lauroyl acyltransferase	**3,16**	0,0035
Y11_15331		Apo-citrate lyase phosphoribosyl-dephospho-CoA transferase	**3,15**	0,0332
Y11_33801	*yifK*	Putative transport protein yifK	**3,14**	0,0070
Y11_07411		Putative DNA-binding protein	**3,13**	0,0283
Y11_19791	*ybbK*	Putative activity regulator of membrane protease YbbK	**3,12**	0,0328
Y11_19731		Uncharacterized metabolite ABC transporter in Enterobacteriaceae	**3,09**	0,0304
Y11_19751		Arylesterase	**3,06**	0,0148
Y11_08241	*ycfS*	L,D-transpeptidase YcfS	**3,06**	0,0008
Y11_20961		Gamma-glutamyltranspeptidase (EC 2.3.2.2)	**3,02**	0,0212
Y11_33081		50S ribosomal protein L36	**2,99**	0,0274
Y11_17341		Uncharacterized protein	**2,99**	0,0067
Y11_06461		Uncharacterized protein	**2,97**	0,0284
Y11_18671		Membrane protein	**2,93**	0,0159
Y11_00741		Phosphocarrier protein of PTS system	**2,90**	0,0033
Y11_02301		Uncharacterized protein	**2,89**	0,0435
Y11_20081		Uncharacterized protein	**2,86**	0,0260
Y11_16641		Glycosyl transferase, group 1 family protein	**2,85**	0,0177
Y11_27701		Maltoporin (Maltose-inducible porin)	**2,77**	0,0213
Y11_19781	*ybbK*	Putative stomatin/prohibitin-family membrane protease subunit YbbK	**2,76**	0,0278
Y11_29421	*dsbA*	Thiol:disulfide interchange protein DsbA	**2,74**	0,0145
Y11_18541		Cytochrome d ubiquinol oxidase subunit II	**2,71**	0,0032
Y11_39291		Transcriptional repressor for pyruvate dehydrogenase complex	**2,70**	0,0290
Y11_23071	*argO*	Arginine exporter protein ArgO	**2,69**	0,0453
Y11_40541		Putative sugar transport protein	**2,66**	0,0151
Y11_28811		2,3-bisphosphoglycerate-independent phosphoglycerate mutase	**2,65**	0,0144

Y11_10641		DNA topoisomerase	**2,65**	0,0017
Y11_10861		Probable intracellular septation protein A	**2,62**	0,0145
Y11_21821		Inner membrane component of tripartite multidrug resistance system	**2,59**	0,0403
Y11_18551		Cytochrome d ubiquinol oxidase subunit I	**2,59**	0,0340
Y11_35851	*dcuA*	C4-dicarboxylate transporter DcuA	**2,59**	0,0026
Y11_11021		Alcohol dehydrogenase Acetaldehyde dehydrogenase	**2,56**	0,0036
Y11_15341		Citrate lyase alpha chain	**2,56**	0,0016
Y11_15311		Citrate Succinate antiporter	**2,54**	0,0179
Y11_22021		Putative Dcu family, anaerobic C4-dicarboxylate transporter	**2,53**	0,0019
Y11_36541		Octaprenyl-diphosphate synthase	**2,52**	0,0367
Y11_10511		Putative exported protein YPO2521	**2,50**	0,0116
Y11_41571	*nrdH*	Glutaredoxin-like protein NrdH	**2,49**	0,0007
Y11_07461		Transposase	**2,44**	0,0488
Y11_26681		Uncharacterized protein	**2,42**	0,0213
Y11_27251		tRNA-dihydrouridine synthase	**2,41**	0,0445
Y11_23821		Inosine-uridine preferring nucleoside hydrolase	**2,41**	0,0005
Y11_09111		NAD(P) transhydrogenase subunit beta	**2,37**	0,0151
Y11_42701	*iscR*	HTH-type transcriptional regulator IscR	**2,35**	0,0113
Y11_10991		Periplasmic oligopeptide-binding protein	**2,33**	0,0435
Y11_09101		NAD(P) transhydrogenase alpha subunit	**2,28**	0,0036
Y11_26581		Endoribonuclease L-PSP	**2,28**	0,0022
Y11_10911		Uncharacterized protein	**2,27**	0,0136
Y11_31101		Dipeptide-binding ABC transporter, periplasmic substrate-binding component	**2,26**	0,0201
Y11_16081		Putative cobalt-precorrin-6A synthase	**2,23**	0,0195
Y11_27741	*malG*	Maltose/maltodextrin ABC transporter, permease protein MalG	**2,23**	0,0033
Y11_15371		[citrate [pro-3S]-lyase] ligase	**2,22**	0,0335
Y11_02521		Tyrosine-specific transport protein	**2,22**	0,0349
Y11_19861		Fosmidomycin resistance protein	**2,22**	0,0284
Y11_05501		NADH dehydrogenase	**2,20**	0,0180
Y11_04161		L-asparaginase	**2,19**	0,0494
Y11_19171		Uncharacterized protein	**2,18**	0,0036
Y11_09691		Uncharacterized protein	**2,17**	0,0106
Y11_03591		Putative membrane protein	**2,17**	0,0080
Y11_01741		Permease of the drug/metabolite transporter (DMT) superfamily	**2,14**	0,0191
Y11_00731		Phosphoenolpyruvate-protein phosphotransferase	**2,14**	0,0019
Y11_38401	*yaaH*	Yaah protein	**2,13**	0,0419
Y11_25171		Phage protein	**2,13**	0,0198
Y11_39351		TonB-dependent receptor Outer membrane receptor for ferric enterobactin and colicins B, D	**2,12**	0,0418
Y11_15991		Substrate-specific component CbiM of cobalt ECF transporter	**2,12**	0,0137
Y11_34101		Glycerol-3-phosphate transporter	**2,11**	0,0030
Y11_32501		Peptidyl-prolyl cis-trans isomerase	**2,11**	0,0427
Y11_11711		4-hydroxy-2-oxoglutarate aldolase 2-dehydro-3-deoxyphosphogluconate aldolase	**2,10**	0,0130
Y11_33881		Adenylate cyclase	**2,07**	0,0233
Y11_17681		Uncharacterized protein	**2,05**	0,0166

Y11_15351		Citrate lyase beta chain	**2,05**	0,0156
Y11_19301	*lipA*	Lipoyl synthase	**2,04**	0,0091
Y11_31711		Inositol 2-dehydrogenase	**2,04**	0,0048
Y11_42761		Ferredoxin, 2Fe-2S	**2,03**	0,0189
Y11_31691		5-keto-2-deoxygluconokinase uncharacterized domain	**2,03**	0,0001
Y11_10711		Pseudouridine synthase	**2,01**	0,0229
Y11_24131	*fliS*	Flagellar biosynthesis protein FliS	**0,50**	0,0448
Y11_28381	*sbp*	Sulfate-binding protein Sbp	**0,50**	0,0345
Y11_20231		Uncharacterized protein	**0,50**	0,0439
Y11_14211	*fliG*	Flagellar motor switch protein FliG	**0,50**	0,0295
Y11_41891		Eukaryotic-type low-affinity urea transporter	**0,50**	0,0052
Y11_27361	*pqaA*	Phop/Q-regulated protein PqaA	**0,50**	0,0164
Y11_35151	*acs*	Acetyl-coenzyme A synthetase	**0,50**	0,0306
Y11_14071	*fliD*	Flagellar hook-associated protein FliD	**0,50**	0,0321
Y11_28701		Integrase	**0,50**	0,0119
Y11_32951		50S ribosomal protein L16	**0,50**	0,0013
Y11_13781		N-acetylneuraminate epimerase	**0,49**	0,0125
Y11_20321		Putative cytoplasmic protein	**0,49**	0,0318
Y11_42461		tRNA-specific adenosine-34 deaminase	**0,49**	0,0371
Y11_15051		Transposase	**0,49**	0,0002
Y11_03481		Methionine ABC transporter ATP-binding protein	**0,49**	0,0256
Y11_14401	*flgF*	Flagellar basal-body rod protein FlgF	**0,49**	0,0250
Y11_38881		Putative transcriptional activator for leuABCD operon	**0,49**	0,0261
Y11_23341	*pilT*	Twitching motility protein PilT	**0,49**	0,0133
Y11_16781		Glucose-1-phosphate thymidylyltransferase	**0,48**	0,0202
Y11_15131		Putative two-component response regulator	**0,48**	0,0315
Y11_33141		Putative cytoplasmic protein	**0,48**	0,0457
Y11_42011		PTS system, chitobiose-specific IIB component	**0,48**	0,0231
Y11_33511		Colicin	**0,48**	0,0057
Y11_14891		Putative histidine acid phosphatase	**0,47**	0,0204
Y11_30211		Putative transport protein Y11_30211	**0,47**	0,0082
Y11_16901		Putative sugar ABC transporter	**0,47**	0,0211
Y11_24211		Uncharacterized protein	**0,47**	0,0223
Y11_09381		Inositol-1-monophosphatase	**0,47**	0,0366
Y11_31351	*yhjG*	Uncharacterized protein YhjG	**0,47**	0,0004
Y11_15581		Argininosuccinate synthase	**0,47**	0,0254
Y11_16211		Propanediol dehydratase reactivation factor small subunit	**0,47**	0,0173
Y11_11011		Putative membrane protein	**0,47**	0,0232
Y11_14471	*flgN*	Flagellar biosynthesis protein FlgN	**0,47**	0,0376
Y11_14381		Flagellar L-ring protein	**0,47**	0,0376
Y11_13861		Uncharacterized protein	**0,46**	0,0096
Y11_06611		Cytosine permease	**0,46**	0,0182
Y11_41751		Nickel ABC transporter, periplasmic nickel-binding protein nikA2	**0,46**	0,0196
Y11_39571		C4-type zinc finger protein, DksA/TraR family	**0,46**	0,0005

Y11_16141		Propanediol diffusion facilitator	**0,46**	0,0073
Y11_28951	*mutM*	Formamidopyrimidine-DNA glycosylase	**0,46**	0,0021
Y11_14251	*fliK*	Flagellar hook-length control protein FliK	**0,46**	0,0446
Y11_40791		Amino-acid acetyltransferase	**0,46**	0,0076
Y11_08951		Uncharacterized protein	**0,45**	0,0106
Y11_18591		Dihydrolipoamide succinyltransferase component (E2) of 2-oxoglutarate dehydrogenase complex	**0,45**	0,0186
Y11_23911		Putative outer membrane lipoprotein	**0,45**	0,0427
Y11_15421	*uhpC*	Hexose phosphate uptake regulatory protein UhpC	**0,45**	0,0387
Y11_21061		Rok family Glucokinase with ambiguous substrate specificity	**0,45**	0,0103
Y11_41961		Protein CrcB homolog	**0,45**	0,0151
Y11_11081		Uncharacterized protein	**0,45**	0,0099
Y11_16911		Uncharacterized protein	**0,45**	0,0233
Y11_37631	*lsrR*	Lsrr, transcriptional repressor of lsr operon	**0,44**	0,0310
Y11_23741		O-demethylpuromycin-O-methyltransferase	**0,44**	0,0234
Y11_00471		Acetyltransferase Y11_00471	**0,44**	0,0092
Y11_13961	*fliY*	Cystine ABC transporter, periplasmic cystine-binding protein FliY	**0,44**	0,0094
Y11_22861		Siroheme synthase	**0,44**	0,0206
Y11_22921		Sulfite reductase [NADPH] flavoprotein alpha-component (SiR-FP)	**0,44**	0,0125
Y11_06681		Hydrolase (HAD superfamily)	**0,43**	0,0223
Y11_37671	*arcD*	Arginine/ornithine antiporter ArcD	**0,43**	0,0276
Y11_00561		N-acetylmannosamine kinase	**0,43**	0,0199
Y11_13991	*fliZ*	Flagellar biosynthesis protein FliZ	**0,43**	0,0217
Y11_37711		Glycerol dehydrogenase	**0,43**	0,0109
Y11_42561		Putative transport system permease protein	**0,42**	0,0252
Y11_01841		Colicin V production protein	**0,42**	0,0055
Y11_13791		Uncharacterized protein	**0,42**	0,0370
Y11_01201	*yceI*	Protein yceI	**0,42**	0,0044
Y11_26511	*yhbH*	Ribosome hibernation protein YhbH	**0,42**	0,0428
Y11_05681		Isocitrate dehydrogenase [NADP]	**0,42**	0,0145
Y11_03191		Proteinase inhibitor	**0,42**	0,0026
Y11_16261	*pduN*	Propanediol utilization polyhedral body protein PduN	**0,42**	0,0424
Y11_24121		Uncharacterized protein	**0,42**	0,0006
Y11_00341		Nitrate/nitrite response regulator protein	**0,41**	0,0034
Y11_14261	*fliL*	Flagellar biosynthesis protein FliL	**0,41**	0,0419
Y11_27871		Transposase	**0,41**	0,0147
Y11_10941		UPF0263 protein Y11_10941	**0,41**	0,0236
Y11_00611	*cysP*	Sulfate and thiosulfate binding protein CysP	**0,41**	0,0005
Y11_07251		Uncharacterized protein	**0,41**	0,0250
Y11_27021		Putative exported protein	**0,41**	0,0242
Y11_10811		Putative lipoprotein	**0,40**	0,0116
Y11_01621		PTS system, cellobiose-specific IIB component	**0,40**	0,0301
Y11_18571		Succinyl-CoA ligase [ADP-forming] subunit alpha	**0,40**	0,0182
Y11_37141		Pe_PGRS (Wag22)	**0,40**	0,0032
Y11_20481		Putative exported protein	**0,40**	0,0157

Y11_31361		CDP-diacylglycerol pyrophosphatase	**0,40**	0,0003
Y11_34741		3-ketoacyl-CoA thiolase	**0,40**	0,0116
Y11_21561		Methylthioribose kinase (MTR kinase)	**0,39**	0,0392
Y11_02911		Carbonic anhydrase	**0,39**	0,0061
Y11_22751	*nlpD*	Lipoprotein NlpD	**0,39**	0,0030
Y11_28091		N-acetyl-gamma-glutamyl-phosphate reductase	**0,39**	0,0336
Y11_17891		Transglycosylase associated protein	**0,38**	0,0213
Y11_08771		Uncharacterized protein	**0,38**	0,0136
Y11_35701	*hmuS*	Hemin transport protein HmuS	**0,38**	0,0338
Y11_41511	*proX*	L-proline glycine betaine binding ABC transporter protein ProX	**0,38**	0,0142
Y11_16951		Cytidine deaminase	**0,37**	0,0396
Y11_13911		Transcriptional repressor of PutA and PUTP Proline dehydrogenase (Proline oxidase) Delta-1-pyrroline-5-carboxylate dehydrogenase	**0,37**	0,0015
Y11_31811		Alpha-acetolactate decarboxylase	**0,37**	0,0498
Y11_08901	*sapB*	Peptide transport system permease protein sapB	**0,37**	0,0230
Y11_07291		Sigma-fimbriae chaperone protein	**0,37**	0,0371
Y11_19521		Uncharacterized protein	**0,37**	0,0091
Y11_30841		Maltoporin	**0,37**	0,0108
Y11_19161		Uncharacterized protein	**0,37**	0,0255
Y11_35711		TonB-dependent hemin , ferrichrome receptor	**0,37**	0,0072
Y11_41881	*ureD*	Urease accessory protein UreD	**0,36**	0,0187
Y11_22911		Sulfite reductase [NADPH] hemoprotein beta-component	**0,36**	0,0032
Y11_22981		Superoxide dismutase [Cu-Zn]	**0,36**	0,0287
Y11_02411		Elab protein	**0,36**	0,0205
Y11_02091		Uncharacterized protein	**0,36**	0,0422
Y11_25641		Putative glutamate/gamma-aminobutyrate antiporter	**0,36**	0,0286
Y11_33331	*ytfQ*	Putative sugar ABC transport system, periplasmic binding protein YtfQ	**0,36**	0,0023
Y11_43241		Probable lipid kinase YegS-like	**0,36**	0,0290
Y11_18611		Succinate dehydrogenase iron-sulfur protein	**0,36**	0,0009
Y11_21031	*phoB*	Phosphate regulon transcriptional regulatory protein PhoB (SphR)	**0,35**	0,0062
Y11_13931		Uncharacterized protein	**0,34**	0,0199
Y11_32651	*tauB*	Taurine transport ATP-binding protein TauB	**0,34**	0,0186
Y11_15491		Transcriptional regulator, TetR family	**0,34**	0,0140
Y11_36371	*ytfJ*	Protein ytfJ	**0,34**	0,0116
Y11_04041		Transposase	**0,34**	0,0019
Y11_21231		Maltose-6'-phosphate glucosidase	**0,34**	0,0023
Y11_04261		Uncharacterized protein	**0,34**	0,0301
Y11_42871		Nucleoside diphosphate kinase	**0,33**	0,0138
Y11_14191	*fliE*	Flagellar hook-basal body complex protein FliE	**0,33**	0,0309
Y11_42621		Flavohemoprotein	**0,33**	0,0192
Y11_20901		Putative signal peptide protein	**0,33**	0,0288
Y11_14081	*fliS*	Flagellar biosynthesis protein FliS	**0,32**	0,0115
Y11_07041		Uncharacterized protein	**0,32**	0,0253
Y11_11281	*msrB*	Peptide methionine sulfoxide reductase MsrB	**0,32**	0,0422
Y11_36511		Arginine repressor	**0,32**	0,0090

Y11_18631		Succinate dehydrogenase hydrophobic membrane anchor protein	**0,32**	0,0460
Y11_10481		Transposase	**0,32**	0,0265
Y11_17471		DNA protection during starvation protein	**0,32**	0,0042
Y11_14701	*uspC*	Universal stress protein C	**0,31**	0,0238
Y11_31451	*uspA*	Universal stress protein A	**0,31**	0,0249
Y11_35141		Putative membrane protein, clustering with ACTP	**0,31**	0,0045
Y11_41861	*ureF*	Urease accessory protein UreF	**0,31**	0,0436
Y11_14411	*flgE*	Flagellar hook protein FlgE	**0,31**	0,0014
Y11_37491		Cytosine permease	**0,31**	0,0061
Y11_08601		Uncharacterized protein	**0,30**	0,0053
Y11_21381		Glycerophosphoryl diester phosphodiesterase family protein	**0,30**	0,0116
Y11_00751		Cysteine synthase	**0,30**	0,0031
Y11_14141		Uncharacterized protein	**0,30**	0,0170
Y11_43061		2-keto-D-gluconate dehydrogenase,membrane-bound, gamma subunit	**0,30**	0,0419
Y11_14451	*flgA*	Flagellar basal-body P-ring formation protein FlgA	**0,30**	0,0068
Y11_41851	*ureE*	Urease accessory protein UreE	**0,30**	0,0127
Y11_11071	*hnr*	Hnr protein	**0,30**	0,0025
Y11_11581		Uncharacterized protein	**0,30**	0,0009
Y11_22831		Adenylyl-sulfate kinase	**0,30**	0,0376
Y11_36341	*ytfE*	Iron-sulfur cluster repair protein YtfE	**0,30**	0,0053
Y11_30641	*xylR*	Xylose activator XylR	**0,29**	0,0113
Y11_03421		TonB-dependent receptor Outer membrane receptor for ferrienterochelin and colicins	**0,29**	0,0020
Y11_20571	*bolA*	Cell division protein BolA	0,29	0,0171
Y11_18641		Succinate dehydrogenase cytochrome b-556 subunit	**0,29**	0,0240
Y11_00641	*cysA*	Sulfate and thiosulfate import ATP-binding protein CysA	**0,29**	0,0023
Y11_16151	*pduA*	Propanediol utilization polyhedral body protein PduA	**0,29**	0,0313
Y11_38001	*osmY*	Osmotically inducible protein OsmY	**0,29**	0,0107
Y11_27851		Malate synthase	**0,28**	0,0249
Y11_22851		Sulfate adenylyltransferase subunit 2	**0,28**	0,0319
Y11_32641	*tauA*	Taurine-binding periplasmic protein TauA	**0,28**	0,0220
Y11_22741		RNA polymerase sigma factor	**0,28**	0,0217
Y11_24541		Cobalt-zinc-cadmium resistance protein CzcA Cation efflux system protein CusA	**0,27**	0,0058
Y11_17531		Putative chemotactic transducer	**0,27**	0,0084
Y11_41871	*ureG*	Urease accessory protein UreG	**0,27**	0,0364
Y11_13031		ISPsy4, transposition helper protein	**0,26**	0,0001
Y11_21281	*crl*	Sigma factor-binding protein crl	**0,26**	0,0054
Y11_12731		Chloramphenicol acetyltransferase	**0,26**	0,0099
Y11_00891		Pyruvate decarboxylase Alpha-keto-acid decarboxylase	**0,26**	0,0181
Y11_41841	*ureC*	Urease subunit alpha	**0,25**	0,0130
Y11_08981		Putative phage protein	**0,25**	0,0184
Y11_41911		Putative exported protein	**0,25**	0,0097
Y11_11411		Alanine racemase, catabolic	**0,24**	0,0400
Y11_03471		Lipoprotein	**0,24**	0,0003
Y11_23861	*proP*	L-proline/Glycine betaine transporter ProP	**0,24**	0,0044

Y11_42571		Uncharacterized protein	**0,24**	0,0100
Y11_22841		Sulfate adenylyltransferase subunit 1	**0,24**	0,0053
Y11_07101	*cutC*	Copper homeostasis protein CutC	**0,23**	0,0003
Y11_14431	*flgC*	Flagellar basal-body rod protein FlgC	**0,23**	0,0177
Y11_14441	*flgB*	Flagellar basal body rod protein FlgB	**0,23**	0,0029
Y11_17971		Uncharacterized protein	**0,23**	0,0004
Y11_32031		Putative exported protein	**0,23**	0,0003
Y11_00481	*ygiW*	Protein ygiW	**0,23**	0,0003
Y11_14421	*flgD*	Flagellar basal-body rod modification protein FlgD	**0,23**	0,0200
Y11_13821	*efeB*	Ferrous iron transport peroxidase EfeB	**0,22**	0,0014
Y11_31821	*alsR*	Transcriptional regulator of alpha-acetolactate operon alsR	**0,22**	0,0454
Y11_31291		C4-dicarboxylate transport protein	**0,22**	0,0235
Y11_23491		Ornithine decarboxylase	**0,21**	0,0431
Y11_03461		2-oxobutyrate oxidase, putative	**0,21**	0,0134
Y11_07311		Sigma-fimbriae uncharacterized paralogous subunit	**0,20**	0,0366
Y11_06711		Putative uroporphyrin-III c-methyltransferase	**0,20**	0,0049
Y11_37461		Acetyltransferase	**0,19**	0,0365
Y11_18351		Putative starvation-inducible protein	**0,19**	0,0289
Y11_34521		5-methyltetrahydropteroyltriglutamate--homocysteine methyltransferase	**0,19**	0,0011
Y11_01871	*hisJ*	Histidine ABC transporter, histidine-binding periplasmic protein HisJ	**0,18**	0,0402
Y11_02741	*ompC*	Outer membrane protein C	**0,18**	0,0098
Y11_30181	*ibpB*	Small heat shock protein IbpB	**0,18**	0,0199
Y11_25651		Glutamate decarboxylase	**0,18**	0,0011
Y11_41831	*ureB*	Urease subunit beta	**0,18**	0,0056
Y11_14721		Mg(2+) transport ATPase protein B	**0,18**	0,0295
Y11_13831		Ferrous iron transport periplasmic protein EfeO,contains peptidase-M75 domain and (Frequently) cupredoxin-like domain	**0,17**	0,0112
Y11_30171		16 kDa heat shock protein A	**0,17**	0,0407
Y11_13841	*efeU*	Ferrous iron transport permease EfeU	**0,17**	0,0023
Y11_11421		D-amino acid dehydrogenase small subunit	**0,16**	0,0424
Y11_02701	*hlyD*	Hlyd family secretion protein	**0,16**	0,0347
Y11_14001	*fliA*	RNA polymerase sigma factor	**0,16**	0,0108
Y11_25661		Glutamate decarboxylase	**0,14**	0,0050
Y11_17621		Aquaporin Z	**0,14**	0,0246
Y11_25681	*hdeD*	Hded protein	**0,14**	0,0150
Y11_18791		Putative exported protein	**0,13**	0,0117
Y11_36161	*yjeT*	Putative inner membrane protein YjeT	**0,13**	0,0034
Y11_08441	*rovA*	Transcriptional regulator RovA (homolog of SlyA)	**0,13**	0,0006
Y11_36151	*hflC*	Hflc protein	**0,13**	0,0313
Y11_41821	*ureA*	Urease subunit gamma	**0,12**	0,0015
Y11_36141	*hflK*	Hflk protein	**0,12**	0,0004
Y11_08991		Putative DNA-binding phage-related protein	**0,09**	0,0464
Y11_28041	*hasA*	Hemophore HasA	**0,08**	0,0023
Y11_14881		Uncharacterized protein	**0,06**	0,0166
Y11_36131	*hflX*	GTPase HflX	**0,05**	0,0070

Table S2. Genes differentially expressed at 37°C in YeO3-*hfq*::Km mutant strain. FC values displayed as ratios that represent the mRNA or protein abundance in YeO3-*hfq*::Km mutant compared with that in the wild-type strain. Values >1 indicate increase, while numbers <1 indicate decrease in the abundance of mRNA in *hfq*::Km strain.

GENE ID	GENE NAME	PROTEIN NAME	FC	P-VALUE
Y11_02141	*rovM*	LysR family transcriptional regulator RovM (homolog of LrhA)	**39,82**	0,0031
Y11_39491		Uncharacterized protein	**21,43**	0,0139
Y11_11991		PTS system, N-acetylgalactosamine-specific IIC component	**18,80**	0,0054
Y11_24181		Uncharacterized protein	**17,82**	0,0018
Y11_28711		P pilus assembly/Cpx signaling pathway,periplasmic inhibitor/zinc-resistance associated protein	**17,39**	0,0002
Y11_11701		Uncharacterized protein	**16,71**	0,0275
Y11_17401	*ompX*	Outer membrane protein X	**16,33**	0,0027
Y11_12671		Uncharacterized protein	**13,15**	0,0113
Y11_21951		Uncharacterized protein	**12,19**	0,0151
Y11_41311	*rcsF*	Protein RcsF	**12,03**	0,0370
Y11_06071		Putative membrane protein	**12,03**	0,0361
Y11_10511		Putative exported protein YPO2521	**11,95**	0,0204
Y11_07461		Transposase	**11,34**	0,0236
Y11_02301		Uncharacterized protein	**11,16**	0,0051
Y11_11291		Uncharacterized protein	**10,32**	0,0245
Y11_04161		L-asparaginase	**10,14**	0,0020
Y11_11981		PTS system, N-acetylgalactosamine-specific IIB component	**9,52**	0,0064
Y11_24501		Uncharacterized protein	**9,48**	0,0030
Y11_06881		Similar to ABC transporter: eg YBJZ_ECOLI hypothetical ABC transporter	**9,35**	0,0385
Y11_04151		L-asparaginase	**9,29**	0,0029
Y11_09491		Uncharacterized protein	**9,18**	0,0144
Y11_15091	*sbcC*	Exonuclease SbcC	**9,10**	0,0069
Y11_10181		Uncharacterized protein	**8,94**	0,0015
Y11_40651		Uncharacterized protein	**8,06**	0,0029
Y11_30741		Histidine ammonia-lyase	**7,86**	0,0009
Y11_05951		Uncharacterized protein	**7,54**	0,0159
Y11_13021		Uncharacterized protein	**7,43**	0,0012
Y11_15241		Fructose-specific phosphocarrier protein HPr PTS system, fructose-specific IIA component	**7,37**	0,0023
Y11_15251		Arabinose-proton symporter	**7,10**	0,0029
Y11_22021		Putative Dcu family, anaerobic C4-dicarboxylate transporter	**6,88**	0,0298
Y11_37591	*lsrB*	Autoinducer 2 (AI-2) ABC transport system, periplasmic AI-2 binding protein LsrB	**6,87**	0,0021
Y11_30031		Ribonuclease P protein component	**6,85**	0,0114
Y11_41561	*nrdI*	Protein NrdI	**6,66**	0,0088
Y11_05361		PTS system, glucose-specific IIB component PTS system, glucose-specific IIC component	**6,65**	0,0060
Y11_35771	*tdcC*	Threonine/serine transporter TdcC	**6,44**	0,0265
Y11_19171		Uncharacterized protein	**6,27**	0,0202
Y11_05031		Putative insecticidal toxin complex	**6,19**	0,0037

Y11_10821	*ompW*	Outer membrane protein W	**6,04**	0,0018
Y11_05161		Putative cytoplasmic protein	**6,02**	0,0123
Y11_39751		Htra protease/chaperone protein	**5,98**	0,0030
Y11_15101		Uncharacterized protein	**5,93**	0,0035
Y11_03551		Serine transporter	**5,80**	0,0127
Y11_23531		Uncharacterized protein	**5,75**	0,0115
Y11_01021		Putative lipoprotein	**5,73**	0,0283
Y11_16381		Ribose/xylose/arabinose/galactoside ABC-type transport systems	**5,69**	0,0001
Y11_17341		Uncharacterized protein	**5,69**	0,0115
Y11_12171		N-formylglutamate deformylase	**5,66**	0,0023
Y11_35441		Uncharacterized protein	**5,54**	0,0134
Y11_34601		Carbon starvation protein A	**5,53**	0,0473
Y11_36101		tRNA dimethylallyltransferase	**5,49**	0,0019
Y11_12001		PTS system, N-acetylgalactosamine-specific IID component	**5,44**	0,0049
Y11_08331		Putative lipoprotein	**5,44**	0,0236
Y11_03911	*cspD*	Cold shock protein CspD	**5,41**	0,0083
Y11_01551		Uncharacterized protein	**5,25**	0,0093
Y11_05741	*lpxR*	Lipid A 3'-acyloxyacyl hydrolase	**5,09**	0,0005
Y11_04571		Ribosome modulation factor (RMF)	**5,08**	0,0016
Y11_28501		Uncharacterized protein	**5,08**	0,0327
Y11_13901		Proline/sodium symporter PUTP	**5,04**	0,0003
Y11_03251		1-phosphofructokinase (EC 2.7.1.56)	**5,02**	0,0031
Y11_19751		Arylesterase (EC 3.1.1.2)	**5,01**	0,0368
Y11_41571	*nrdH*	Glutaredoxin-like protein NrdH	**4,99**	0,0343
Y11_14841		Putative membrane protein	**4,99**	0,0094
Y11_05691		Uncharacterized protein	**4,90**	0,0114
Y11_43221		PTS system, glucitol/sorbitol-specific IIB component and second of two IIC components	**4,90**	0,0073
Y11_34741		3-ketoacyl-CoA thiolase	**4,88**	0,0042
Y11_25581		Beta-hexosaminidase	**4,84**	0,0106
Y11_21901	*yfiA*	Ribosome hibernation protein YfiA	**4,84**	0,0030
Y11_15541		Uncharacterized protein	**4,81**	0,0003
Y11_15231		Nucleoprotein/polynucleotide-associated enzyme	**4,80**	0,0015
Y11_18391		Uncharacterized protein	**4,76**	0,0496
Y11_31101		Dipeptide-binding ABC transporter, periplasmic substrate-binding component	**4,72**	0,0002
Y11_21001	*brnQ*	Branched-chain amino acid transport system carrier protein	**4,70**	0,0238
Y11_30351		PTS system, mannitol-specific IIC component PTS system, mannitol-specific IIB component PTS system, mannitol-specific IIA component	**4,69**	0,0231
Y11_03271		PTS system, fructose-specific IIB component PTS system, fructose-specific IIC component	**4,62**	0,0436
Y11_28721	*cpxR*	Copper-sensing two-component system response regulator CpxR	**4,61**	0,0003
Y11_03241		Fructose-specific phosphocarrier protein HPr PTS system, fructose-specific IIA component	**4,54**	0,0097
Y11_18001	*ybiH*	Transcriptional regulator YbiH, TetR family	**4,54**	0,0087
Y11_06251		Ferrichrome-iron receptor	**4,52**	0,0127
Y11_26301		Uncharacterized protein	**4,51**	0,0410

Y11_15561		Putative membrane protein	**4,49**	0,0038
Y11_19831		Ybak family protein	**4,44**	0,0024
Y11_08461		Uncharacterized protein	**4,44**	0,0287
Y11_15551		Putative membrane protein	**4,43**	0,0162
Y11_39271	*aroP*	Aromatic amino acid transport protein AroP	**4,42**	0,0251
Y11_41551		Ribonucleoside-diphosphate reductase	**4,39**	0,0010
Y11_07941		Putative exported protein	**4,33**	0,0000
Y11_24771		Methylglyoxal reductase, acetol producing 2,5-diketo-D-gluconate reductase A	**4,33**	0,0045
Y11_26581		Endoribonuclease L-PSP	**4,33**	0,0029
Y11_15321		Probable 2-(5''-triphosphoribosyl)-3'-dephosphocoenzyme-A synthase	**4,31**	0,0133
Y11_21161		Putative exported protein YPO3518	**4,29**	0,0215
Y11_24721		Mota/TolQ/ExbB proton channel family protein	**4,28**	0,0042
Y11_34561		Transposase	**4,28**	0,0027
Y11_28621		Uncharacterized protein	**4,27**	0,0410
Y11_11691	*mtdJ*	Spermidine export protein MdtJ	**4,26**	0,0160
Y11_03261		PTS system, fructose-specific IIB component PTS system, fructose-specific IIC component	**4,25**	0,0498
Y11_21721		Uncharacterized protein	**4,24**	0,0407
Y11_12851		Uncharacterized protein	**4,23**	0,0007
Y11_30671		Usg protein	**4,23**	0,0028
Y11_10991		Periplasmic oligopeptide-binding protein	**4,20**	0,0048
Y11_29461	*mobB*	Molybdopterin-guanine dinucleotide biosynthesis protein MobB	**4,20**	0,0013
Y11_15331		Apo-citrate lyase phosphoribosyl-dephospho-CoA transferase	**4,17**	0,0036
Y11_05731		ISsod5, transposase	**4,15**	0,0293
Y11_39891		Uncharacterized protein	**4,14**	0,0181
Y11_31441		Glutamate dehydrogenase	**4,11**	0,0027
Y11_18211		Putative phosphatase	**4,09**	0,0051
Y11_28261		Glycerol uptake facilitator protein	**4,04**	0,0309
Y11_29451		Molybdenum cofactor guanylyltransferase	**4,00**	0,0045
Y11_17951		Uncharacterized protein	**4,00**	0,0379
Y11_28731	*cpxA*	Copper sensory histidine kinase CpxA	**3,98**	0,0105
Y11_12021		Putative galactosamine-6-phosphate isomerase	**3,98**	0,0121
Y11_23731		Ferric anguibactin-binding protein	**3,95**	0,0011
Y11_06311		Uncharacterized protein	**3,95**	0,0445
Y11_07051		Phosphate starvation-inducible protein PhoH,predicted ATPase	**3,91**	0,0230
Y11_42191		Autonomous glycyl radical cofactor	**3,91**	0,0041
Y11_04441		Putative outer membrane porin C protein	**3,90**	0,0011
Y11_13911		Transcriptional repressor of PutA and PUTP Proline dehydrogenase	**3,88**	0,0248
Y11_19631		Inorganic pyrophosphatase/exopolyphosphatase	**3,83**	0,0064
Y11_39961		Putative membrane protein hemolysin III homolog	**3,82**	0,0002
Y11_20711		Exodeoxyribonuclease 7 small subunit	**3,79**	0,0094
Y11_30041		Uncharacterized protein	**3,78**	0,0084
Y11_11971		Tagatose-6-phosphate kinase AgaZ	**3,77**	0,0188
Y11_01071		Ferric iron ABC transporter, iron-binding protein	**3,74**	0,0068

Y11_10831		Ferredoxin	**3,72**	0,0017
Y11_19721	*ybbP*	Uncharacterized metabolite ABC transporter in Enterobacteriaceae, permease protein EC-YbbP	**3,70**	0,0006
Y11_34171	*tusA*	Sulfurtransferase TusA	**3,69**	0,0024
Y11_02921		ISsod5, transposase	**3,69**	0,0066
Y11_24001		Hydrogenase-2 operon protein hybE	**3,68**	0,0167
Y11_37581	*lsrF*	Autoinducer 2 (AI-2) aldolase LsrF	**3,67**	0,0485
Y11_35741		Putative heme iron utilization protein	**3,65**	0,0126
Y11_12661		Glycine cleavage system transcriptional activator	**3,60**	0,0010
Y11_01971		Transposase	**3,55**	0,0011
Y11_10401		Carbon starvation protein A paralog	**3,55**	0,0029
Y11_12161		Imidazolonepropionase	**3,55**	0,0069
Y11_40731		Prepilin peptidase dependent protein C	**3,52**	0,0093
Y11_06301		PTS system, mannose-specific IIA component PTS system, mannose-specific IIB component	**3,50**	0,0304
Y11_16891		Putative membrane protein	**3,42**	0,0236
Y11_10911		Uncharacterized protein	**3,42**	0,0089
Y11_15361		Citrate lyase acyl carrier protein	**3,42**	0,0185
Y11_08531		Uncharacterized protein	**3,40**	0,0066
Y11_12371		Calcium/proton antiporter	**3,40**	0,0000
Y11_35761		Threonine dehydratase, catabolic	**3,39**	0,0122
Y11_09691		Uncharacterized protein	**3,39**	0,0066
Y11_12361		Iron-chelator utilization protein	**3,36**	0,0027
Y11_10901		Uncharacterized protein	**3,36**	0,0386
Y11_19741		Uncharacterized metabolite ABC transporter in Enterobacteriaceae, ATP-binding protein EC-YbbA	**3,35**	0,0380
Y11_40171		ISsod5, transposase	**3,33**	0,0457
Y11_30751		Urocanate hydratase	**3,33**	0,0171
Y11_33181		Uncharacterized protein	**3,32**	0,0116
Y11_37721	*dhaK*	Phosphoenolpyruvate-dihydroxyacetone phosphotransferase, dihydroxyacetone binding subunit DhaK	**3,29**	0,0097
Y11_15371		[citrate [pro-3S]-lyase] ligase	**3,29**	0,0000
Y11_20181		Uncharacterized protein	**3,29**	0,0105
Y11_00411		Nadp-dependent malic enzyme	**3,27**	0,0065
Y11_35751	*hutW*	Radical SAM family protein HutW	**3,25**	0,0150
Y11_10981	*oppB*	Oligopeptide transport system permease protein OppB	**3,25**	0,0061
Y11_31901		Uncharacterized protein	**3,25**	0,0070
Y11_07831		Uncharacterized protein	**3,25**	0,0387
Y11_41541		Ribonucleoside-diphosphate reductase subunit beta	**3,24**	0,0161
Y11_24061		Putative outer membrane lipoprotein Pcp	**3,24**	0,0099
Y11_31291		C4-dicarboxylate transport protein	**3,24**	0,0041
Y11_38301		Uncharacterized protein	**3,23**	0,0181
Y11_18051		Putative membrane protein	**3,22**	0,0361
Y11_24711		Biopolymer transport protein ExbD/TolR	**3,22**	0,0000
Y11_34751		Fatty acid oxidation complex subunit alpha	**3,20**	0,0082
Y11_26141		Uncharacterized protein	**3,18**	0,0167
Y11_20331		Haemolysin expression modulating protein	**3,17**	0,0065

Y11_06201	*ftsI*	Cell division protein FtsI	**3,17**	0,0011
Y11_04951		Glucans biosynthesis protein C	**3,15**	0,0056
Y11_23461		Probable Fe(2+)-trafficking protein	**3,15**	0,0287
Y11_12011		PTS system, N-acetylgalactosamine-and galactosamine-specific IIA component	**3,12**	0,0158
Y11_38541		Threonine efflux protein	**3,12**	0,0040
Y11_12031	*agaY*	Tagatose-1,6-bisphosphate aldolase AgaY	**3,11**	0,0282
Y11_23261	*sprT*	Protein SprT	**3,11**	0,0152
Y11_30301		Acetyltransferase	**3,10**	0,0114
Y11_15341		Citrate lyase alpha chain	**3,10**	0,0053
Y11_01641		Glucose-1-phosphatase	**3,10**	0,0084
Y11_15281		Trap-type C4-dicarboxylate transport system,periplasmic component	**3,10**	0,0033
Y11_12271		Succinylornithine transaminase	**3,09**	0,0005
Y11_30481		Formate dehydrogenase O beta subunit	**3,08**	0,0041
Y11_15111		Metallo-beta-lactamase family protein	**3,08**	0,0072
Y11_37641	*lsrK*	Autoinducer 2 (AI-2) kinase LsrK	**3,08**	0,0163
Y11_17171	*mglB*	Galactose/methyl galactoside ABC transport system, D-galactose-binding periplasmic protein	**3,06**	0,0026
Y11_19841		UDP-sugar hydrolase 5'-nucleotidase	**3,06**	0,0093
Y11_07741		Membrane-bound lytic murein transglycosylase E	**3,06**	0,0368
Y11_10101		L-arabinose-binding periplasmic protein AraF	**3,04**	0,0134
Y11_43411		Putative exported protein	**3,03**	0,0496
Y11_26831		Soluble cytochrome b562	**3,02**	0,0016
Y11_10091	*araG*	L-arabinose transport ATP-binding protein AraG	**3,01**	0,0237
Y11_04781		Sulfurtransferase	**3,01**	0,0002
Y11_33981		Tim-barrel signal transduction protein	**3,00**	0,0058
Y11_37251		Uncharacterized protein	**3,00**	0,0158
Y11_25571		Uncharacterized protein	**2,99**	0,0041
Y11_25081		Uncharacterized protein	**2,98**	0,0218
Y11_24511		Aatd	**2,98**	0,0101
Y11_10861		Probable intracellular septation protein A	**2,97**	0,0270
Y11_28651		Uncharacterized protein	**2,96**	0,0151
Y11_10551		Uncharacterized protein	**2,95**	0,0032
Y11_36931		Putative sugar binding protein, ABC transport system	**2,95**	0,0103
Y11_16511		Nucleoside-diphosphate-sugar epimerases	**2,94**	0,0086
Y11_10431	*yciT*	Transcriptional regulatory protein YciT	**2,93**	0,0478
Y11_04051		ISsod5, transposase	**2,91**	0,0167
Y11_04721		Succinyl-CoA synthetase, alpha subunit-related enzymes	**2,91**	0,0003
Y11_31671		5-deoxy-glucuronate isomerase	**2,90**	0,0492
Y11_10501		Orotidine 5'-phosphate decarboxylase	**2,89**	0,0035
Y11_08851		Peroxiredoxin	**2,88**	0,0232
Y11_32151	*ompR*	Two-component system response regulator OmpR	**2,87**	0,0060
Y11_36441		Uncharacterized protein	**2,86**	0,0114
Y11_10971		Oligopeptide transport system permease protein OppC	**2,86**	0,0126
Y11_23471		Membrane-bound lytic murein transglycosylase C	**2,85**	0,0246

Y11_28271		Glycerol kinase	**2,85**	0,0003
Y11_12131		Uncharacterized protein	**2,84**	0,0034
Y11_00711		Putative two-component system sensor kinase	**2,83**	0,0024
Y11_32071		Ferrous iron transport protein A	**2,83**	0,0362
Y11_42311	*rseB*	Sigma factor RpoE negative regulatory protein RseB	**2,83**	0,0005
Y11_19131	*gltJ*	Glutamate Aspartate transport system permease protein GltJ	**2,81**	0,0107
Y11_25551		Putative bacteriophage integrase	**2,80**	0,0127
Y11_36991	*stbD*	Stbd replicon stabilization protein (Antitoxin to StbE)	**2,79**	0,0198
Y11_07531		Sugar-binding protein	**2,79**	0,0016
Y11_32161	*envZ*	Osmolarity sensory histidine kinase EnvZ	**2,78**	0,0018
Y11_23961	*hypD*	[NiFe] hydrogenase metallocenter assembly protein HypD	**2,78**	0,0087
Y11_39951		Hydrolase (HAD superfamily)	**2,77**	0,0011
Y11_03521		D-alanyl-D-alanine carboxypeptidase	**2,77**	0,0018
Y11_09901		Integral membrane protein (Rhomboid family)	**2,77**	0,0161
Y11_32481		6-phospho-beta-glucosidase	**2,76**	0,0176
Y11_41611		Uncharacterized protein	**2,76**	0,0171
Y11_29031		Uncharacterized protein	**2,76**	0,0396
Y11_11411		Alanine racemase, catabolic	**2,76**	0,0459
Y11_30311		DNA-3-methyladenine glycosylase	**2,75**	0,0014
Y11_12741		Uncharacterized protein	**2,74**	0,0074
Y11_33621		Exo-poly-alpha-D-galacturonosidase	**2,74**	0,0028
Y11_35781		Propionate kinase Acetate kinase	**2,73**	0,0164
Y11_06281		PTS system, mannose-specific IID component	**2,73**	0,0478
Y11_23691	*fecE*	Iron(III) dicitrate transport ATP-binding protein FecE	**2,73**	0,0149
Y11_29441	*yihD*	Protein yihD	**2,72**	0,0091
Y11_41371		3-oxoacyl-[ACP] synthase	**2,72**	0,0049
Y11_25881		Putative lipoprotein	**2,71**	0,0149
Y11_43231		PTS system, glucitol/sorbitol-specific IIC component	**2,70**	0,0268
Y11_37431		ISPsy4, transposition helper protein	**2,69**	0,0023
Y11_06811		Glutaminase	**2,69**	0,0397
Y11_37611	*lsrC*	Autoinducer 2 (AI-2) ABC transport system,membrane channel protein LsrC	**2,69**	0,0125
Y11_43211		PTS system, glucitol/sorbitol-specific IIA component	**2,68**	0,0042
Y11_16801		Uncharacterized protein	**2,68**	0,0022
Y11_25611		N-acetylmuramic acid 6-phosphate etherase	**2,68**	0,0405
Y11_35961		Fumarate reductase subunit D (Fumarate reductase 13 kDa hydrophobic protein)	**2,66**	0,0347
Y11_13651		D-serine/D-alanine/glycine transporter	**2,65**	0,0094
Y11_03411	*fhuC*	Ferrichrome transport ATP-binding protein FhuC	**2,64**	0,0205
Y11_11431		Uncharacterized protein	**2,64**	0,0416
Y11_00601		Putative sialic acid transporter (Sialic acid permease)	**2,62**	0,0005
Y11_26211		Monofunctional biosynthetic peptidoglycan transglycosylase	**2,62**	0,0013
Y11_08251		Pyruvate kinase	**2,61**	0,0014
Y11_32681		Putative sugar transferase	**2,61**	0,0011
Y11_12341		Transposase	**2,60**	0,0313
Y11_06191		Inner membrane protein	**2,59**	0,0000

Y11_28631	*sugR*	Putative ATP binding protein SugR	**2,58**	0,0271
Y11_17511		Glutamate transport membrane-spanning protein	**2,57**	0,0160
Y11_27451		Guanine-hypoxanthine permease	**2,57**	0,0450
Y11_00231		Uncharacterized protein	**2,56**	0,0010
Y11_03801		Uncharacterized protein	**2,55**	0,0055
Y11_20961		Gamma-glutamyltranspeptidase	**2,55**	0,0283
Y11_12261		Arginine N-succinyltransferase	**2,52**	0,0059
Y11_18681		Membrane protein	**2,52**	0,0137
Y11_24011		Hydrogenase maturation protease	**2,52**	0,0119
Y11_30961		ISsod5, transposase	**2,52**	0,0281
Y11_16641		Glycosyl transferase, group 1 family protein	**2,52**	0,0168
Y11_34101		Glycerol-3-phosphate transporter	**2,51**	0,0209
Y11_12481		Glycerophosphoryl diester phosphodiesterase family protein	**2,50**	0,0184
Y11_37881		Periplasmic binding protein	**2,50**	0,0064
Y11_07441	*kdgR*	Transcriptional regulator KdgR, KDG operon repressor	**2,50**	0,0080
Y11_19731		Uncharacterized metabolite ABC transporter in Enterobacteriaceae, permease protein EC-YbbP	**2,49**	0,0080
Y11_08741		Phage shock protein D	**2,49**	0,0155
Y11_39131		Secretion monitor	**2,48**	0,0187
Y11_03151		Mannonate dehydratase	**2,48**	0,0082
Y11_10881	*tonB*	Ferric siderophore transport system, periplasmic binding protein TonB	**2,47**	0,0326
Y11_31951	*malT*	HTH-type transcriptional regulator MalT	**2,47**	0,0142
Y11_21501		Acyl-CoA dehydrogenase, short-chain specific	**2,47**	0,0048
Y11_10691		Cob(I)alamin adenosyltransferase	**2,47**	0,0026
Y11_15021		LysR-family transcriptional regulatory protein	**2,46**	0,0007
Y11_40721		Uncharacterized protein	**2,46**	0,0300
Y11_36541		Octaprenyl-diphosphate synthase	**2,46**	0,0016
Y11_20351		Methylated-DNA--protein-cysteine methyltransferase-related protein	**2,46**	0,0012
Y11_08701		Psp operon transcriptional activator	**2,45**	0,0478
Y11_04751		Uncharacterized protein	**2,44**	0,0279
Y11_29861		Putative periplasmic solute-binding protein	**2,44**	0,0207
Y11_29431	*yihE*	YihE protein, a ser/thr kinase implicated in LPS synthesis and Cpx signalling	**2,44**	0,0134
Y11_41621		Acid shock protein 2	**2,44**	0,0159
Y11_13621		Biotin synthesis protein bioC	**2,44**	0,0108
Y11_30471		Formate dehydrogenase chain D	**2,41**	0,0014
Y11_28111		Uncharacterized protein	**2,41**	0,0012
Y11_11131		Formyltetrahydrofolate deformylase	**2,41**	0,0085
Y11_26031		Aldo-keto reductase	**2,40**	0,0231
Y11_27471		Uncharacterized protein	**2,40**	0,0474
Y11_05461	*lpoB*	Penicillin-binding protein activator LpoB	**2,40**	0,0026
Y11_10961	*oppD*	Oligopeptide transport ATP-binding protein OppD	**2,39**	0,0012
Y11_34181		Lead, cadmium, zinc and mercury transporting ATPase Copper-translocating P-type ATPase	**2,39**	0,0199
Y11_17161	*mglA*	Galactose/methyl galactoside ABC transport system, ATP-binding protein MglA	**2,39**	0,0023
Y11_15521		Transcriptional repressor of aga operon	**2,39**	0,0046

Y11_00021	*yfgC*	Exported zinc metalloprotease YfgC	**2,39**	0,0057
Y11_22191		Protein Implicated in DNA repair function with RecA and MutS	**2,39**	0,0007
Y11_06701		Putative ROK-family transcriptional regulator	**2,38**	0,0168
Y11_13831	*efeO*	Ferrous iron transport periplasmic protein EfeO	**2,38**	0,0188
Y11_33901		Putative lipoprotein	**2,36**	0,0468
Y11_29551	*rbsC*	Ribose ABC transport system, permease protein RbsC	**2,36**	0,0063
Y11_28851		Putative TRANSmembrane protein	**2,36**	0,0019
Y11_12201	*ompC*	Outer membrane protein C	**2,35**	0,0104
Y11_18781		Uncharacterized protein	**2,35**	0,0034
Y11_42411	*gntP*	Fructuronate transporter GntP	**2,34**	0,0180
Y11_20581	*yajG*	Hypothetical lipoprotein YajG	**2,34**	0,0046
Y11_06361	*nudL*	Uncharacterized Nudix hydrolase NudL	**2,34**	0,0246
Y11_43201		Sorbitol-6-phosphate 2-dehydrogenase	**2,34**	0,0032
Y11_06211	*ftsI*	Cell division protein FtsI	**2,34**	0,0113
Y11_06961		Ferric reductase	**2,31**	0,0127
Y11_01901	*hisP*	Histidine ABC transporter, ATP-binding protein HisP	**2,31**	0,0024
Y11_06341		L-serine dehydratase	**2,31**	0,0047
Y11_29021		Transposase for IS1668	**2,31**	0,0475
Y11_37601	*lsrD*	Autoinducer 2 (AI-2) ABC transport system,membrane channel protein LsrD	**2,30**	0,0310
Y11_05421		Putative transport protein	**2,30**	0,0187
Y11_30361		Mannitol-1-phosphate 5-dehydrogenase	**2,29**	0,0029
Y11_42601		Protein containing PTS-regulatory domain	**2,29**	0,0146
Y11_40621		Oxidoreductase, aldo/keto reductase family	**2,29**	0,0018
Y11_32581		Phosphoribulokinase	**2,27**	0,0065
Y11_08291		Putative transport protein	**2,27**	0,0046
Y11_21911	*bamD*	Outer membrane protein assembly factor BamD	**2,27**	0,0008
Y11_35861		Aspartate ammonia-lyase	**2,26**	0,0026
Y11_36861		Acetyltransferase	**2,26**	0,0469
Y11_14821		ISsod5, transposase	**2,25**	0,0082
Y11_42111		Putative oligoketide cyclase/lipid transport protein	**2,25**	0,0223
Y11_43091		Transposase	**2,24**	0,0095
Y11_17211		GTP cyclohydrolase 1	**2,24**	0,0003
Y11_36351		2',3'-cyclic-nucleotide 2'-phosphodiesterase	**2,24**	0,0236
Y11_07061		Uncharacterized protein	**2,24**	0,0200
Y11_01541		3-oxoacyl-[acyl-carrier-protein] synthase, KASI	**2,23**	0,0224
Y11_42701	*iscR*	HTH-type transcriptional regulator IscR	**2,23**	0,0071
Y11_26011		Alcohol dehydrogenase	**2,23**	0,0030
Y11_20931		Acyl carrier protein phosphodiesterase (ACP phosphodiesterase)	**2,23**	0,0092
Y11_38891		Long-chain-fatty-acid--CoA ligase	**2,23**	0,0170
Y11_12231		Succinylarginine dihydrolase	**2,22**	0,0293
Y11_32851		Bacterioferritin-associated ferredoxin	**2,22**	0,0381
Y11_36781		Uncharacterized protein	**2,22**	0,0214
Y11_38741		Putative membrane protein	**2,22**	0,0348
Y11_01721		Transcriptional regulator, GntR family domain Aspartate aminotransferase	**2,21**	0,0425

Y11_02891		PTS system, beta-glucoside-specific IIB component PTS system, beta-glucoside-specific IIC component PTS system,beta-glucoside-specific IIA component	**2,21**	0,0208
Y11_32191		Phosphoenolpyruvate carboxykinase	**2,21**	0,0390
Y11_08561		Glyoxalase family protein	**2,21**	0,0362
Y11_22141	*ygaB*	Putative phosphatase YqaB	**2,20**	0,0145
Y11_26541		Phosphocarrier protein, nitrogen regulation associated	**2,20**	0,0122
Y11_02761	*ampH*	Penicillin-binding protein AmpH	**2,20**	0,0355
Y11_27481		Hipa protein	**2,20**	0,0039
Y11_19961		Uncharacterized protein	**2,19**	0,0006
Y11_35851	*dcuA*	C4-dicarboxylate transporter DcuA	**2,19**	0,0052
Y11_18621		Succinate dehydrogenase flavoprotein subunit	**2,19**	0,0226
Y11_00011		Arsenate reductase	**2,19**	0,0127
Y11_12251		N-succinylglutamate 5-semialdehyde dehydrogenase	**2,18**	0,0072
Y11_37631	*lsrR*	Lsrr, transcriptional repressor of lsr operon	**2,18**	0,0088
Y11_34761		Xaa-Pro dipeptidase	**2,18**	0,0087
Y11_21791		Transcription repressor	**2,18**	0,0055
Y11_11271	*yeaC*	Uncharacterized protein YeaC	**2,18**	0,0301
Y11_15351		Citrate lyase beta chain	**2,18**	0,0316
Y11_25121		Transposase	**2,18**	0,0048
Y11_24751	*yghC*	Hypothetical transcriptional regulator YqhC	**2,17**	0,0137
Y11_18961		N-acetylglucosamine-regulated outer membrane porin	**2,17**	0,0394
Y11_28821		Cell wall endopeptidase, family M23/M37	**2,17**	0,0039
Y11_40801		N-acetylmuramoyl-L-alanine amidase	**2,17**	0,0255
Y11_02871		Phosphosugar-binding transcriptional regulator, RpiR family	**2,16**	0,0034
Y11_42101		SsrA-binding protein	**2,16**	0,0104
Y11_00461		Coproporphyrinogen-III oxidase, aerobic	**2,15**	0,0008
Y11_36361		3'(2'),5'-bisphosphate nucleotidase	**2,15**	0,0030
Y11_11781	*znuA*	Zinc ABC transporter, periplasmic-binding protein ZnuA	**2,14**	0,0091
Y11_09631		Putative phage-related membrane protein	**2,14**	0,0083
Y11_12061		Transposase for IS1668	**2,14**	0,0125
Y11_09361		Transposase	**2,14**	0,0252
Y11_33931	*xerC*	Tyrosine recombinase XerC	**2,13**	0,0150
Y11_35031	*rsd*	Regulator of sigma D	**2,13**	0,0387
Y11_41791		Nickel transport ATP-binding protein nikE2	**2,13**	0,0006
Y11_37741		Phosphoenolpyruvate-dihydroxyacetone phosphotransferase, subunit DhaM DHA-specific IIA component DHA-specific phosphocarrier protein HPr DHA-specific EI component	**2,12**	0,0009
Y11_35821		Glycerate kinase	**2,12**	0,0020
Y11_24871	*cpdA*	3',5'-cyclic adenosine monophosphate phosphodiesterase CpdA	**2,12**	0,0031
Y11_33791	*yifK*	Putative transport protein yifK	**2,12**	0,0015
Y11_31051	*uhpA*	Transcriptional regulatory protein UhpA	**2,12**	0,0087
Y11_26101		DNA-cytosine methyltransferase	**2,11**	0,0008
Y11_04591		Transcriptional regulator, HxlR family	**2,11**	0,0030
Y11_40281		Transcriptional regulator, HxlR family	**2,11**	0,0066
Y11_42301	*rseA*	Sigma factor RpoE negative regulatory protein RseA	**2,11**	0,0057
Y11_04881	*ypeR*	Quorum-sensing transcriptional activator YpeR	**2,11**	0,0207

Y11_40291		Carbonic anhydrase	**2,11**	0,0181
Y11_13891		Transposase	**2,11**	0,0061
Y11_38151		Transcriptional regulator	**2,10**	0,0329
Y11_19941		Undecaprenyl-phosphate N-acetylglucosaminyl 1-phosphate transferase	**2,10**	0,0037
Y11_15121		Uncharacterized protein	**2,10**	0,0013
Y11_25801	*sstT*	Serine/threonine transporter SstT	**2,10**	0,0024
Y11_25951	*ygiF*	Inner membrane protein YqjF	**2,10**	0,0351
Y11_08191	*sufB*	Iron-sulfur cluster assembly protein SufB	**2,09**	0,0177
Y11_05451		Ycfl protein: an outer membrane lipoprotein that is part of a salvage cluster	**2,09**	0,0089
Y11_16391		ABC-type sugar transport system, ATP-binding protein	**2,09**	0,0021
Y11_35641		Ferrichrome-iron receptor	**2,09**	0,0293
Y11_25621		PTS system, sucrose-specific IIB component PTS system, sucrose-specific IIC component	**2,09**	0,0105
Y11_22871		Alkaline phosphatase isozyme conversion protein	**2,09**	0,0023
Y11_19951		Glycosyltransferase	**2,09**	0,0084
Y11_00391	*napC*	Cytochrome c-type protein NapC	**2,09**	0,0147
Y11_37731	*dhaL*	Phosphoenolpyruvate-dihydroxyacetone phosphotransferase, ADP-binding subunit DhaL	**2,08**	0,0099
Y11_42611		Uncharacterized protein	**2,08**	0,0034
Y11_10261		Right origin-binding protein	**2,07**	0,0052
Y11_18611		Succinate dehydrogenase iron-sulfur protein	**2,07**	0,0275
Y11_00861		Putative exported protein	**2,07**	0,0401
Y11_14881		Uncharacterized protein	**2,07**	0,0235
Y11_05771		Putative O-antigen biosynthesis protein	**2,07**	0,0286
Y11_19291		Octanoyltransferase	**2,06**	0,0157
Y11_10491		Uncharacterized protein	**2,06**	0,0002
Y11_23071	*argO*	Arginine exporter protein ArgO	**2,06**	0,0053
Y11_43421		Magnesium transporter	**2,06**	0,0049
Y11_05001		Multidrug-efflux transporter, major facilitator superfamily (MFS)	**2,06**	0,0283
Y11_30421		Virulence associated protein C	**2,06**	0,0023
Y11_35171		Secretion system regulator of DegU/UvrY/BvgA type	**2,06**	0,0034
Y11_05171		DNA-damage-inducible protein I	**2,06**	0,0325
Y11_17021		Hydrogenase-4 component C	**2,06**	0,0046
Y11_09541		Transcriptional regulator, MarR family	**2,05**	0,0434
Y11_34811		Transposase	**2,05**	0,0067
Y11_36921		Putative exported protein	**2,05**	0,0277
Y11_08571		Dipeptide and tripeptide permease A	**2,05**	0,0120
Y11_35981		Succinate dehydrogenase iron-sulfur protein	**2,05**	0,0080
Y11_20721		Octaprenyl-diphosphate synthase Dimethylallyltransferase Geranyltranstransferase (Farnesyldiphosphate synthase) Geranylgeranyl pyrophosphate synthetase	**2,05**	0,0077
Y11_36601	*basR*	Transcriptional regulatory protein basR/pmrA	**2,05**	0,0113
Y11_03541		L-serine dehydratase	**2,05**	0,0004
Y11_37651		Lipopolysaccharide heptosyltransferase III	**2,05**	0,0381
Y11_11361		Uncharacterized protein	**2,05**	0,0049
Y11_42711		Cysteine desulfurase	**2,04**	0,0207
Y11_33571		Outer membrane usher protein FIMD	**2,04**	0,0301

Y11_36521		Malate dehydrogenase	**2,04**	0,0040
Y11_41131	*fabZ*	3-hydroxyacyl-[acyl-carrier-protein] dehydratase FabZ	**2,04**	0,0156
Y11_39741		Deoxyguanosinetriphosphate triphosphohydrolase	**2,03**	0,0094
Y11_28841		Uncharacterized protein	**2,03**	0,0026
Y11_29561	*rbsA*	Ribose ABC transport system, ATP-binding protein RbsA	**2,03**	0,0156
Y11_17521		Glutamate transport ATP-binding protein	**2,03**	0,0069
Y11_25141		Gene D protein	**2,02**	0,0488
Y11_00001	*hda*	DnaA-homolog protein hda	**2,02**	0,0050
Y11_00191		Transposase	**2,02**	0,0473
Y11_32761		Peptidyl-prolyl cis-trans isomerase	**2,02**	0,0183
Y11_01011		Uncharacterized protein	**2,02**	0,0476
Y11_36981		UPF0306 protein Y11_36981	**2,01**	0,0473
Y11_23951	*hypE*	[NiFe] hydrogenase metallocenter assembly protein HypE	**2,01**	0,0271
Y11_12141		Formiminoglutamic iminohydrolase	**2,01**	0,0176
Y11_39561		Glutamyl-Q tRNA(Asp) synthetase	**2,01**	0,0189
Y11_35791		2-ketobutyrate formate-lyase Pyruvate formate-lyase	**2,01**	0,0044
Y11_03301		Ph 6 antigen adhesin	**2,00**	0,0012
Y11_33371	*hdfR*	HTH-type transcriptional regulator HdfR	**2,00**	0,0181
Y11_30211		Putative transport protein Y11_30211	**2,00**	0,0074
Y11_42221		Putative phospholipase A accessory protein	**2,00**	0,0367
Y11_40791		Amino-acid acetyltransferase	**0,50**	0,0224
Y11_02031		Phosphate acetyltransferase	**0,50**	0,0141
Y11_38421	*dnaJ*	Chaperone protein DnaJ	**0,50**	0,0025
Y11_16431		Putative inner membrane protein	**0,50**	0,0163
Y11_33111		30S ribosomal protein S4	**0,50**	0,0046
Y11_31471		Low-affinity inorganic phosphate transporter	**0,49**	0,0013
Y11_11611		Cell division topological specificity factor	**0,49**	0,0122
Y11_11051		UDP-glucose dehydrogenase	**0,49**	0,0199
Y11_32951		50S ribosomal protein L16	**0,49**	0,0278
Y11_03771	*artP*	Arginine ABC transporter, ATP-binding protein ArtP	**0,49**	0,0130
Y11_32331		Shikimate kinase 1 (SK 1)	**0,49**	0,0029
Y11_05281		3-oxoacyl-[acyl-carrier protein] reductase	**0,48**	0,0074
Y11_16731		dTDP-4-dehydrorhamnose 3,5-epimerase	**0,48**	0,0250
Y11_39411		S-adenosylmethionine decarboxylase proenzyme	**0,48**	0,0031
Y11_36581		GTPase obg	**0,48**	0,0085
Y11_17361		Putative ATPase component of ABC transporter with duplicated ATPase domain	**0,48**	0,0079
Y11_30911		Uncharacterized protein	**0,47**	0,0123
Y11_16901		Putative sugar ABC transporter	**0,47**	0,0436
Y11_05141		Putative LuxR-family regulatory protein	**0,47**	0,0380
Y11_28091		N-acetyl-gamma-glutamyl-phosphate reductase	**0,47**	0,0048
Y11_24851		Topoisomerase IV subunit B	**0,47**	0,0018
Y11_04141		Uncharacterized protein	**0,47**	0,0262
Y11_36301		50S ribosomal protein L9	**0,47**	0,0075

Y11_05621		Putative lipoprotein	**0,47**	0,0038
Y11_23491		Ornithine decarboxylase	**0,47**	0,0080
Y11_42961		Uncharacterized protein	**0,45**	0,0047
Y11_01091		Putrescine importer	**0,45**	0,0448
Y11_33101		SSU ribosomal protein S11p (S14e)	**0,45**	0,0008
Y11_14721		Mg(2+) transport ATPase protein B	**0,45**	0,0059
Y11_03581		Putative permease	**0,44**	0,0134
Y11_37491		Cytosine permease	**0,44**	0,0035
Y11_25681	*hdeD*	Hded protein	**0,44**	0,0032
Y11_28171		50S ribosomal protein L31	**0,43**	0,0114
Y11_07101	*cutC*	Copper homeostasis protein CutC	**0,43**	0,0055
Y11_34891	*nusG*	Transcription antitermination protein nusG	**0,43**	0,0067
Y11_15581		Argininosuccinate synthase	**0,42**	0,0030
Y11_05301		3-oxoacyl-[acyl-carrier-protein] synthase 2	**0,42**	0,0033
Y11_08991		Putative DNA-binding phage-related protein	**0,42**	0,0154
Y11_33091		SSU ribosomal protein S13p (S18e)	**0,41**	0,0018
Y11_34901		50S ribosomal protein L11	**0,41**	0,0103
Y11_36741		30S ribosomal protein S15	**0,41**	0,0406
Y11_36711		Translation initiation factor IF-2	**0,41**	0,0019
Y11_41531	*proV*	L-proline glycine betaine ABC transport system permease protein ProV	**0,41**	0,0081
Y11_07311		Sigma-fimbriae uncharacterized paralogous subunit	**0,41**	0,0207
Y11_32871		30S ribosomal protein S10	**0,41**	0,0121
Y11_23861	*proP*	L-proline/Glycine betaine transporter ProP	**0,41**	0,0069
Y11_14991		ABC-type sugar transport system, periplasmic component	**0,40**	0,0058
Y11_08441	*rovA*	Transcriptional regulator RovA (homolog of SlyA)	**0,40**	0,0001
Y11_36751		Polyribonucleotide nucleotidyltransferase	**0,40**	0,0022
Y11_34911		50S ribosomal protein L1	**0,40**	0,0052
Y11_07371		Gaf domain-containing protein	**0,40**	0,0180
Y11_21581		Methylthioribose-1-phosphate isomerase	**0,39**	0,0462
Y11_24951		3,4-dihydroxy-2-butanone 4-phosphate synthase	**0,39**	0,0278
Y11_14711	*yncB*	Putative oxidoreductase YncB	**0,38**	0,0033
Y11_16461		Putrescine importer	**0,37**	0,0113
Y11_36691	*rimP*	Ribosome maturation factor RimP	**0,37**	0,0007
Y11_23201		Biosynthetic arginine decarboxylase	**0,36**	0,0123
Y11_33131		50S ribosomal protein L17	**0,35**	0,0036
Y11_16521		ATP phosphoribosyltransferase	**0,35**	0,0216
Y11_14701	*uspC*	Universal stress protein C	**0,35**	0,0024
Y11_16441		Nucleoside-diphosphate-sugar epimerases	**0,35**	0,0204
Y11_27261		DNA-binding protein fis	**0,34**	0,0058
Y11_38001	*osmY*	Osmotically inducible protein OsmY	**0,34**	0,0259
Y11_04221		Integration host factor subunit beta	**0,34**	0,0077
Y11_06981	*pgaA*	Biofilm PGA outer membrane secretin PgaA	**0,34**	0,0086
Y11_43341	*yegD*	Putative heat shock protein YegD	**0,33**	0,0034
Y11_28031	*hasA*	Hemophore HasA	**0,32**	0,0122

Y11_22071		30S ribosomal protein S16	**0,32**	0,0019
Y11_37271		Ornithine carbamoyltransferase, catabolic	**0,32**	0,0062
Y11_06491		Ferritin-like protein 2	**0,32**	0,0037
Y11_30171		16 kDa heat shock protein A	**0,31**	0,0228
Y11_36161	*yjeT*	Putative inner membrane protein YjeT	**0,31**	0,0111
Y11_20031	*htpG*	Chaperone protein HtpG	**0,31**	0,0019
Y11_33991	*corA*	Magnesium and cobalt transport protein CorA	**0,31**	0,0058
Y11_25641		Putative glutamate/gamma-aminobutyrate antiporter	**0,31**	0,0117
Y11_33411		Acetolactate synthase	**0,31**	0,0168
Y11_00481	*ygiW*	Protein ygiW	**0,30**	0,0031
Y11_25631		Glutaminase	**0,30**	0,0310
Y11_04211		30S ribosomal protein S1	**0,29**	0,0000
Y11_12951		Tail fiber assembly protein	**0,28**	0,0416
Y11_22051		tRNA (guanine-N(1)-)-methyltransferase	**0,27**	0,0010
Y11_36701	*nusA*	Transcription termination protein NusA	**0,26**	0,0008
Y11_17991	*rhlE*	ATP-dependent RNA helicase RhlE	**0,26**	0,0017
Y11_30181	*ibpB*	Small heat shock protein IbpB	**0,25**	0,0064
Y11_07321		Sigma-fimbriae uncharacterized paralogous subunit	**0,25**	0,0103
Y11_22041		50S ribosomal protein L19	**0,24**	0,0008
Y11_36771		Cold-shock DEAD-box protein A	**0,24**	0,0003
Y11_36151	*hflC*	Hflc protein	**0,23**	0,0001
Y11_22061	*rimM*	Ribosome maturation factor RimM	**0,21**	0,0001
Y11_25661		Glutamate decarboxylase	**0,20**	0,0025
Y11_23221		S-adenosylmethionine synthase	**0,20**	0,0042
Y11_25651		Glutamate decarboxylase	**0,19**	0,0080
Y11_36141	*hflK*	Hflk protein	**0,17**	0,0009
Y11_28041	*hasS*	Hemophore HasA	**0,12**	0,0104
Y11_36131	*hflX*	GTPase HflX	**0,06**	0,0082
Y11_14731		Mg(2+) transport ATPase protein C	**0,04**	0,0052

Table S3. Genes differentially expressed between the wild type and the YeO3-*hfq*::Km mutant strains at both RT and 37°C. FC value is the ratio between the FPKM values of the YeO3-*hfq*::Km and wild-type strains. The values >1 indicate increase, while numbers <1 indicate decrease in the abundance of mRNA in the YeO3-*hfq*::Km strain. Genes for which opposite changes took place depending on the growth temperature are marked with exclamation marks.

GENE ID	GENE NAME	PROTEIN NAME	FC (22°C)	FC (37°C)	!
Y11_02141	*rovM*	LysR family transcriptional regulator RovM (homolog of LrhA)	7,77	39,82	
Y11_11701		Uncharacterized protein	23,65	16,71	
Y11_17401	*ompX*	Outer membrane protein X	11,27	16,33	
Y11_28711		P pilus assembly/Cpx signaling pathway,periplasmic inhibitor/zinc-resistance associated protein	5,91	17,39	
Y11_09491		Uncharacterized protein	10,17	9,18	
Y11_21001	*brnQ*	Branched-chain amino acid transport system carrier protein	13,07	4,70	
Y11_05361		PTS system, glucose-specific IIB component PTS system, glucose-specific IIC component (EC 2.7.1.69)	9,46	6,65	
Y11_10511		Putative exported protein YPO2521	2,50	11,95	
Y11_02301		Uncharacterized protein	2,89	11,16	
Y11_07461		Transposase	2,44	11,34	
Y11_43221		PTS system, glucitol/sorbitol-specific IIB component and second of two IIC components (EC 2.7.1.69)	7,95	4,90	
Y11_31441		Glutamate dehydrogenase	8,44	4,11	
Y11_04161		L-asparaginase (EC 3.5.1.1)	2,19	10,14	
Y11_43201		Sorbitol-6-phosphate 2-dehydrogenase (EC 1.1.1.140)	9,71	2,34	
Y11_03551		Serine transporter	5,87	5,80	
Y11_36101		tRNA dimethylallyltransferase (EC 2.5.1.75)	6,10	5,49	
Y11_23531		Uncharacterized protein	4,47	5,75	
Y11_28731	*cpxA*	Copper sensory histidine kinase CpxA	5,62	3,98	
Y11_22021		Putative Dcu family, anaerobic C4-dicarboxylate transporter	2,53	6,88	
Y11_43211		PTS system, glucitol/sorbitol-specific IIA component (EC 2.7.1.69)	6,71	2,68	
Y11_28721	*cpxR*	Copper-sensing two-component system response regulator CpxR	4,61	4,61	
Y11_17341		Uncharacterized protein	2,99	5,69	
Y11_06251		Ferrichrome-iron receptor	3,96	4,52	
Y11_19171		Uncharacterized protein	2,18	6,27	
Y11_08251		Pyruvate kinase (EC 2.7.1.40)	5,66	2,61	
Y11_19751		Arylesterase (EC 3.1.1.2)	3,06	5,01	
Y11_18211		Putative phosphatase	3,88	4,09	
Y11_28111		Uncharacterized protein	5,55	2,41	
Y11_35641		Ferrichrome-iron receptor	5,74	2,09	
Y11_19721		Uncharacterized metabolite ABC transporter in Enterobacteriaceae, permease protein EC-YbbP	4,10	3,70	
Y11_41571	*nrdH*	Glutaredoxin-like protein NrdH	2,49	4,99	
Y11_15331		Apo-citrate lyase phosphoribosyl-dephospho-CoA transferase (EC 2.7.7.61)	3,15	4,17	
Y11_43231		PTS system, glucitol/sorbitol-specific IIC component (EC 2.7.1.69)	4,51	2,70	
Y11_12371		Calcium/proton antiporter	3,67	3,40	
Y11_08531		Uncharacterized protein	3,63	3,40	
Y11_31101		Dipeptide-binding ABC transporter, periplasmic substrate-binding component	2,26	4,72	

Y11_33791	*yifK*	Putative transport protein yifK	4,71	2,12	
Y11_26581		Endoribonuclease L-PSP	2,28	4,33	
Y11_10991		Periplasmic oligopeptide-binding protein	2,33	4,20	
Y11_03521		D-alanyl-D-alanine carboxypeptidase (EC 3.4.16.4)	3,74	2,77	
Y11_06341		L-serine dehydratase	3,89	2,31	
Y11_31951	*malT*	HTH-type transcriptional regulator MalT (ATP-dependent transcriptional activator MalT)	3,59	2,47	
Y11_03541		L-serine dehydratase (EC 4.3.1.17)	3,90	2,05	
Y11_10911		Uncharacterized protein	2,27	3,42	
Y11_15341		Citrate lyase alpha chain (EC 4.1.3.6)	2,56	3,10	
Y11_42711		Cysteine desulfurase (EC 2.8.1.7)	3,57	2,04	
Y11_10861		Probable intracellular septation protein A	2,62	2,97	
Y11_19731		Uncharacterized metabolite ABC transporter in Enterobacteriaceae, permease protein EC-YbbP	3,09	2,49	
Y11_20961		Gamma-glutamyltranspeptidase (EC 2.3.2.2)	3,02	2,55	
Y11_09691		Uncharacterized protein	2,17	3,39	
Y11_15371		[citrate [pro-3S]-lyase] ligase (EC 6.2.1.22)	2,22	3,29	
Y11_02761	*ampH*	Penicillin-binding protein AmpH	3,27	2,20	
Y11_16641		Glycosyl transferase, group 1 family protein	2,85	2,52	
Y11_34741		3-ketoacyl-CoA thiolase (EC 2.3.1.16) (Acetyl-CoA acyltransferase) (Beta-ketothiolase) (Fatty acid oxidation complex subunit beta)	0,40	4,88	!
Y11_36541		Octaprenyl-diphosphate synthase	2,52	2,46	
Y11_35851	*dcuA*	C4-dicarboxylate transporter DcuA	2,59	2,19	
Y11_23071	*argO*	Arginine exporter protein ArgO	2,69	2,06	
Y11_34101		Glycerol-3-phosphate transporter	2,11	2,51	
Y11_42701	*iscR*	HTH-type transcriptional regulator IscR	2,35	2,23	
Y11_13911		Transcriptional repressor of PutA and PUTP Proline dehydrogenase (Proline oxidase) Delta-1-pyrroline-5-carboxylate dehydrogenase (EC 1.5.1.12) (EC 1.5.99.8)	0,37	3,88	!
Y11_15351		Citrate lyase beta chain (EC 4.1.3.6)	2,05	2,18	
Y11_31291		C4-dicarboxylate transport protein	0,22	3,24	!
Y11_11411		Alanine racemase, catabolic (EC 5.1.1.1)	0,24	2,76	!
Y11_37631	*lsrR*	LsrR, transcriptional repressor of lsr operon	0,44	2,18	!
Y11_13831	*efeO*	Ferrous iron transport periplasmic protein EfeO,contains peptidase-M75 domain and (Frequently) cupredoxin-like domain	0,17	2,38	!
Y11_30211		Putative transport protein Y11_30211	0,47	2,00	!
Y11_18611		Succinate dehydrogenase iron-sulfur protein (EC 1.3.99.1)	0,36	2,07	!
Y11_14881		Uncharacterized protein	0,06	2,07	!
Y11_32951		50S ribosomal protein L16	0,50	0,49	
Y11_40791		Amino-acid acetyltransferase (EC 2.3.1.-) (EC 2.3.1.1) (N-acetylglutamate synthase)	0,46	0,50	
Y11_16901		Putative sugar ABC transporter	0,47	0,47	
Y11_15581		Argininosuccinate synthase (EC 6.3.4.5) (Citrulline--aspartate ligase)	0,47	0,42	
Y11_28091		N-acetyl-gamma-glutamyl-phosphate reductase (AGPR) (EC 1.2.1.38) (N-acetyl-glutamate semialdehyde dehydrogenase)	0,39	0,47	
Y11_37491		Cytosine permease	0,31	0,44	
Y11_23491		Ornithine decarboxylase (EC 4.1.1.17)	0,21	0,47	
Y11_25641		Putative glutamate/gamma-aminobutyrate antiporter	0,36	0,31	
Y11_07101	*cutC*	Copper homeostasis protein CutC	0,23	0,43	
Y11_14701	*uspC*	Universal stress protein C	0,31	0,35	

Y11_23861	*proP*	L-proline/Glycine betaine transporter ProP	0,24	0,41	
Y11_38001	*osmY*	Osmotically inducible protein OsmY	0,29	0,34	
Y11_14721		Mg(2+) transport ATPase protein B	0,18	0,45	
Y11_07311		Sigma-fimbriae uncharacterized paralogous subunit	0,20	0,41	
Y11_25681	*hdeD*	Hded protein	0,14	0,44	
Y11_08441	*rovA*	Transcriptional regulator RovA (homolog of SlyA)	0,13	0,40	
Y11_00481	*ygiW*	Protein ygiW	0,23	0,30	
Y11_08991		Putative DNA-binding phage-related protein	0,09	0,42	
Y11_30171		16 kDa heat shock protein A	0,17	0,31	
Y11_36161	*yjeT*	Putative inner membrane protein YjeT (Clustered with HflC)	0,13	0,31	
Y11_30181		Small heat shock protein IbpB (16 kDa heat shock protein B)	0,18	0,25	
Y11_25651		Glutamate decarboxylase (EC 4.1.1.15)	0,18	0,19	
Y11_36151	*hflC*	Hflc protein	0,13	0,23	
Y11_25661		Glutamate decarboxylase (EC 4.1.1.15)	0,14	0,20	
Y11_36141	*hflK*	Hflk protein	0,12	0,17	
Y11_28041	*hesA*	Hemophore HasA	0,08	0,12	
Y11_36131	*hflX*	GTPase HflX (GTP-binding protein HflX)	0,05	0,06	

Table S4. Validation of the RNA-seq data by RT-qPCR. Shown are the YeO3-*hfq*::Km to wt and YeO3-*hfq*::Km/p*hfq* to wt ratios obtained in RT-qPCR and RNAseq. The *yopE* and *yopH* values are missing from the *phfq* and RNA-seq columns as the RNA was isolated from virulence plasmid-cured strains.

	RT-qPCR		RNAseq
gene	***hfq*::Km**	**p*hfq***	***hfq*::Km**
rovM	54.44 ± 3.64	5.46 ± 0.95	39.82
rovA	0.10 ± 0.09	0.59 ± 0.02	0.40
ureA	0.12 ± 0.12	0.59 ± 0.12	0.53
ureB	0.28 ± 0.12	1.37 ± 0.00	0.62
yopE	0.99 ± 0.10	-	-
yopH	0.87 ± 0.06	-	-

Table S5. Proteins differentially expressed at 37°C in YeO3-*hfq*::Km mutant strain in comparison to the wild type strain. In the FC column, the ↑ sign or value >1 show increased, while the ↓ sign or value <1 show decreased protein abundance. The proteins were considered as differentially expressed in the YeO3-*hfq*::Km mutant when compared to the wild type strain if in LC-MS/MS analysis they showed two-fold or greater difference in abundance with the p-value below 0.05. The corresponding RNA-sequencing values are shown for comparison.

Inf, the protein was detected only in the YeO3-*hfq*::Km mutant or the wild type strain. **NDE**, no significant differential expression in the RNA-sequencing analysis. **OP**, significantly inconsistent expression in proteomics and transcriptomics. **The grey color** indicates different pattern of expression in proteomics and transcriptomics.

					RNA SEQ		
ENTRY	PROTEIN	DESCRIPTION	FC	P-VALUE	FC	*P*	
YP_006004598.1		periplasmic oligopeptide-binding protein	inf ↑	0,0069	4,20	0,005	
YP_006007821.1		PTS system, glucitol/sorbitol-specific IIB component and second of two IIC components	inf ↑	0,0002	4,90	0,007	
YP_006007188.1		ornithine decarboxylase	inf ↑	0,0009	1,00	0,983	NDE
YP_006007418.1		GMP reductase	inf ↑	0,0051	0,96	0,232	NDE
YP_006003713.1	RovM	LysR family transcriptional regulator (homolog of LrhA)	inf ↑	0,0000	39,82	0,003	
YP_006007774.1	HscA	chaperone protein HscA	inf ↑	0,0073	1,48	0,029	NDE
YP_006005860.1		ornithine decarboxylase	inf ↑	0,0000	1,03	0,715	NDE
YP_006005146.1		glycerol dehydrogenase	inf ↑	0,0450	1,75	0,017	NDE
YP_006004654.1		fumarylacetoacetate hydrolase	inf ↑	0,0179	1,06	0,377	NDE
YP_006005778.1		2-c-methyl-D-erythritol 2,4-cyclodiphosphate synthase	inf ↑	0,0000	1,88	0,009	NDE
YP_006003853.1		L-serine dehydratase	inf ↑	0,0428	2,05	0,000	
YP_006006461.1		aspartate--ammonia ligase	inf ↑	0,0272	1,08	0,544	NDE
YP_006006609.1		dipeptide ABC transporter substrate-binding protein	inf ↑	0,0024	4,72	0,000	
YP_006006375.1		serine acetyltransferase	inf ↑	0,0020	1,54	0,007	NDE
YP_006004252.1		sugar-binding protein	inf ↑	0,0133	2,79	0,002	
YP_006007634.1		D-glycero-D-manno-heptose 1,7-bisphosphate phosphatase	inf ↑	0,0031	1,79	0,006	NDE
YP_006005434.1		putative cold-shock protein	inf ↑	0,0308	1,01	0,963	NDE
YP_006004062.1		adenylosuccinate lyase	17,50	0,0107	0,72	0,037	NDE
YP_006006665.1		methylmalonate-semialdehyde dehydrogenase	16,77	0,0041	2,01	0,153	NDE
YP_006005405.1		tRNA-i(6)A37 methylthiotransferase	12,40	0,0460	1,56	0,033	NDE
YP_006005687.1		CDP-diacylglycerol--serine O-phosphatidyltransferase	12,40	0,0108	1,81	0,016	NDE
YP_006007819.1		sorbitol-6-phosphate 2-dehydrogenase	12,40	0,0023	2,34	0,003	
YP_006006478.1	PstS	phosphate ABC transporter substrate-binding protein PstS	11,67	0,0049	0,73	0,172	NDE
YP_006006387.1		2-amino-3-ketobutyrate coenzyme A ligase	11,30	0,0031	1,88	0,001	NDE
YP_006006643.1		nadp-specific glutamate dehydrogenase	9,84	0,0298	4,11	0,003	
YP_006005249.1		glutamine ABC transporter, periplasmic glutamine-binding protein	9,50	0,0488	1,95	0,003	NDE
YP_006005684.1		thioredoxin 2	9,47	0,0458	0,95	0,764	NDE
YP_006004045.1	YcfM	lipoprotein YcfM	8,75	0,0019	2,40	0,003	
YP_006006465.1	GidA	tRNA uridine 5-carboxymethylaminomethyl modification protein GidA	8,75	0,0019	0,89	0,240	NDE
YP_006004331.1		superoxide dismutase	8,75	0,0219	1,40	0,099	NDE
YP_006005726.1		class I fumarate hydratase	8,39	0,0153	1,85	0,039	NDE

YP_006005144.1		exodeoxyribonuclease I	8,03	0,0421	1,92	0,010	NDE
YP_006003900.1	LolA	outer membrane lipoprotein carrier protein LolA	8,02	0,0394	0,68	0,021	NDE
YP_006006669.1		epi-inositol hydrolase	7,54	0,0039	1,61	0,300	NDE
YP_006006182.1		soluble cytochrome b562	7,30	0,0143	3,02	0,002	
YP_006007321.1		soluble lytic murein transglycosylase	7,29	0,0132	1,60	0,031	NDE
YP_006007010.1		IMP cyclohydrolase; Phosphoribosylaminoimidazolecarboxamide formyltransferase	6,57	0,0050	1,21	0,078	NDE
YP_006004244.1		N-acetylmuramoyl-L-alanine amidase	6,56	0,0072	1,04	0,161	NDE
YP_006005690.1		putative component of the lipoprotein assembly complex	6,02	0,0094	2,27	0,001	
YP_006005997.1		ADP-heptose synthase; D-glycero-beta-D-manno-heptose 7-phosphate kinase	5,84	0,0281	1,33	0,097	NDE
YP_006005697.1		chorismate mutase I; Prephenate dehydratase	5,84	0,0140	1,91	0,030	NDE
YP_006004744.1		putative oxidoreductase component of anaerobic dehydrogenases	5,84	0,0279	1,30	0,005	NDE
YP_006005340.1		2-keto-3-deoxy-D-arabino-heptulosonate-7-phosphate synthase I alpha	5,83	0,0266	0,97	0,596	NDE
YP_006006253.1		replicative DNA helicase	5,83	0,0266	1,51	0,044	NDE
YP_006006371.1	CpxR	copper-sensing two-component system response regulator CpxR	5,83	0,0266	4,61	0,000	
YP_006006714.1	OmpR	two-component system response regulator OmpR	5,59	0,0252	2,87	0,006	
YP_006005349.1		mota/TolQ/ExbB proton channel family protein	5,10	0,0413	1,15	0,501	NDE
YP_006004664.1		hypothetical protein	5,10	0,0409	0,65	0,052	NDE
YP_006005626.1		glutamate 5-kinase	5,10	0,0409	0,94	0,324	NDE
YP_006004035.1		PTS system, glucose-specific IIB component; PTS system, glucose-specific IIC component	5,07	0,0058	6,65	0,006	
YP_006006337.1	Sbp	sulfate-binding protein Sbp	5,03	0,0004	1,20	0,525	NDE
YP_006005187.1		methionyl-tRNA synthetase	4,74	0,0247	0,92	0,144	NDE
YP_006006767.1		putative sugar transferase	4,74	0,0247	2,61	0,001	
YP_006003504.1		thiol peroxidase, Bcp-type	4,74	0,0235	1,59	0,005	NDE
YP_006006965.1	TatA	twin-arginine translocation protein TatA	4,47	0,0127	1,45	0,042	NDE
YP_006005402.1	NagD	phosphatase NagD	4,38	0,0201	1,02	0,776	NDE
YP_006005495.1		hypothetical protein	4,38	0,0201	2,19	0,001	
YP_006006289.1	BtuB	outer membrane vitamin B12 receptor BtuB	4,38	0,0201	0,69	0,016	NDE
YP_006007468.1		putative iron binding protein from the HesB_IscA_SufA family	4,38	0,0201	0,98	0,886	NDE
YP_006007622.1	YaeO	rho-specific inhibitor of transcription termination (YaeO)	4,38	0,0201	0,55	0,087	NDE
YP_006007626.1		copper homeostasis protein CutF precursor; Lipoprotein NlpE involeved in surface adhesion	4,38	0,0201	1,07	0,330	NDE
YP_006007735.1		ribonuclease III	4,38	0,0201	0,93	0,043	NDE
YP_006006264.1		glycerol-3-phosphate acyltransferase	4,38	0,0361	1,64	0,015	NDE
YP_006003849.1		cystathionine gamma-lyase	4,14	0,0236	1,05	0,889	NDE
YP_006007267.1		arginine deiminase	4,13	0,0308	1,16	0,155	NDE
YP_006006924.1	FtsY	signal recognition particle receptor protein FtsY (=alpha subunit)	4,09	0,0422	1,30	0,049	NDE
YP_006006750.1		hypothetical protein	4,01	0,0425	1,32	0,156	NDE
YP_006007351.1		carbamoyl-phosphate synthase small subunit	3,89	0,0370	0,83	0,456	NDE
YP_006006399.1		deoxyuridine 5'-triphosphate nucleotidohydrolase	3,77	0,0061	1,57	0,027	NDE
YP_006005976.1		methylglyoxal reductase, acetol producing; 2,5-diketo-D-gluconate reductase A	3,72	0,0057	4,33	0,005	
YP_006007762.1		serine hydroxymethyltransferase	3,38	0,0017	0,82	0,008	NDE

YP_006006440.1		DNA polymerase I	3,23	0,0329	1,72	0,020	NDE
YP_006007633.1		methionine ABC transporter ATP-binding protein	3,12	0,0254	1,40	0,019	NDE
YP_006003540.1		nadp-dependent malic enzyme	2,99	0,0273	3,27	0,007	
YP_006007233.1	PepA	cytosol aminopeptidase PepA	2,99	0,0133	1,07	0,550	NDE
YP_006006404.1		orotate phosphoribosyltransferase	2,98	0,0235	0,93	0,604	NDE
YP_006007480.1		CTP synthase	2,83	0,0450	0,70	0,025	NDE
YP_006003761.1		ribonucleotide reductase of class Ia (aerobic),alpha subunit	2,79	0,0137	0,64	0,017	NDE
YP_006004290.1		integration host factor alpha subunit	2,75	0,0084	0,69	0,087	NDE
YP_006006755.1		cyclic AMP receptor protein	2,75	0,0336	1,53	0,002	NDE
YP_006006533.1		hypothetical protein	2,72	0,0423	1,23	0,208	NDE
YP_006006534.1		PTS system, mannitol-specific IIC component; PTS system, mannitol-specific IIB component; PTS system, mannitol-specific IIA component	2,67	0,0486	4,69	0,023	
YP_006006320.1	HslV	ATP-dependent protease HslV	2,59	0,0276	1,57	0,006	NDE
YP_006007718.1		pyruvate formate-lyase	2,55	0,0004	3,91	0,004	
YP_006007307.1		purine nucleoside phosphorylase	2,49	0,0371			
YP_006005399.1		N-acetylglucosamine-6-phosphate deacetylase	2,47	0,0114	1,08	0,537	NDE
YP_006007352.1		carbamoyl-phosphate synthase large subunit	2,46	0,0352	0,61	0,029	NDE
YP_006005816.1	YggG	putative metalloprotease yggG	2,46	0,0134	0,79	0,059	NDE
YP_006007790.1		1-hydroxy-2-methyl-2-(E)-butenyl 4-diphosphate synthase	2,44	0,0378	0,70	0,014	NDE
YP_006006133.1		putative cytochrome d ubiquinol oxidase subunit III (Cytochrome bd-I oxidase subunit III)	2,43	0,0140	1,12	0,364	NDE
YP_006006275.1		glucose-6-phosphate isomerase	2,43	0,0399	1,10	0,086	NDE
YP_006005606.1		DNA recombination-dependent growth factor C	2,39	0,0158	0,73	0,025	NDE
YP_006007361.1		survival protein SurA precursor (Peptidyl-prolyl cis-trans isomerase SurA)	2,36	0,0309	1,06	0,102	NDE
YP_006006476.1		N-acetylglucosamine-1-phosphate uridyltransferase;glucosamine-1-phosphate N-acetyltransferase	2,33	0,0489	1,06	0,290	NDE
YP_006006500.1		inner membrane protein translocase component YidC, long form	2,26	0,0019	1,03	0,046	NDE
YP_006007733.1		hypothetical protein	2,20	0,0009	0,92	0,306	NDE
YP_006006638.1		glutathione reductase	2,14	0,0026	1,10	0,216	NDE
YP_006006975.1	PepQ	xaa-Pro dipeptidase PepQ	2,14	0,0351	2,18	0,009	
YP_006005354.1		cytochrome d ubiquinol oxidase subunit I	2,11	0,0384	1,14	0,363	NDE
YP_006003704.1		acetate kinase	2,07	0,0338	1,00	0,993	NDE
YP_006006324.1		putative cytoplasmic protein	2,04	0,0249	1,73	0,012	NDE
YP_006003877.1		putative lipoprotein	0,53	0,0386	1,12	0,047	NDE
YP_006007681.1		urease subunit gamma	0,53	0,0209	0,53	0,083	NDE
YP_006005359.1		2-oxoglutarate dehydrogenase E1 component	0,53	0,0043	1,54	0,054	NDE
YP_006005361.1		succinate dehydrogenase flavoprotein subunit	0,43	0,0143	2,19	0,023	OP
YP_006005589.1		putative signal peptide protein	0,36	0,0105	1,45	0,178	NDE
YP_006003718.1		NADH-ubiquinone oxidoreductase subunit F	0,36	0,0018	0,90	0,071	NDE
YP_006004319.1	SufC	iron-sulfur cluster assembly ATPase protein SufC	0,36	0,0076	1,79	0,012	NDE
YP_006006194.1		putative toxin subunit	0,18	0,0372	1,08	0,677	NDE
YP_006007114.1	HflC	hflc protein	0,09	0,0015	0,23	0,000	
YP_006007113.1	HflK	hflk protein	0,03	0,0004	0,17	0,001	
YP_006004604.1		UDP-glucose dehydrogenase	inf ↓	0,0322	0,49	0,020	

YP_006005173.1		ABC transporter	inf ↓	0,0322	1,07	0,618	NDE
YP_006005232.1	MoeB	molybdopterin biosynthesis protein MoeB	inf ↓	0,0322	1,81	0,024	NDE
YP_006007472.1		5'-methylthioadenosine nucleosidase; S-adenosylhomocysteine nucleosidase	inf ↓	0,0322	1,01	0,949	NDE
YP_006007717.1		uracil-DNA glycosylase, family 1	inf ↓	0,0322	1,30	0,050	NDE
YP_006004681.1	RuvB	Holliday junction ATP-dependent DNA helicase RuvB	inf ↓	0,0000	1,15	0,213	NDE
YP_006006726.1		multimodular transpeptidase-transglycosylase	inf ↓	0,0000	0,79	0,151	NDE
YP_006007804.1		hypothetical protein	inf ↓	0,0000	1,13	0,746	NDE

Table S6. Proteins differentially expressed at RT in YeO3-*hfq*::Km mutant strain in comparison to the wild type strain. In the FC column, the ↑ sign or value >1 show increased, while the ↓ sign or value <1 show decreased protein abundance. The proteins were considered as differentially expressed in the YeO3-*hfq*::Km mutant when compared to the wild type strain if in LC-MS/MS analysis they showed two-fold or greater difference in abundance with the p-value below 0.05. The corresponding RNA-sequencing values are shown for comparison.

Inf, the protein was detected only in the YeO3-*hfq*::Km mutant or the wild type strain. **NDE**, no significant differential expression in the RNA-sequencing analysis. **OP**, significantly inconsistent expression in proteomics and transcriptomics. **The grey color** indicates different pattern of expression in proteomics and transcriptomics.

					RNA SEQ		
ENTRY	PROTEIN	DESCRIPTION	FC	P-VALUE	FC	*P*	
YP_006003871.1	ArtJ	arginine ABC transporter periplasmic substrate-binding protein	inf ↑	0,0357	0,76	0,214	NDE
YP_006005034.1		citrate lyase subunit beta	inf ↑	0,0391	2,05	0,016	
YP_006005137.1		ribose/xylose/arabinose/galactoside ABC-type transport systems, periplasmic sugar binding protein	inf ↑	0,0002	1,36	0,017	NDE
YP_006005143.1		nucleoside-diphosphate-sugar epimerase	inf ↑	0,0357	0,56	0,003	NDE
YP_006005150.1		nucleoside-diphosphate-sugar epimerase	inf ↑	0,0000	1,20	0,405	NDE
YP_006005189.1		putative sugar ABC transporter	inf ↑	0,0089	0,47	0,021	OP
YP_006005643.1		Na(+)-translocating NADH-quinone reductase subunit C	inf ↑	0,0223	2,06	0,303	NDE
YP_006005645.1		Na(+)-translocating NADH-quinone reductase subunit A	inf ↑	0,0247	3,07	0,143	NDE
YP_006005701.1		putative Dcu family, anaerobic C4-dicarboxylate transporter	inf ↑	0,0391	2,53	0,002	
YP_006005868.1	FecE	iron(III) dicitrate transport ATP-binding protein FecE	inf ↑	0,0111	1,87	0,112	NDE
YP_006006372.1	CpxA	copper sensory histidine kinase CpxA	inf ↑	0,0223	5,62	0,029	
YP_006006523.1		glyoxylate reductase-Hydroxypyruvate reductase; 2-ketoaldonate reductase, broad specificity	inf ↑	0,0028	1,96	0,006	NDE
YP_006006767.1		putative sugar transferase	inf ↑	0,0002	2,04	0,063	
YP_006007187.1	PotE	putrescine/proton symporter, putrescine/ornithine antiporter PotE	inf ↑	0,0180	0,70	0,243	NDE
YP_006007188.1		ornithine decarboxylase	inf ↑	0,0002	0,73	0,400	NDE
YP_006006643.1		nadp-specific glutamate dehydrogenase	43,59	0,0002	8,44	0,002	
YP_006003915.1		L-asparaginase, partial	31,49	0,0008	2,19	0,049	
YP_006003853.1		L-serine dehydratase	28,81	0,0000	3,90	0,000	
YP_006007727.1		L-aspartate oxidase	28,22	0,0144	1,94	0,062	NDE
YP_006007821.1		PTS system, glucitol/sorbitol-specific IIB component and second of two IIC components	16,16	0,0006	7,95	0,042	
YP_006007076.1		L-threonine transporter, anaerobically inducible	14,80	0,0023	1,08	0,777	NDE
YP_006007416.1		hypothetical protein	12,64	0,0005	2,02	0,183	NDE
YP_006006909.1		glycerol-3-phosphate transporter	11,26	0,0007	2,11	0,003	
YP_006006906.1		cof protein, HD superfamily hydrolase	11,16	0,0047	1,93	0,118	NDE
YP_006007633.1		methionine ABC transporter ATP-binding protein	10,77	0,0123	3,45	0,023	
YP_006004035.1		PTS system, glucose-specific IIB component; PTS system, glucose-specific IIC component	10,54	0,0016	9,46	0,001	
YP_006005033.1		citrate lyase subunit alpha	10,02	0,0009	2,56	0,002	
YP_006006573.1		histidine ammonia-lyase	8,60	0,0127	1,05	0,694	NDE
YP_006007153.1		octaprenyl-diphosphate synthase	7,82	0,0149	2,52	0,037	
YP_006007148.1		UDP-N-acetylmuramate:L-alanyl-gamma-D-glutamyl-meso-diaminopimelate ligase	7,80	0,0131	0,80	0,118	NDE

YP_006004133.1		L-serine dehydratase	7,73	0,0001	3,89	0,020	
YP_006006461.1		aspartate--ammonia ligase	7,51	0,0041	0,91	0,798	NDE
YP_006007109.1		tRNA delta(2)-isopentenylpyrophosphate transferase, partial	6,74	0,0423	6,10	0,002	
YP_006004395.1		fmn-dependent NADH-azoreductase	6,14	0,0048	1,04	0,907	NDE
YP_006005992.1		glutathionylspermidine synthase, group 1	5,50	0,0212	3,73	0,005	
YP_006004766.1		hypothetical protein	5,27	0,0045	6,75	0,052	
YP_006006859.1	PpiC	peptidyl-prolyl cis-trans isomerase ppiC	5,04	0,0289	1,05	0,768	NDE
YP_006004300.1	PmrJ	polymyxin resistance protein PmrJ	5,00	0,0021	1,86	0,221	NDE
YP_006007068.1		periplasmic hemin-binding protein	4,67	0,0408	0,49	0,066	NDE
YP_006006380.1		2,3-bisphosphoglycerate-independent phosphoglycerate mutase	4,40	0,0105	2,65	0,014	
YP_006005569.1	ThiI	thiamine biosynthesis protein thiI	4,09	0,0226	1,80	0,079	NDE
YP_006005465.1		hypothetical protein	3,93	0,0351	1,19	0,418	NDE
YP_006004128.1		PTS system mannose-specific transporter subunit IIC	3,84	0,0148	2,22	0,064	
YP_006006966.1	TatB	twin-arginine translocation protein TatB	3,77	0,0200	1,62	0,306	NDE
YP_006003854.1		serine transporter	3,46	0,0172	5,87	0,008	
YP_006004391.1		D-lactate dehydrogenase	3,37	0,0416	1,24	0,124	NDE
YP_006004735.1		iron-chelator utilization protein	3,34	0,0175	1,85	0,088	NDE
YP_006004495.1		fumarate hydratase class II	3,32	0,0121	0,66	0,019	NDE
YP_006004630.1	YeaD	aldose 1-epimerase family protein YeaD	3,31	0,0122	1,05	0,420	NDE
YP_006006534.1		PTS system, mannitol-specific IIC component; PTS system, mannitol-specific IIB component; PTS system, mannitol-specific IIA component	3,23	0,0447	0,84	0,096	NDE
YP_006007474.1		htra protease/chaperone protein	3,22	0,0118	1,75	0,005	NDE
YP_006003577.1		DNA ligase	3,20	0,0066	1,18	0,354	NDE
YP_006007254.1		putative glycoprotein/receptor	3,19	0,0268	0,78	0,305	NDE
YP_006003888.1	MacA	macrolide-specific efflux protein MacA	3,15	0,0253	1,77	0,098	NDE
YP_006006134.1	DegQ	outer membrane stress sensor protease DegQ,serine protease	2,97	0,0003	1,76	0,043	NDE
YP_006007509.1		peptide chain release factor 2; programmed frameshift-containing, partial	2,96	0,0312	3,52	0,049	
YP_006004598.1		periplasmic oligopeptide-binding protein	2,90	0,0357	2,33	0,044	
YP_006005477.1	YbbK	putative stomatin/prohibitin-family membrane protease subunit YbbK	2,75	0,0175	2,76	0,028	
YP_006005354.1		cytochrome d ubiquinol oxidase subunit I	2,69	0,0220	2,59	0,034	
YP_006006714.1	OmpR	two-component system response regulator OmpR	2,67	0,0255	1,49	0,231	NDE
YP_006004239.1	HtpX	putative protease HtpX	2,66	0,0131	1,37	0,137	NDE
YP_006004563.1		DNA topoisomerase I	2,60	0,0254	2,65	0,002	
YP_006007774.1		chaperone protein HscA	2,59	0,0075	3,92	0,019	
YP_006006670.1	HscA	myo-inositol 2-dehydrogenase 1	2,46	0,0001	2,04	0,005	
YP_006007069.1	HmuS	hemin transport protein HmuS	2,41	0,0008	0,38	0,034	OP
YP_006005483.1		UDP-sugar hydrolase; 5'-nucleotidase	2,32	0,0151	0,78	0,204	NDE
YP_006007366.1	RapA	RNA polymerase associated protein RapA	2,30	0,0065	1,38	0,067	NDE
YP_006006609.1		dipeptide ABC transporter substrate-binding protein	2,26	0,0011	2,26	0,020	
YP_006006326.1		glycerol kinase	2,24	0,0155	1,17	0,315	NDE
YP_006005411.1	GltI	glutamate Aspartate periplasmic binding protein precursor GltI	0,50	0,0069	0,30	0,050	
YP_006007092.1		entericidin B	0,47	0,0094	2,14	-	NDE

YP_006007147.1		fructose-1,6-bisphosphatase, type I	0,46	0,0184	0,86	0,096	NDE
YP_006006471.1		ATP synthase subunit delta	0,44	0,0021	1,08	0,372	NDE
YP_006005790.1		sulfite reductase [NADPH] hemoprotein beta-component	0,43	0,0052	0,36	0,003	
YP_006006091.1	YgiD	membrane protein YqjD	0,42	0,0302	0,67	0,003	NDE
YP_006007306.1		phosphopentomutase	0,40	0,0243	0,59	0,002	NDE
YP_006007682.1		urease subunit beta	0,39	0,0079	0,18	0,006	
YP_006007128.1		30S ribosomal protein S18	0,38	0,0258	1,19	0,649	NDE
YP_006007267.1		arginine deiminase	0,38	0,0219	0,73	0,213	NDE
YP_006003823.1		fructose-specific phosphocarrier protein HPr; PTS system, fructose-specific IIA component	0,35	0,0353	0,82	0,358	NDE
YP_006007683.1		urease alpha subunit	0,32	0,0333	0,25	0,013	
YP_006004209.1	CutC	cytoplasmic copper homeostasis protein CutC	0,30	0,0206	0,23	0,000	
YP_006004150.1	YobA	protein yobA	0,30	0,0192	0,40	0,070	
YP_006003740.1		elab protein	0,29	0,0325	0,36	0,021	
YP_006003547.1	YgiW	protein ygiW	0,27	0,0043	0,23	0,000	
YP_006005469.1		phosphoribosylaminoimidazole carboxylase catalytic subunit	0,26	0,0127	0,69	0,156	NDE
YP_006003846.1		methionine ABC transporter substrate-binding protein	0,25	0,0238	0,24	0,000	
YP_006007299.1	OsmY	osmotically inducible protein OsmY	0,21	0,0401	0,29	0,011	
YP_006004343.1	RovA	transcriptional regulator (homolog of SlyA)	0,19	0,0001	0,13	0,001	
YP_006007650.1	ProX	L-proline glycine betaine binding ABC transporter protein ProX	0,18	0,0090	0,38	0,014	
YP_006003724.1		NADH-ubiquinone oxidoreductase subunit L	0,17	0,0088	1,10	0,800	NDE
YP_006006188.1		succinate-semialdehyde dehydrogenase	0,15	0,0033	0,96	0,702	NDE
YP_006005556.1	BolA	cell division protein BolA	0,13	0,0262	0,29	0,017	
YP_006006090.1	YgiC	periplasmic protein YqjC	0,13	0,0071	0,54	0,039	NDE
YP_006004087.1		nadph:quinone oxidoreductase 2	0,13	0,0410	0,64	0,041	NDE
YP_006007684.1	UreE	urease accessory protein UreE	0,11	0,0096	0,30	0,013	
YP_006004890.1		transcriptional repressor of PutA and PUTP; Proline dehydrogenase	0,11	0,0156	0,37	0,001	
YP_006006973.1		3-ketoacyl-CoA thiolase @ Acetyl-CoA acetyltransferase	0,09	0,0300	0,40	0,012	
YP_006007113.1		hflk protein	0,07	0,0016	0,12	0,000	
YP_006005296.1		hypothetical protein	0,06	0,0020	0,23	0,000	
YP_006007693.1		potassium channel protein	0,05	0,0005	0,53	0,091	NDE
YP_006004204.1		phosphate starvation-inducible protein PhoH	inf ↓	0,0036	0,21	0,128	
YP_006004228.1		sigma-fimbriae chaperone protein	inf ↓	0,0085	0,37	0,037	
YP_006004882.1		ferrous iron transport periplasmic protein EfeO,contains peptidase-M75 domain and (frequently) cupredoxin-like domain	inf ↓	0,0194	0,17	0,011	
YP_006005332.1		galactokinase	inf ↓	0,0238	1,06	0,758	NDE
YP_006005885.1	ProP	L-proline/Glycine betaine transporter ProP	inf ↓	0,0194	0,24	0,004	
YP_006006704.1		ferrous iron transport protein B	inf ↓	0,0011	0,55	0,001	NDE
YP_006007114.1	HflC	hflc protein	inf ↓	0,0000	0,13	0,031	
YP_006007651.1	ProW	L-proline glycine betaine ABC transport system permease protein ProW	inf ↓	0,0447	0,49	0,065	NDE
YP_006007823.1		transcription regulator	inf ↓	0,0032	0,36	0,029	

Table S7. A list of sRNA species identified from the *Y. enterocolitica* O:3 strain Y11 genome (accession number FR729477) analyzed in this work

	Location in the Y11 genome	
sRNA	*start*	end
ryfA	198163	198461
micF	280362	280452
rybB	373459	373539
sraC	684431	684546
ryeB	684453	684552
rprA	842565	842673
ryhB2	899508	899615
fnrS	914737	914857
rtt	1138115	1138274
sroB	2002864	2002946
ffs	2053260	2053359
ryfD	2237776	2237914
sraD	2256448	2256522
rnpA	2645937	2646086
csrC	3011650	3011850
spot42	3013098	3013215
ryhB2	3290008	3290114
glmZ	3499765	3499833
rTT	3613574	3613729
sraG	3812285	3812465
ssrS	4172106	4172288
sraE	4238999	4239093
gcvB	4274338	4274443
csrB	4284182	4284498
tff	4291658	4291830
ssrA	4396448	4396828
cyaR	4517116	4517216

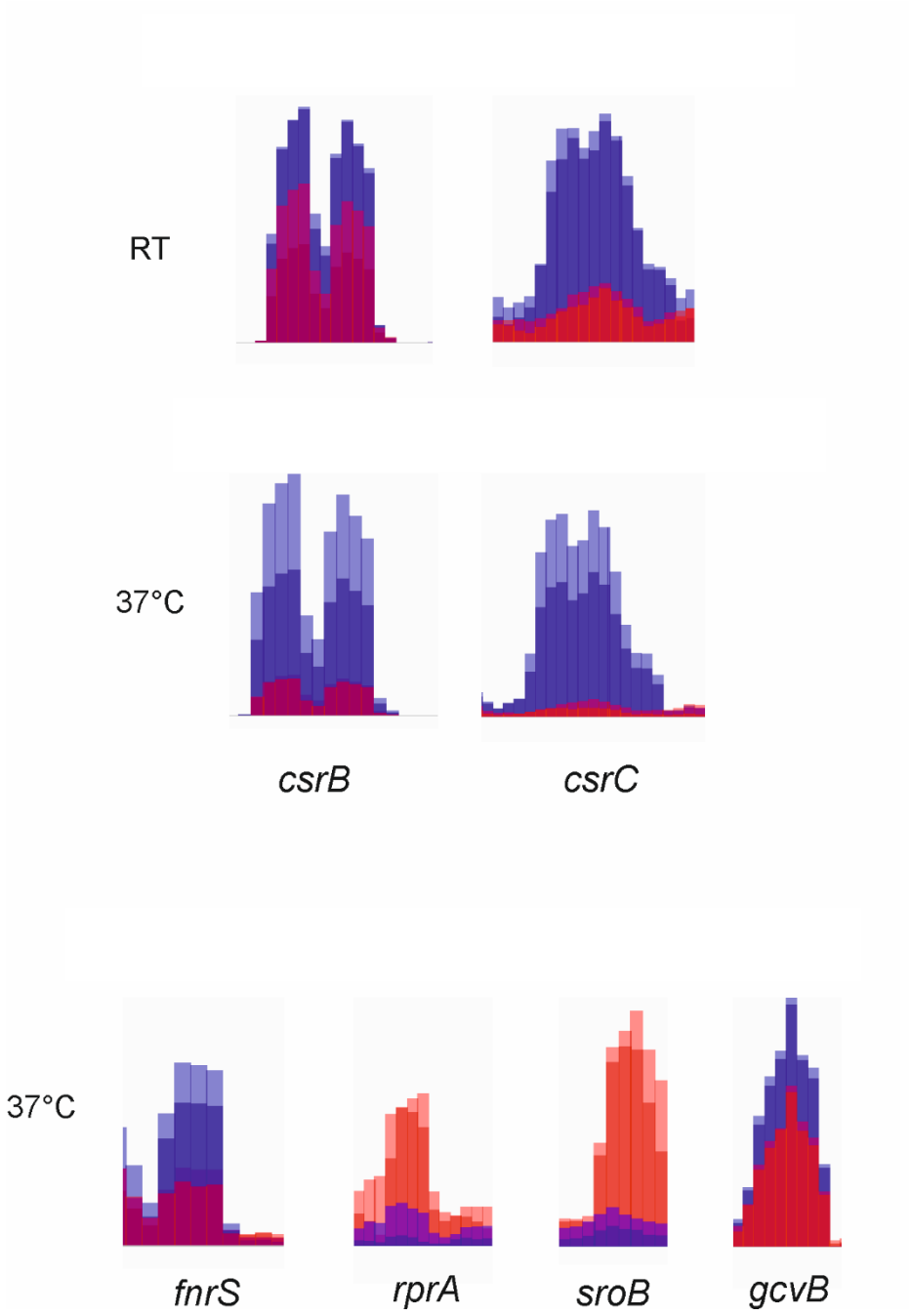

Figure S1. Differentially expressed sRNAs in YeO3 strain and the *hfq* mutant of *Y. enterocolitica* O:3 at RT and 37°C. Alignments of the read coverages from two biological replicates for both strains are shown. Data were processed using the Integrative Genomics Viewer (Broad Institute). Each bar shows the mean read coverage of a window of 25 nt. The wild type data are shown in shades of blue and the YeO3-*hfq*::Km mutant are shown in pink and red. The read coverage ranges were adjusted for each sRNA panel separately.

Table S8. Bacterial counts on day 5 post-infection in mouse organs after intragastric infection with ca. 10^9 CFU of bacteria.

Mouse single infection (I.G. route)				
Strain (Dose)	**Organ**	**CFU/g**		
		Mouse 1	**Mouse 2**	**Mouse 3**
YeO3-wt ($0.8x10^9$)	Spleen	3×10^8 †	0	0
	Liver	1×10^6 †	0	0
	Peyer's patches	2×10^5 †	8×10^5	9×10^6
YeO3-*hfq*::Km ($2.7x10^9$)	Spleen	4×10^3 †	0	0
	Liver	0 †	0	0
	Peyer's patches	0 †	3×10^5	2×10^5
YeO3- *rovM*-*hfq*::Km ($2.7x10^9$)	Spleen	0	1×10^3	0
	Liver	0	0	0
	Peyer's patches	4×10^5	5×10^3	2×10^5
YeO3-*hfq*::Km/p*hfq* ($0.4x10^9$)	Spleen	0	0	0
	Liver	0	0	0
	Peyer's patches	1×10^6	4×10^6	1×10^6

†, found dead on day 2 post-infection

A

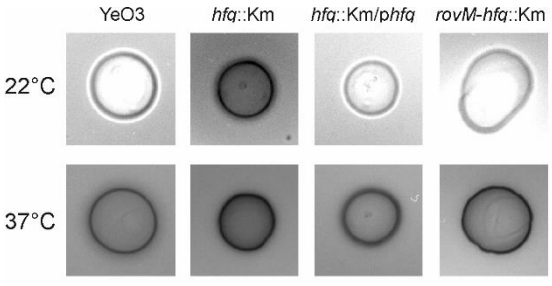

B

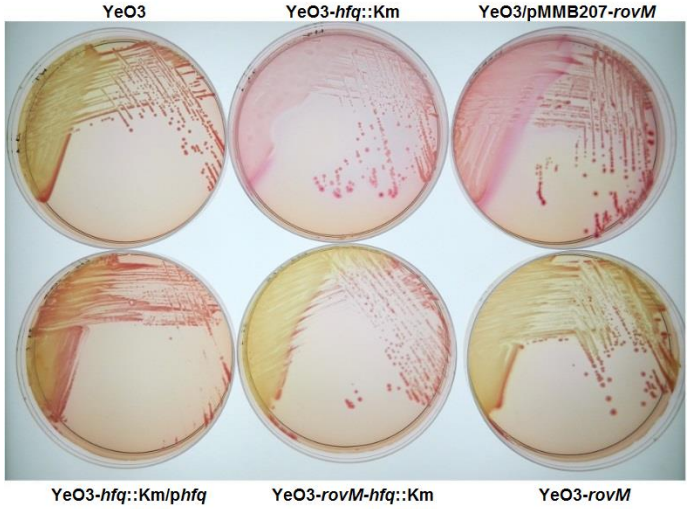

C

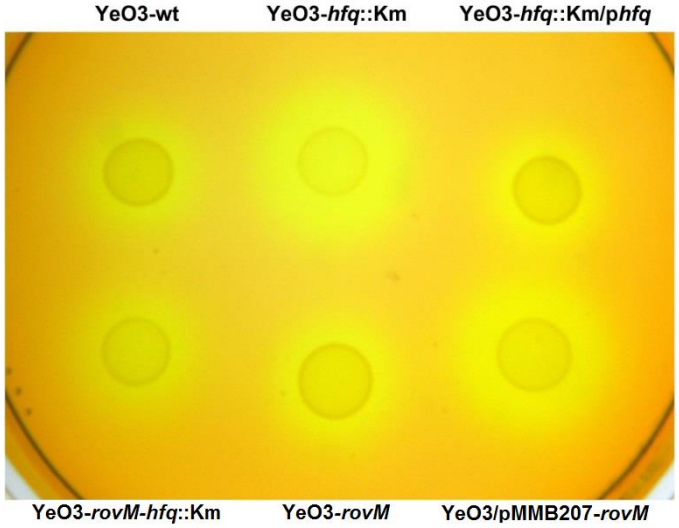

Figure S2. Influence of RovM derepression on the carbohydrate metabolism. **(A)** Colony morphology of bacteria grown on CIN-agar plates. Five µl of bacterial culture grown aerated overnight in LB at 22°C was spotted on CIN agar plate that was subsequently incubated at 22 or 37 °C. Images of the colonies were taken with the background UV light. **(B)** Bacteria grown on CIN agar plates for 48h at RT. Both the YeO3-*hfq*::Km and YeO3/pMMB207-*rovM* bacteria displayed a violet halo surrounding the growth. All the other strains presented growth typical for YeO3-wt. **(C)** Overexpression of RovM leads to higher rate of mannitol utilization. Ten µl of bacteria was spotted on mannitol plates and incubated for 48h at RT. Both YeO3-*hfq*::Km and YeO3/pMMB207-*rovM* displayed larger halos surrounding the bacterial growth indicating higher rates of acidification of the medium.

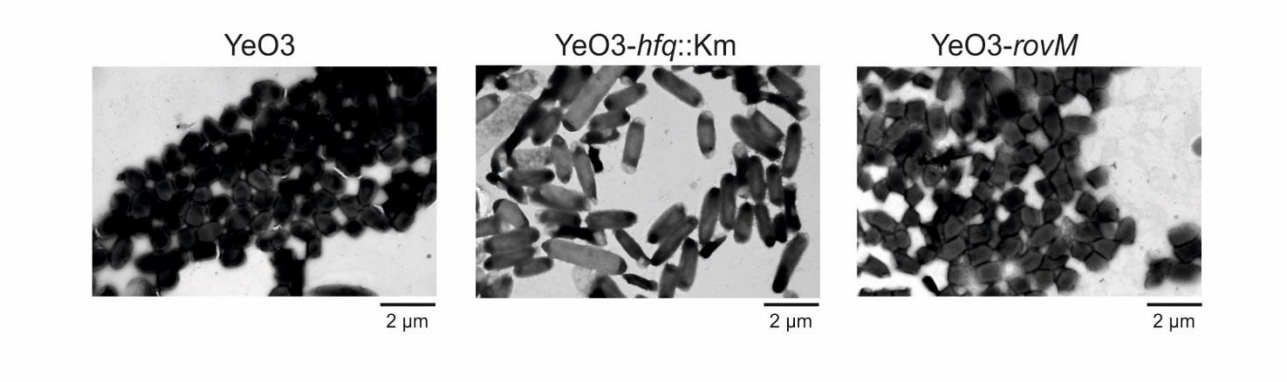

Figure S3. Transmission electron microscopy images of wild type (left image), YeO3-*hfq*::Km (middle image) and YeO3-*rovM* bacteria (right image) stained with uranyl acetate.

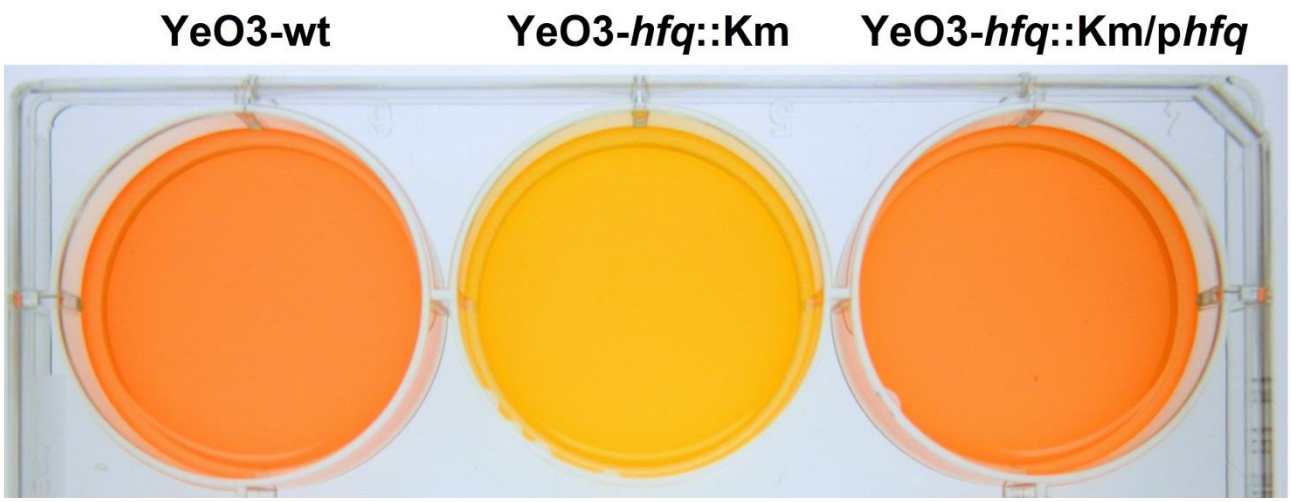

Figure S4. Urease activity in *Y. enterocolitica* is Hfq-dependent. Bacteria were grown for 24h at 37°C in medium containing urea, 0.1% of glucose, and phenol red as the pH indicator. The urease activity was not present in the YeO3-*hfq*::Km bacteria. The complementation of the mutant restored the urease activity.

Table S9. Bacterial counts in mouse organs on day 5 after intraperitoneal infection with 1 x 10^9 CFU of bacteria.

Mouse single infection (I.P. route)				
Strain (Dose)	**Organ**	**CFU/g**		
		Mouse 1	**Mouse 2**	**Mouse 3**
YeO3-wt ($0.8x10^9$)	Spleen	6 x 10^4	2 x 10^4	4 x 10^3
	Liver	5 x 10^5	4 x 10^6	5 x 10^2
	Peyer's patches	6 x 10^7	9 x 10^6	5 x 10^6
YeO3-*hfq*::Km ($2.7x10^9$)	Spleen	1 x 10^7 †	1 x 10^7 †	5 x 10^4
	Liver	1 x 10^6 †	1 x 10^6 †	1 x 10^5
	Peyer's patches	2 x 10^6 †	2 x 10^6 †	1 x 10^5
YeO3- *rovM-hfq*::Km ($2.7x10^9$)	Spleen	4 x 10^8 ††	2 x 10^8 †	6 x 10^7 †††
	Liver	7 x 10^6 ††	1 x 10^7 †	3 x 10^6 †††
	Peyer's patches	1 x 10^7 ††	6 x 10^7 †	1 x 10^7 †††

†, found dead on day 2 post-infection; ††, found dead on day 1 post-infection; †††, killed on day 2 post-infection due to severe signs of illness.

Table S10. The spleen weights of the mice infected with the different strains.

Strain	**Spleen weight [g]**					
	I.G. infection			**I.P. infection**		
	Mouse 1	**Mouse 2**	**Mouse 3**	**Mouse 1**	**Mouse 2**	**Mouse 3**
YeO3-wt	0.073 †	0.083	0.123	0.258	0.276	0. 337
YeO3-*hfq*::Km	0.094 †	0.125	0.166	0.075 †	0.074 †	0.216
YeO3- *rovM-hfq*::Km	0.104	0.105	0.078	0.096 †	0.063 †	0.097 ††
YeO3-*hfq*::Km/p*hfq*	0.095	0.086	0.088			

†, found dead on day 2 post-infection; ††, killed on day 2 post-infection due to severe signs of illness

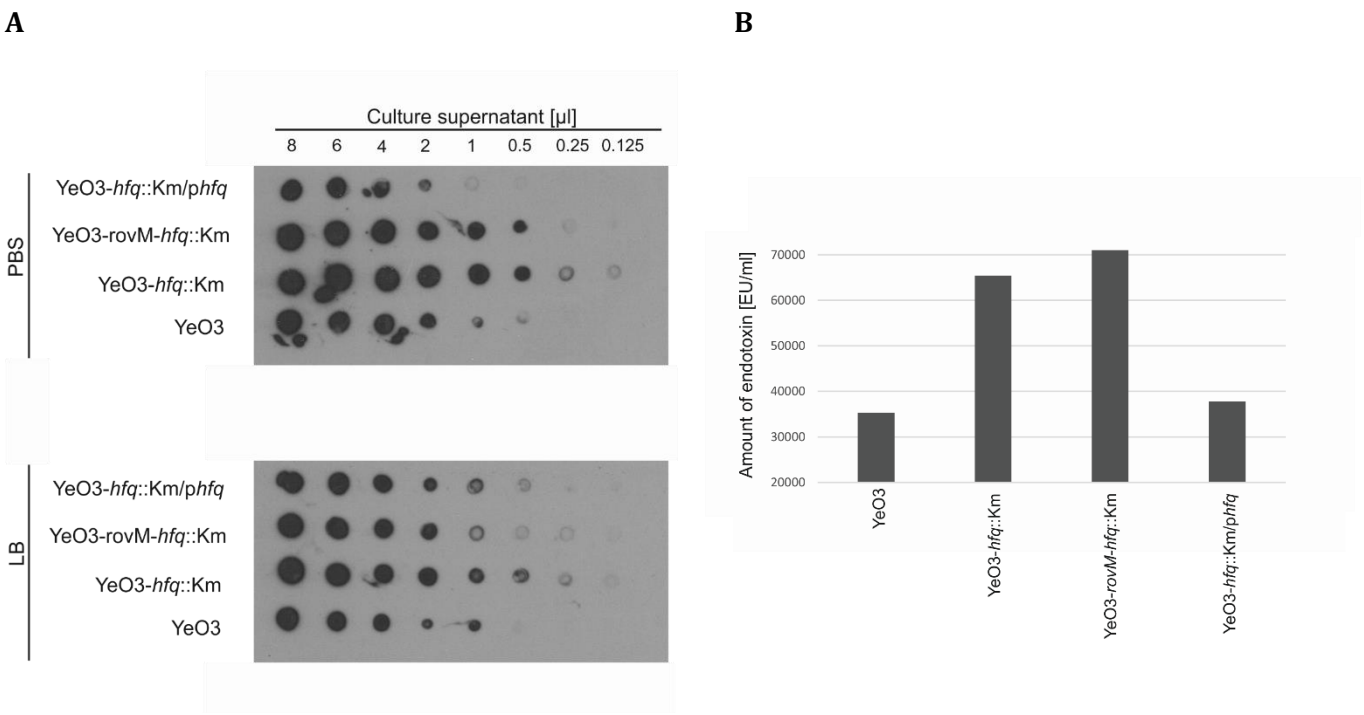

Figure S5. The release of LPS to culture medium. **(A)** The dot blotting of culture supernatants showed increased release of LPS from the YeO3-hfq::Km and YeO3-rovM-hfq::Km bacteria when compared to wild type bacteria (YeO3) and *trans*-complemented *hfq*-mutant. The presence of O-antigen in the culture medium supernatant was detected by dot-immunoblotting using mAb TomA6 (Pekkola-Heino *et al.,* 1987. Monoclonal antibodies reacting selectively with core and O-polysaccharide of *Yersinia enterocolitica* O:3 lipopolysaccharide. APMIS 95:27-34). Overnight bacterial cultures were diluted to OD_{600} = 2.0 and incubated for 2h at 37°C in either LB or PBS with vigorous shaking. After the incubation, bacterial cells were centrifuged down and discarded. The amounts of the supernatant spotted (in 2 µl volumes of undiluted and appropriately diluted supernatants) to the dots on the membrane are indicated above the picture. **(B)** The quantity of endotoxin in the supernatants was measured using the Endosafe-PTS system (Charles River Laboratories). Only the results of the PBS supernatants are shown due to inhibitors interfering with the measurements present in the LB supernatants.

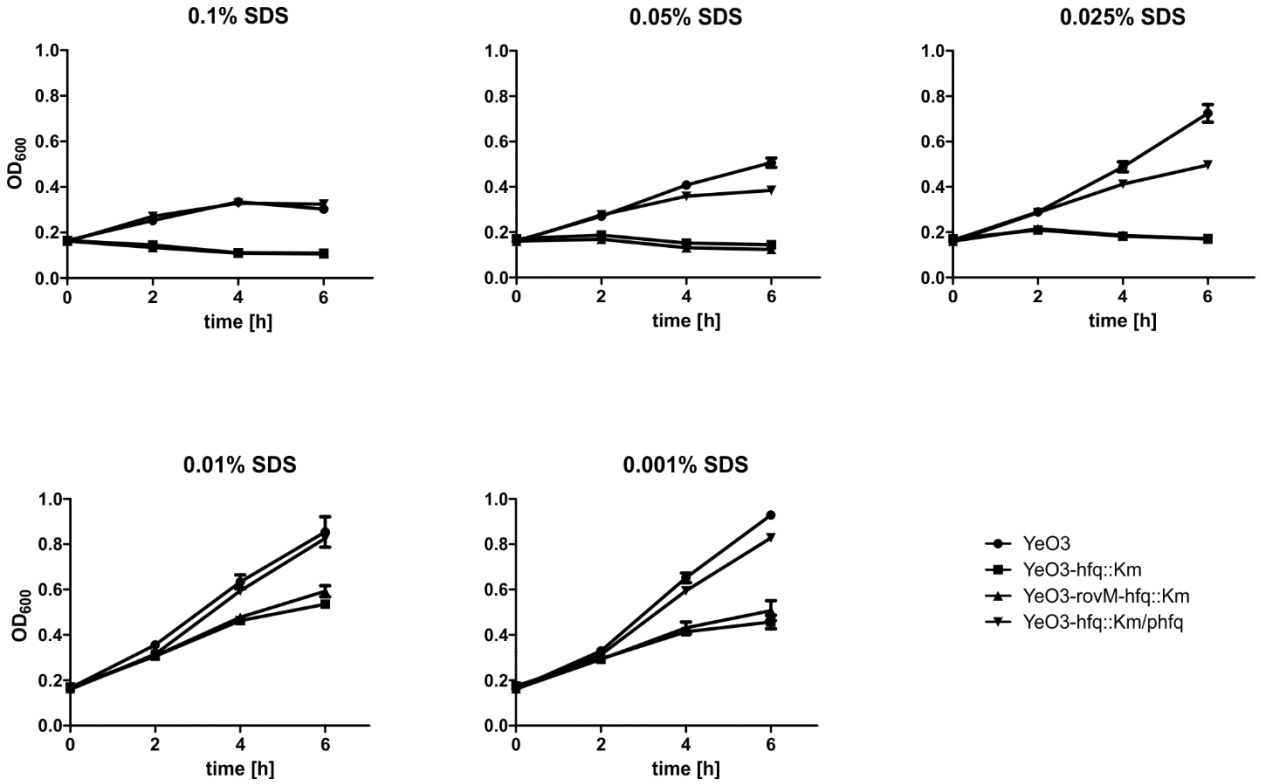

Figure S6. The YeO3-*hfq*::Km and YeO3-*rovM-hfq*::Km bacteria highly sensitive to SDS. Shown are the growth curves of wild type, mutant and *trans*-complemented strains in the presence of 0.1%, 0.05%, 0.025, 0.01%, and 0.001% SDS. Each point represents the average of ten replicates and the vertical bars indicate the standard deviations (mostly covered by the symbol). The symbols of the curves are indicated at the bottom right. Bacteria grown overnight (12-16 h) at RT were diluted into fresh LB medium supplemented with different concertrations of SDS and 200 µl aliquots were distributed into honeycomb plate wells (Growth Curves Ab Ltd). The growth experiment was carried out at 37°C using the Bioscreen C incubator (Growth Curves Ab Ltd) with continuous shaking. OD_{600} was measured every 2h. The growth of the wild type and the *trans*-complemented bacteria was partially inhibited by 0.1 % SDS while that of the mutant bacteria was completely inhibited still by the 0.025 % SDS. Note also that the growth rates of the mutant bacteria is slower than that of the wild type and the *trans*-complemented bacteria.

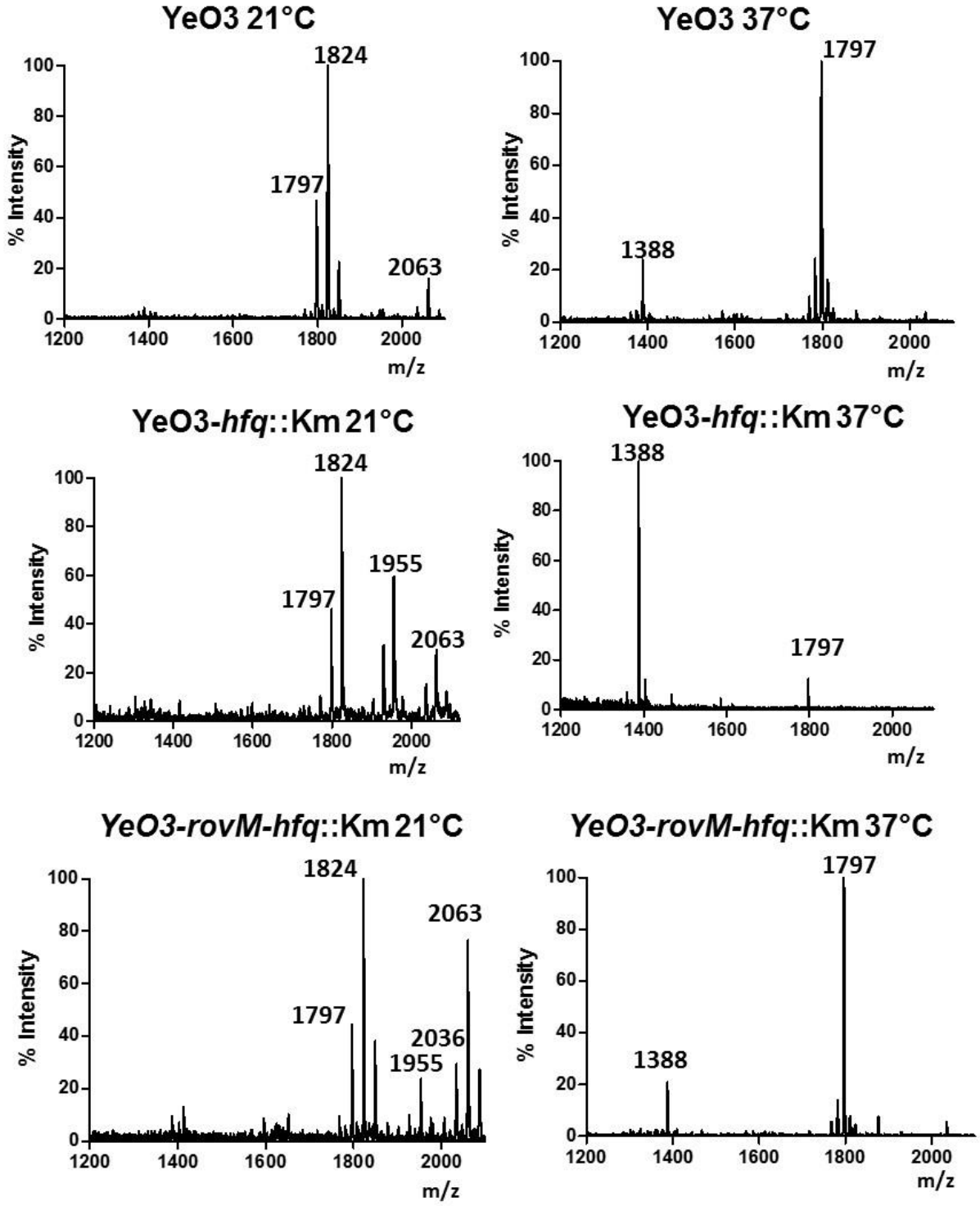

Figure S7. Lipid A analysis of *Y. enterocolitica* O:3 wild type, YeO3-*hfq*::Km and YeO3-*rovM-hfq*::Km. Negative ion MALDI-TOF mass spectrometry spectra of lipid A isolated from the bacteria grown at 21°C and 37°C.

The Lipid A was extracted and analyzed as described before (Reinés M, Llobet E, Dahlström KM, Pérez-Gutiérrez C, Llompart CM, et al. (2012) Deciphering the acylation pattern of *Yersinia enterocolitica* Lipid A. PLoS Pathog 8(10): e1002978. doi:10.1371/journal.ppat.1002978).

Y11_04281

YeO3-wt
(RT, forward strand)

YeO3-*hfq*::Km
(RT, forward strand)

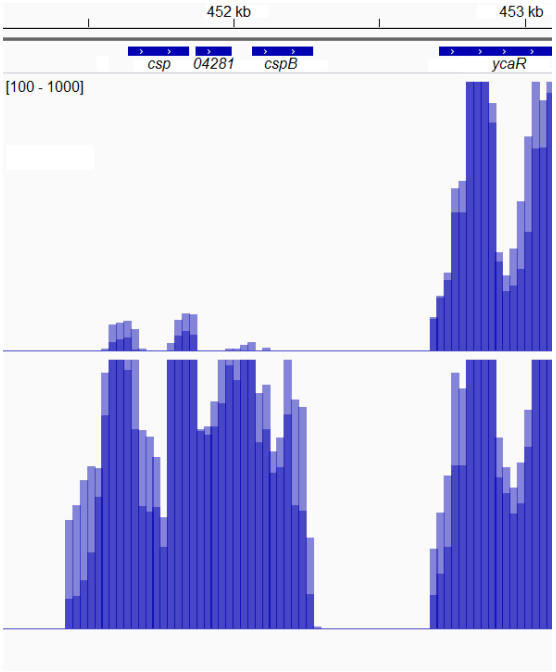

Y11_11701

YeO3-wt
(RT, reverse strand)

YeO3-*hfq*::Km
(RT, reverse strand)

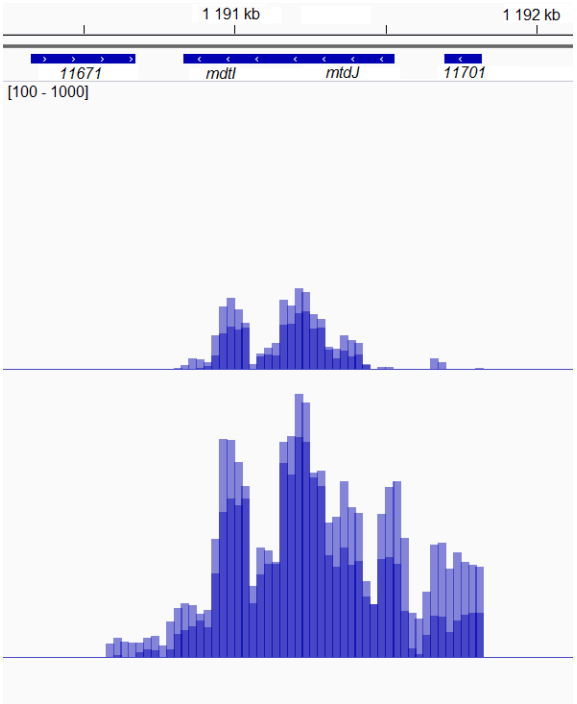

Figure S8. RNA-seq read alignments of the two most up-regulated genes, Y11_04281 and Y11_11701, in the YeO3-*hfq*::Km bacteria. Visualization was done using Integrative Genomics Viewer (Broad Institute). Each bar shows the mean read coverage of a window of 25 nt. Each graph presents an overlay of two replicates.

Table S11. Primers used in this work.

Primer	Sequence	Acc. no	Purpose
hfq-F1	GGCAGATCTCCAGAGCACTGGAAGTTTTT		Amplification of *hfq* and flanking regions, 1367 bp, BglII sites
hfq-R1	GGCAGATCTACCAAACGAGTCGCAATATG		
hfq-F2	GGCGGATCCAACCATGACGGGGAACATAA		Plasmid PCR, deletion of *hfq* gene from the 1367 bp fragment, BamHI sites
hfq-R2	GGCGGATCCTCGGCTCGAAAATAAACTGC		
Km-GB66-f	GGAAAGCCACGTTGTGTCTCAAA	X06404	Amplification of Km-Genblock cassette, 1156 bp
Km-GB66-r	CATCATCCAGCCAGAAAGTGAGG		
M-lrhA-F	CGCGGATCCGCATCTGATGATACTGCCG		Amplification of a 437 bp internal fragment of the *rovM* gene, BamHI sites
M-lrhA-R	CGCGGATCCGCATCTGATGATACTGCCG		
G-lrhA-F	CTTAGCGTTGTCCCTTATTGATG		Amplification of the *rovM* gene, EcoRI site
G-lrhA-R	CGCGAATTCCTTAGCTTGACCTGCTCGAATTA		
P-lrhA-F	CGCGGATCCTGCTTATCAATTATCAATTCTTACCAC		Amplification of the *rovM* promoter region, BamHI site
P-lrhA-R	CGCGGATCCAGCAGAGGCAAACGTATTCAA		
csrA-F1	CGCGAATTCTTTTCAAGGAGCAAAGAATGC		Amplification of the *csrA* gene, EcoRI/BamHI site
csrA-R1	CGCGGATCCGCAGTAGCGCCTCGTGTAAC		
pMMB207polylinker-R	AGCGGATAACAATTTCACACAGGAA		sequencing
pMMB207polylinker-F	AGACCGCTTCTGCGTTCTGATTTA		
csrA-F2	GCCGGATCCCGAAATTGGTCAATGGTGTG		Construction of pKNG101-*csrA*::CAT plasmid
csrA-R4	CGCGGATCCGGATTCGAACCCTCGATACA		
CAT_upF	CAAGGAGCAAAGAATGGAGAAAAAAATCACTG		Construction of pKNG101-*csrA*::CAT plasmid
CAT_upR	GTGATTTTTTTCTCCATTCTTTGCTCCTTGAA		
CAT_downF	CAGGGCGGGGCGTGAAGAAGCGTCTCGTG		Construction of pKNG101-*csrA*::CAT plasmid
CAT_downR	GAGACGCTTCTTCACGCCCCGCCCTGCCAC		
lrhA q F	CAAGGTCGACAACCATCCTC		RT-qPCR, quantification of *rovM* expression
lrhA q R	GCCATATCACGGAATGGACT		
slyA q F	AAACGCATTGGGTTACCTTG		RT-qPCR, quantification of *rovA* expression
slyA q R	CACAGGTATGGCGTGTGATT		

ureA q F	GCTCACCCCAAGAGAAGTTG	RT-qPCR, quantification of *ureA* expression
ureA q R	TCCTCTACGGATTTGCCATC	
ureB q F	CGTTGATTCCTTTTGGTGGT	RT-qPCR, quantification of *ureB* expression
ureB q R	AGACGATTTGAAGCCACGTT	
yopE q F	GCCCACTCTGTGATTGGATT	RT-qPCR, quantification of *yopE* expression
yopE q R	TGTATTTTGGCAGCGTCTCA	
yopH q F	TACAAGACGCCAAAGTGCTG	RT-qPCR, quantification of *yopH* expression
yopH q R	CAACGGTGGAGTTCTGGAGT	
csrA q F	ACACTCATGATTGGCGATGA	RT-qPCR, quantification of *csrA* expression
csrA q R	CAGAAACCTCTTTCGGAGCA	

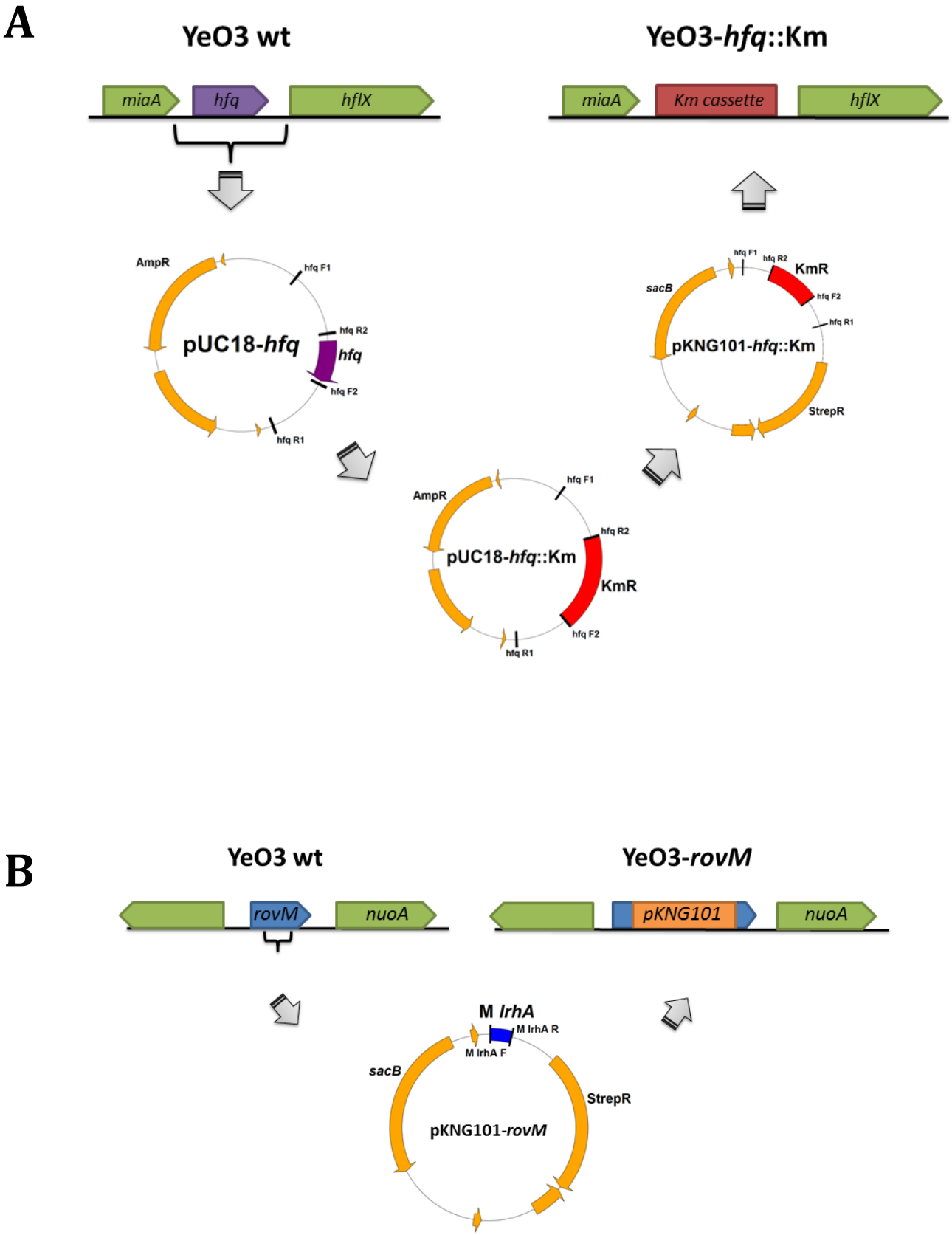
A
YeO3 wt
YeO3-hfq::Km
miaA
hfq
hflX
miaA
Km cassette
hflX
AmpR
hfq F1
pUC18-hfq
hfq R2
hfq
hfq F2
hfq R1
hfq F1
hfq R2
KmR
sacB
hfq F2
pKNG101-hfq::Km
hfq R1
StrepR
AmpR
hfq F1
pUC18-hfq::Km
hfq R2
KmR
hfq F2
hfq R1
B
YeO3 wt
YeO3-rovM
rovM
nuoA
pKNG101
nuoA
M lrhA
M lrhA R
M lrhA F
sacB
StrepR
pKNG101-rovM

C

YeO3-*hfq*::Km/p*hfq*

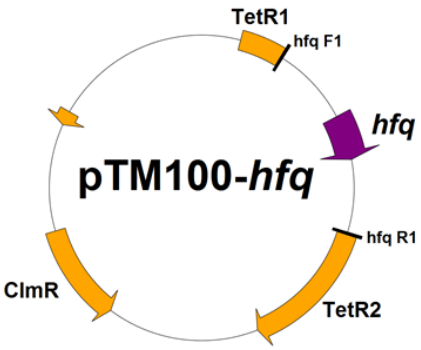

YeO3/pMMB207-*rovM*

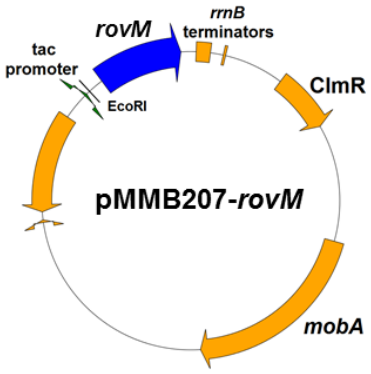

D

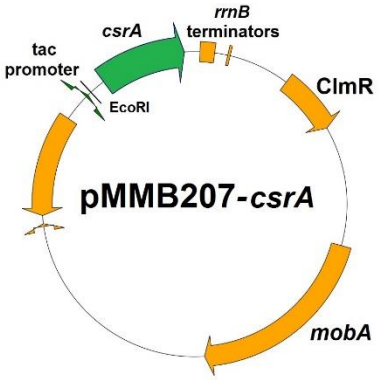

YeO3-wt/pMMB207-csrA

YeO3-hfq::Km/pMMB207-csrA

YeO3/pLux232oT-rovM /pMMB207-csrA

E

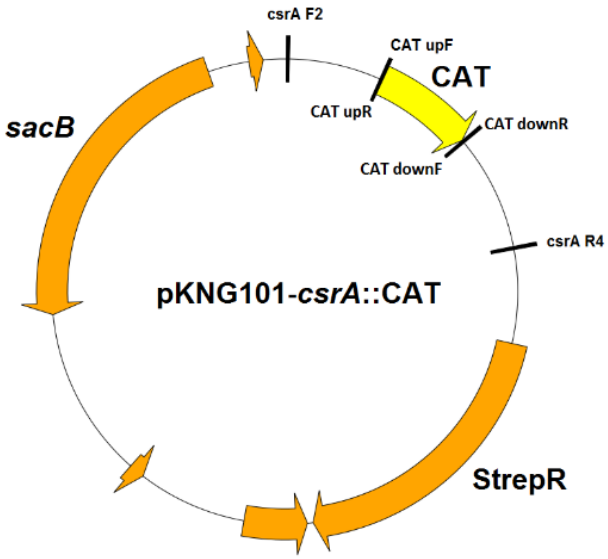

..

Figure S9. Schematic presentation of the construction of the the *Y. enterocolitica* O:3 strains and plasmids used in this study.

Panel A. Construction of YeO3-*hfq*::Km mutant. A 1367 bp fragment of the *hfq* gene with its flanking region was amplified with primers hfq F1 and hfq F2, and ligated with pUC18. Subsequently, the obtained pUC18-*hfq* plasmid was used as a template for PCR reaction with primers hfq F2 and hfq R2. The amplified PCR fragment was ligated with kanamycin resistance GenBlock (KmR) to obtain plasmid pUC18-*hfq*::Km. The plasmid was used as a template in PCR with primers hfq F1 and hfq R1 and the amplified fragment was ligated with the suicide vector pKNG101. The obtained plasmid pKNG101-*hfq*::Km was used in allelic exchange to replace the *hfq* gene with kanamycin resistance casette.

Panel B. Construction of YeO3-*rovM* and YeO3-*rovM-hfq*::Km mutants. The *rovM* knock-out mutants were generated by insertion mutagenesis using a single site homologous recombination approach. An internal fragment of the *rovM* gene was ligated with the suicide vector pKNG101 to obtain plasmid pKNG101-*rovM*, which was subsequently used to generate single and double mutant strains YeO3-*rovM* and YeO3-*rovM-hfq*::Km.

Panel C. Construction of the *hfq* and *rovM* complementation and overexpression plasmids. The complete *hfq* gene along with its promoter region was amplified using the primers hfq F1 and hfq R1, and ligated with pTM100. The complete *rovM* gene was amplified using the primers G lrhA F and G lrhA R, and the obtained fragment was ligated with pMMB207 downstream of the *tac* promotor. The obtained plasmids pTM100-*hfq* and pMMB207-*rovM* were mobilized into the YeO3-*hfq*::Km and YeO3-wt strains, respectively.

Panel D. Construction of the *csrA* overexpression plasmid. The complete *csrA* gene of *Y. enterocolitica* O:3 strain 6471/76 was amplified with Phusion DNA polymerase using primers csrA-F1 and csrA-R1 (Table S1). The obtained fragment was digested with BamHI and EcoRI and ligated into BamHI and EcoRI digested, SAP-treated pMMB207. The ligation mixture was electroporated into *E. coli* ω7249 cells. The resulting construct (pMMB207-*csrA*) was verified by restriction digestion and by sequencing with csrA-R1 and the pMMB207 specific primers. The plasmid pMMB207-*csrA* was then mobilized into the YeO3-wt, YeO3-*hfq*::Km and YeO3/pLux232oT-*rovM* strains by diparental conjugation as described earlier (Biedzka-Sarek *et al.*, 2005).

Panel E. Construction of suicide vector for allelic exchange mutagenesis of the *csrA* gene. Generation of the allelic exchange insert for the knock-out of the *csrA* gene was carried out with the overlapping extension PCR (Ho *et al.*, 1989) using Phusion DNA polymerase (Thermo Scientific). The initial PCR reactions were performed as follows: Genomic DNA of strain 6471/76 was used as a template to amplify the upstream region of the *csrA* gene by PCR using primers csrA-F2 and CAT_upR, and the downstream region of the *csrA* gene using primers CAT_downF and csrA-R4. The promoterless *CAT* gene fragment (coding for chloramphenicol acetyltransferase) from start to stop codon was amplified by PCR using plasmid pACYC184 DNA as template with primers CAT_upF and CAT_downR. All three PCR fragments contain overlapping regions, as the primer CAT_upR has a CAT_upF-, and primer CAT_downF has a CAT_downR-complementary region in their 5' ends, respectively. The fragments were electrophoretically purified, mixed in equal molar amounts and subjected to another round of PCR using the external primers (csrA-F2 and csrA-R4) in order to get the three fragments joined together. The resulting PCR fragment was digested with BamHI and ligated with BamHI-digested and phosphatase-treated pKNG101 (Kaniga *et al.*, 1991). The resulting plasmid was electrotransformed into *E. coli* strain ω7249. Restriction digestions and PCR confirmed that the CAT gene flanked by the *csrA* upstream and downstream fragments had been inserted in the same direction to the streptomycin resistance gene. The constructed plasmid (pKNG101-*csrA*::CAT) was then mobilized to the YeO3-wt and YeO3-*hfq*::Km by diparental conjugation. The resulting merodiploid strains (Clm^R Str^R $sucrose^S$) were confirmed by PCR. However, although Clm^R Str^S $sucrose^R$ colonies were obtained none of them was the desired allelic exchange mutant, thus the construction of the *csrA* mutant strain was unsuccessful.

Vectors were drawn using rf-cloning (http://www.rf-cloning.org/savvy.php)

REFERENCES:

Biedzka-Sarek, M., R. Venho & M. Skurnik, (2005) Role of YadA, Ail, and Lipopolysaccharide in Serum Resistance of *Yersinia enterocolitica* Serotype O:3. *Infection and immunity* **73**: 2232-2244.

Ho, S.N., H.D. Hunt, R.M. Horton, J.K. Pullen & L.R. Pease, (1989) Site-directed mutagenesis by overlap extension using the polymerase chain reaction. *Gene* **77**: 51-59.

Kaniga, K., I. Delor & G.R. Cornelis, (1991) A wide-host-range suicide vector for improving reverse genetics in gram-negative bacteria: inactivation of the blaA gene of *Yersinia enterocolitica*. *Gene* **109**: 137-141.

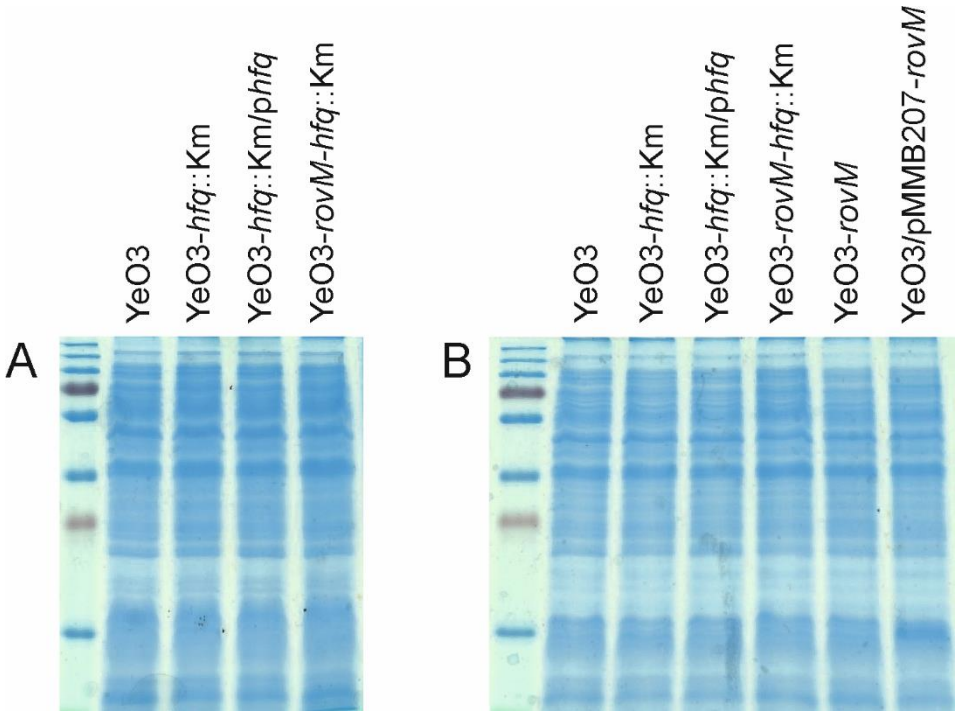

Figure S10. Loading control of samples used for Western Blotting with anti-flagellin (A) and anti-RpoS (B) antibodies. Same amount of each sample was applied on the 12% SDS-PAGE gel. After the electrophoresis, the gel was stained with InstantBlue (Expedon) and scanned.